Model Based Control of Resonating Processes Using Kautz Models

Rajasekhara Reddy B.

Reg. No : 10610708

Thesis submitted for

the award of the degree of

Doctor of Philosophy

Department of Chemical Engineering,

Indian Institute of Technology Guwahati, India.

August, 2017

Department of Chemical Engineering
Indian Institute of Technology Guwahati
India

Certificate

This is to certify that the thesis entitled, **Model Based Control of Resonating Processes Using Kautz Models**, being submitted by **Rajasekhara Reddy B.** for the award of the degree of Doctor of Philosophy, is an authentic record of the research carried out by him in the Department of Chemical Engineering, Indian Institute of Technology Guwahati under my supervision. The work documented in this thesis has not been submitted to any other university or institute for the award of any degree or diploma.

Prof. Prabirkumar Saha,
Department of Chemical Engineering,
Indian Institute of Technology Guwahati,
India.

Date :

Dedicated to

My wife, **Sushma**, My Daughter, **Sanvitha**

& **My Parents**

Abstract

Resonating processes are a special class of systems which display oscillatory dynamics around the operating point. Very common examples of resonating systems are power electronic devices, mechanical spring-mass-damping systems, electro-mechanical systems and chemical reactors. In general the electrical and/or mechanical systems are either linear or mildly nonlinear in nature, whereas the chemical reactors are highly nonlinear in nature. Hence control of resonating nonlinear chemical processes is always a challenging problem for control researchers community. Although the traditional PI(D) controller is very popular and well established control algorithm, its design procedure is not very clear for resonating systems. Hence Model Based Control(hereafter referred to as MBC) is a preferred candidate for controlling such systems. However not much has been addressed so far on this issue in the control engineering literature.

Model Predictive Control (hereafter referred to as MPC) and Internal Model Control (hereafter referred to as IMC) are the two important branches of MBC theory and are effective approaches for controlling constrained processes. As the name sounds, MBC design needs an explicit model of the process while computing the optimal control input. An efficient model and the closed-loop stability are the two major issues in this controller design procedure. The scope of this thesis broadly spans two areas: firstly the system identification of resonating systems and secondly the design of stable MBC of such resonating systems. In system identification, *Kautz model* and its nonlinear version in *Wiener* structure have been developed, which are novel in their kind. Kautz functions are derived in a standard state space

form in order to approximate the behavior of linear/mildly nonlinear resonating systems. In its nonlinear version (a.k.a *Kautz-Wiener model*) the linear dynamic part is formed by the Kautz filters while the static nonlinear mapping is described via two independent means, *viz*, wavelet decomposition and least squares support vector machine (hereafter referred to as LSSVM). The performance of the developed models are compared with that of similar models of the same class through suitable examples of case studies comprising of continuous stirred tank reactor (a.k.a CSTR) which is a reasonably nonlinear resonating system. Degree of nonlinearity as well as resonance were enhanced with series-connected CSTRs.

Kautz functions are formulated in a recursive fashion in order to compute the future incremental control effort of MPC. Use of Kautz functions in the optimization procedure leads to parsimonious representation. The efficacy of the proposed Kautz-MPC is tested on two case studies, *viz.* linear highly oscillatory mechanical system and mildly nonlinear magnetic ball suspension system. Performance of Kautz-MPC is compared against already published literature on Laguerre model based MPC. Stability of the Kautz-MPC is established through Lyapunov criteria.

On the other hand nonlinear Kautz-Wiener models have further been employed in the present thesis for developing nonlinear MBC strategies and their closed-loop control performance have been evaluated through simulation case studies involving CSTRs. Two types of model based control strategies are adopted *viz.* nonlinear MPC and nonlinear IMC. In case of nonlinear IMC, the problem of model inversion has been addressed, first of its kind in approach, through tactful modification of Wiener model coupled with optimization technique. Deletion of positive zeros from orthogonal basis filters while modifying Wiener model is the uniqueness of this thesis and it ensures stability of the controller.

Acknowledgements

This thesis has been completed during the years that I have spent as a PhD student at IITGuwahati.

First and foremost, I wish to thank my mentor, Professor Prabirkumar Saha, who gave me the great opportunity to come to IITG and guided my research. Many thanks to him for the fruitful discussions and for inspiring many of the ideas and results that are presented in this thesis. Above all, I thank him for his trust and his guidance during my PhD period in IITGuwahati. I have also learned from him many great scientific skills which will be helpful for my future career.

I would also like to thank Prof. Pallab Ghosh, Prof. Ramgopal Uppaluri and Dr. Indrani Kar for kindly accepting to serve as my doctoral committee members. Their comments, suggestions and criticism have all helped me to make the thesis to the present form. I would also like to take this opportunity to specially thank Prof. Bishnupada Mandal, Prof. Mihir K. Purkait and Prof. Pugazhenthi for their interest in the progress of my work and my career, although they are not anyway related to my thesis.

Guwahati, December 30, 2017 (Rajasekhara Reddy.B)

Contents

List of Figures

List of Tables

Nomenclature

$\beta_{()}, \beta^*_{()}$	n^{th} Kautz function's poles
$\boldsymbol{\alpha}$	Linear coefficient vector in LSSVM
$\boldsymbol{x}_o\left(\right), \boldsymbol{x}_e\left(\right)$	Newly defied odd, even Kautz states
δ_{ij}	kronecker delta function
Δu	incremental control action
Δu_{max}	maximum value of incremental control signal
Δu_{min}	minimum value of incremental control signal
γ	smoothness parameter in LSSVM
Λ, Υ, Ξ	Augmented system matrices
$\psi(x)$	wavelet function
$\Psi_{2n-1}()$	Odd Kautz functions
$\Psi_{2n}()$	Even Kautz functions
σ^2	RBF parameter in LSSVM
Θ	Linear regression coefficient vector
A, B, C	State space system matrices
a_i	dilation parameter in wavelet functions

a_l	Laguerre filter parameter
b_i	translation parameter in wavelet functions
b_{bias}	bias term in LSSVM
C_ψ	admissibility condition of wavelet
$C_o^{(n)}, C_e^{(n)}$	Odd and even Kautz functions coefficients
$G(T_s), H(T_s)$	State and input matrices in discrete time state model
$h_1^{()}, h_2^{()}$	Kautz model parameters
j	Complex number operator
K_{mpc}	State feedback controller gain
l_k	Laguerre filter state
N_c	Control horizon
N_p	Prediction horizon
Q	error weighted matrix
q	Shift operator
R	input weighted matrix
T_s	Sampling time
$V(k)$	Control Lyapunov Function
$V_{sub-opt}()$	sub optimal value of control Lyapunov function
$W_{a,b}^i$	wavelet network coefficient
z	z transforms operator
CLF	Control Lyapunov Function

Fig.	Figure
FIR	Finite Impulse Response
GOBF	Generalized Orthonormal Basis Filters
IIR	Infinite Impulse Response
IMC	Internal Model Control
ISE	Integral Square Error
LSSVM	Least Squares Support Vector Machine
MBSS	Magnetic Ball Suspension System
MPC	Model Predictive Control
RBF	Radial Basis Function
SISO	Single Input Single Output
SSE	Sum Square Error
VAF	Variance Accounted For

Chapter 1

Introduction

Resonating systems are also referred to as oscillatory systems. Several electrical, mechanical and chemical systems show resonating characteristics(Henson and Seborg, 1990). The resonating characteristics of a process is observed mainly due to more than one forces acting on the process variable. These forces may be due to the nature of the process itself or due to one or more external input(s). The resonating characteristics of a process yields oscillatory behavior when the process is subjected to changes in input(s). Linearization of such process around the operating point results in one or more pair(s) of complex poles and these complex poles lead to such resonating characteristics. Examples of such resonating processes can be found in robotics, power system electronics, mechanical systems etc. The resonating characteristics are also observed in large scale chemical processes, where multiple recycle loops exist in the process network and/or the case of a cascade control with the primary loop cut off (Huang and Chou, 1994). Modeling of such resonating systems is a critical yet essential pre-requisite, when process optimization and/or optimal control (especially model based control) happens to be the primary objective.

Although the conventional PID controller is an well established and industrially accepted technique, its design procedure is not very clear for the processes with resonating characteristics. It is particularly very cumbersome in case of large scale systems. There is no profound mathematical background for designing the

classical PID controllers for resonating systems. In many situations, Model Based Control(hereafter termed as MBC) strategies are proven to be good alternatives for PID controller. Model predictive controller and internal model controller (hereafter termed as MPC and IMC respectively) are the two important branches of MBC strategies that have a wide range of applications in the field of chemical process control (Henson and Seborg, 1990; Nahas et al., 1992; Yousefzadeh and Jahanian, 2017; Huang et al., 2000; Prakash and Srinivasan, 2009; Afram et al., 2017; Wang et al., 2017; Forlenza et al., 2017). Performance of these controllers mainly depends on the accuracy of the underlying model of the process on which the control schemes are designed.

Traditional MBC design techniques need an appropriate model for describing the system to be controlled. An accurate model of the system under consideration plays a significant role and model of the system is the key issue for the success of the developed control strategy. Modelling of the resonating systems in particular needs a special attention as the existing theory of identification and/or control is not so much focused on the resonating systems.

Over the years, dynamic modelling of process(also referred as system identification) has become one of the major research areas for applied control engineering researchers and there has been a significant progress in developing various linear and nonlinear models through system identification. The dynamic modeling of any systems can be obtained in three different ways:

First principles model: the first principle modeling or white-box modeling technique needs extensive knowledge about the systems of one's interest which is not a probable situation all the times.

Grey-box model: which needs partial information of the process and some of the model parameters are fixed using process input-output data. They are rarely preferred because of the complexity involved in model development.

Black-box model: which needs only input - output data of the process under consideration.

For poorly understood systems, the development of white-box models is almost impossible. Complexity of these models is also one of the main concerns as they require a high simulation time, hence they are not best suited for on-line optimization based control calculations. On the other hand, black-box models are the most preferred in the field of MBC strategies as their model structure is best suited for MBC applications and the model structure can be defined *a priori*. A brief discussion of system identification and aspects of MBC would help one to identify the gap areas of the state of the art research status and also assist one to zero in on the measurable objectives of the thesis.

1.1 System Identification

The art of system identification plays an important role in various engineering fields and has got many applications including automatic control, applied time series analysis, fault tolerant control and so on (Billings and Fakhouri, 1982; Boutayeb and Darouach, 1995; Chen and Billings, 1992; Lakshminarayanan et al., 1995; Saha, 1998; Manohar and Das, 2017; He et al., 2017b; Dijoux et al., 2017). Among the various system identification techniques the black box identification is quite famous particularly in the area of advanced control engineering for various reasons such as predefined model structure, simplicity and ease of building. The black box models need only the input - output data of the process and is independent of process characteristics information. In the literature, many linear and nonlinear system identifications techniques have been proposed (Cai et al., 2013; Wang et al., 2014, 2015; Abdollahzade and Kazemi, 2015; Linhares et al., 2015; Münker and Nelles, 2016; Ding et al., 2016). The applicability of the available linear and nonlinear models is limited to one particular class of systems, called well damped systems. However, the system identification and advanced control for resonating systems is not addressed extensively till now. This demands a complete theoretical background for development of suitable linear and/or nonlinear identification techniques for resonating systems.

1.1.1 Linear Modelling

Identification of various physical and engineering systems has a long historical background. A good overview, basic concepts and development procedures of system identification is presented by Ljung (1999). In the area of linear system modelling, step response models, Finite Impulse Response(FIR)(Shen et al., 2017) models and ARX models are very popular for approximating linear system dynamics. Shen et al. (2017) adopted FIR modelling in order to approximate the first order system with time delay. The advantages of their proposed method lie in the aspects of simplicity in model structure with a small number of basis models and ability to determine basis models with limited prior process information, which is beneficial for practical implementations. Rahman (2016) discussed ARX modelling technique by optimizing the ARX model parameters in order to identify twin rotor system using chaotic fractal search algorithm. Firstly, the improved Fractal Search algorithms were evaluated using 4 well-known classical benchmark functions with different dimension levels. Then, the modified Fractal Search algorithms are employed to optimize the parameters for an ARX model of twin rotor system in hovering mode. The final results found that Chaotic Fractal Search algorithm with Gauss/Mouse map shows superiority over other enhanced Stochastic Fractal Search algorithms when applied both in Diffusion Process and Updating Process.

These models are structure specific and need huge number of model parameters to model the dynamic systems, hence they are non-parsimonious in nature. A wide-variety of rigorous statistical metrics ar in place to balance model parsimony and predictive power (Mangan et al., 2017) including popular methods such as the Akaike information criterion (AIC), Bayesian information criterion (BIC), cross-validation (CV), deviance information criterion (DIC), and minimum description length (MDL). Methods such as AIC explicitly balance parsimony and relative information loss across models, penalizing the number of parameters in the model to avoid overfitting. The problem of non-parsimonious nature of these models can otherwise be overcome by adopting Orthogonal Basis Functions (hereafter refereed

to as OBFs) for dynamic system modelling.

1.1.2 OBF type Modelling

OBFs are very popular in developing various engineering and physical system models(Chou, 2017). Any function $f \in L^2$ is said to be orthogonal if it obeys the following property:

$$\delta_{ij} = \sum_{k=0}^{\infty} f_i(k) f_j(k) \tag{1.1}$$

where δ_{ij} is the kronecker delta function. The orthogonality property of OBFs will lead to parsimonious representation in the resulting model.

Laguerre functions (Wahlberg and Mäkilä, 1996; Wang, 2004; Bouzrara et al., 2012; Garna et al., 2013b) are quite popular OBFs because they can be parameterized by a single real-valued pole and they are parsimonious in nature too. The recursive nature of Laguerre construction makes it easy to compute. Because of its real valued pole, the Laguerre basis is preferable in representing well damped dynamic system. Systems with poorly damped dynamics, however, cannot be accurately described by Laguerre functions i.e. these functions are not appropriate for approximating signals having strong oscillatory behavior. This drawback has led to an increasing interest in the Kautz functions (Kautz, 1954; Benlahrache et al., 2016). Kautz filters are more generalized structure of Laguerre filters and a model developed with these filters deals with complex poles; thus facilitates an efficient modeling of resonant systems. Although the OBF based models are parsimonious and efficient in modelling linear dynamic systems, they fail to represent nonlinear systems.

Even though electrical and mechanical systems exhibit resonating characteristics they are mostly linear or mildly nonlinear in nature, whereas the chemical processes exhibit high nonlinearity and resonance. A linear model fails to represent such system(s). An obvious solution to this problem is to use nonlinear models for identifying the highly nonlinear dynamics. Mechanistic models are capable of representing any nonlinear system over the entire range of operation, however development of such models is very difficult and/or sometimes impossible. On the other hand, black-box

nonlinear identification technique is an elegant one even in presence of time delay.

1.1.3 Nonlinear Modelling

Polynomial models (especially NARMAX model)(Zabidi et al., 2017), neural network (He et al., 2017a) and fuzzy logic (Pasieka et al., 2017) are some of the successful tools to develop nonlinear system identification techniques. Polynomial models (Ying and Joseph, 1999a,c; Cheng et al., 2017) are quite efficient in approximating global information of any nonlinear system but the approximation of local information leads to non- parsimonious representation. Although neural network can effectively represent any nonlinear system with good accuracy, lack of a specified structured construction is the main drawback. Fuzzy logic based models are quite effective in identifying the installed nonlinearities such as saturation and discontinuous jumps. All of these nonlinear tools suffer from the problem of non-parsimonious nature, which can be overcome by combining them with OBF linear models called in *Wienertype structure*.

1.1.4 Wiener type Modelling

One of the major contribution of this thesis is to develop a certain class of nonlinear models, called *Wiener model*, specifically for resonating systems. A Wiener model is depicted in Figure 1.1. It is composed of a linear dynamic part along with a static nonlinear mapping. The input $u(k)$ and output $y(k)$ are measurable, the intermediate signal $v(k)$ can't be measured. In many situations, nonlinear black-box models based on Wiener framework are proved to be better alternatives. Various techniques have been reported in the literature to develop black-box Wiener models using open-loop input-output dataset of the process. Model parsimony, cost of development, time required for development and accuracy of the developed model are the important consideration which are needed to be taken care of while developing the model. In many situations, there should always be a compromise between the above said modelling specifications, however no modelling technique is expected to

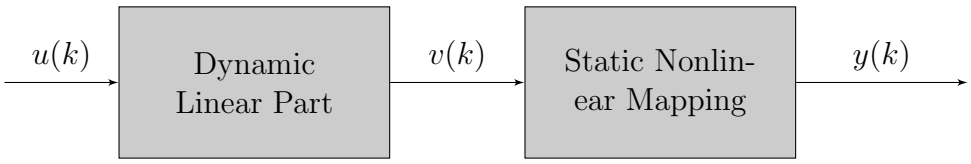

Figure 1.1: Wiener Model Structure

satisfy all the above said specifications.

The available literature on Wiener modelling for system identification is exhaustive, such as Aadaleesan et al. (2008); Al Seyab and Cao (2006); Babuska and Verbruggen (2003); Billings and Fakhouri (1982); Garna et al. (2013a); Kalafatis et al. (1995); Qing-chao Wang (2011); Saha et al. (2004); Tang et al. (2016); Tiels and Schoukens (2014); Totterman and Toivonen (2009) to name a few. In a work by Oliveira et al. (2012), a detailed overview of system identification using OBF is presented. The key operating units in process control such as CSTR, pH neutralization process, distillation column and bio reactor are the main case studies for the various developed nonlinear models. A few researchers (Qing-chao Wang, 2011; Saha et al., 2004) developed OBF based Wiener models in order to model the pH neutralization process. Others (Aadaleesan et al., 2008; Saha et al., 2004) used OBF based Wiener models to identify and/or control a bio reactor system which exhibits severe nonlinear characteristics. In some cases (Bloemen et al., 2001a) Wiener model was used to identify the dynamics of distillation column.

Over the years, many researchers have been applying the Wiener modelling technique for various engineering applications, especially, in the area of process control. OBFs are known for their parsimony and are very useful in construction of Wiener model (Aadaleesan et al., 2008; Alci and Asyali, 2009; Mahmoodi et al., 2009; Qing-chao Wang, 2011; Saha et al., 2004; Wahlberg, 1991b; Stanisawski et al., 2014; Zabiri et al., 2013, 2014a, 2016, 2014b). A residuals-based sequential identification algorithm using parallel integration of linear OBFs-Auto regressive with exogenous input (OBFARX) and a nonlinear neural network (NN) models was developed and analyzed by Zabiri et al. (2014a,b, 2018) under range extrapolations. A linear OBF model was integrated with nonlinear Wavelet Network model in parallel structure.

The overall nonlinear model was taken as the sum of these two models and analyzed using Van de Vusse reactor to observe the effectiveness and its performance within the model development region as well as under extrapolating conditions. The result showed that the proposed parallel OBF-WN performed better than other conventional model.

Laguerre basis function (*a.k.a* Laguerre filter) is very popular in representing the linear dynamic part of the Wiener model (Stanisawski et al., 2014), however they are limited primarily to systems with real poles. Stanisawski et al. (2014) presented a new implementable strategy for modeling and identification of a fractional-order discrete-time nonlinear block-oriented SISO Wiener system. The concept of modeling of a linear dynamics by means of OBF was employed in order to separate linear and nonlinear submodels, which enables a linear regression formulation of the parameter estimation problem. Discrete-time Laguerre filters were uniquely embedded in modeling of the fractional-order dynamics, eliminating the bilinearity issue. Very good identification performance for a fractional-order Laguerre-based Wiener model was observed through simulation studies, both in terms of low prediction errors and accurate reconstruction of the actual system characteristics.

However, the existing theory is limited to a certain class of systems called, *well damped systems*. Whereas, the problems associated with modelling and/or control of resonating systems (also called as under damped systems) is not addressed much in the control literature. Use of Laguerre filters in resonating system is not explicitly advocated by any researcher. On the other hand, Kautz filters have the ability to deal with the systems having multiple pairs of complex poles. Even though they were first introduced by Kautz (1954) in 1954, a thorough literature survey reveals that very few works (da Rosa et al., 2009; Zenan Šehiċ, 2012; Khan et al., 2011; Benlahrache et al., 2016; Vairetti et al., 2014; Mittal and Aadaleesan, 2012; Chen and Ljung, 2015) have been reported so far in the literature that deal Kautz filter based modelling technique. In the work by Zenan Šehiċ (2012), two-parametric Kautz model is employed to describe the control input trajectory of well damped linear system with time delay which can be more effectively controlled by using

Laguerre model with proper choice of Laguerre model parameter. In the work by Khan et al. (2011), the authors have presented Kautz functions as an alternative to Laguerre functions to parameterize the degrees of freedom in the predictions. It has been argued that the capability of handling complex poles gives Kautz function the edge (over Laguerre function) to maximize the feasible region of MPC. The Kautz network has been formulated with only one pair of complex poles and implemented on an LTI system.

Vairetti et al. (2014) worked on modeling of room (description of the sound field inside a room) where OBF models can include knowledge about the room resonances as a set of poles, which appear nonlinearly in the structure. Vairetti et al. (2014) exploited some properties of Kautz models, such as orthogonality and linearity-in-the-parameters and proposed a novel algorithm that avoid nonlinearity problem by iteratively estimating the poles and building the model. Mittal and Aadaleesan (2012) proposed a newer type of black box nonlinear model in Hammerstein structure which has Wavelet Network coupled with Kautz Functions. Wavelet basis functions have the property of localization which enables wavelet networks to approximate severe non-linearities using few number of parameters. On the other hand Kautz functions possess the ability to approximate any linear time invariant system using appropriate basis functions. Chen and Ljung (2015) tackled the regularized system identification using Kautz functions.

In OBF-Wiener modelling, the different Wiener models are categorized on the basis of description of static nonlinear mapping. In the work by Saha et al. (2004), the OBF-Wiener models are developed by two nonlinear mappings *viz.,* quadratic polynomial mapping and artificial neural networks mapping. Wavelet decomposition property was exercised by Aadaleesan et al. (2008) to develop OBF-Wiener models where the nonlinear mapping parameters were selected optimally by network based optimization. In some works (Qing-chao Wang, 2011; Totterman and Toivonen, 2009) Support Vector Machine(SVM) is used as a nonlinear mapping tool. However neither wavelet decomposition nor SVMs had ever been employed in the context of identification of resonating systems. Wiener structure modelling was explored by

Ławryńczuk (2013) where multi-layer perceptron feedforward neural network was used as the steady-state nonlinear part. However the algorithm does not need the model inversion yet yields better performance in controlling highly nonlinear polymerization and neutralization reactors.

In the field of process control, the Wiener models are primarily used to design MBC algorithms because the static nonlinear mapping of the Wiener models is generally invertible via certain mathematical manipulation.

1.2 Model Based Control

Model Based Control(or MBC), as the name sounds, completely depends on the accuracy of the model developed. Model Predictive Control(or MPC) and Internal Model Control(or IMC) are the two important sub branches of model based control.

1.2.1 Model Predictive Control

MPC works on the basis of optimization of a pre-defined objective function and it offers a way to resolve the difficulties posed by classical control problems by defining an open loop optimal control problem iteratively, forming a closed loop feedback control structure. In early $1960's$ MPC was first introduced by (Propoi, 1963) in the form of linear programming, but was ignored for almost two decades. In $1970's$ and $1980's$ MPC has enjoyed significant attention in industrial control applications and it is worth to mention the work reported by Shell oil industry in the form of Model Predictive Heuristic Control(MPHC) and Dynamic Matrix Control(DMC) (Cutler and Ramaker, 1980) that opened up new horizon to process control applications. Identification and Control(IDCOM)(Richalet et al., 1978), Generalised Predictive Control(GPC)(Patwardhan et al., 1998), Quadratic Dynamic Matrix Control(QDMC) (Niva and Yli-Korpela, 2012) and Model Algorithmic Control(MAC)(Rouhani and Mehra, 1982) are few other form of MPC. These techniques successfully resolved the

problems associated with constraints and nonlinear dynamics, however the issues like stability and robustness are not yet guaranteed. In the last decade NMPC has been extensively studied by several other researchers (Cao and Chen, 2014; Chen and Cao, 2012; Atuonwu et al., 2010; Seyab and Cao, 2008a,b; Al Seyab and Cao, 2006; Seyab et al., 2006; Cao, 2005).

The capabilities of MPC in dealing with nonlinear processes in presence of process constraints had made it very attractive in industrial control applications(Ying and Joseph, 1999b; Srinivasagupta et al., 2004). Various Wiener type models have been tried by the control engineers for severely nonlinear processes such as pH neutralization process (Mahmoodi et al., 2009), industrial C $_2$-splitter (Norquay et al., 1999), distillation column (Bloemen et al., 2001b), bioreactor (Saha et al., 2004), ALSTROM gasifier (Al Seyab and Cao, 2006), neutralization reactor (Ławryńczuk, 2013, 2016a), polymerization reactor (Shafiee et al., 2008; Ławryńczuk, 2013), Variable area tank (Arasu et al., 2016), heat exchanger (Ławryńczuk, 2016b), Piezoelectric Actuators (Cheng et al., 2015), Wastewater Treatment Process (Han and Qiao, 2014), composite manufacturing process (Voorakaranam and Joseph, 1999) *etc.* MPC of networked industrial process are proposed by Wang et al. (2016) and Lu et al. (2015). However, none of these techniques/applications are meant for resonating processes. In recent past, the theory of MPC has reached significant maturity and a good review of recent trends and future directions of MPC is presented by Xi et al. (2013) and Mayne (2014). Use of state-space models made it more useful because of the simplicity and generalization. State estimation techniques such as Kalman filtering (Senthil et al., 2006) were used when some of the process states are not measurable for any reason. Wiener and Hammerstein-Wiener model based NMPC were extensively studied by Ławrynczuk (Ławryńczuk, 2010, 2013, 2015, 2016b).

1.2.2 Internal Model Control

Unlike MPC, IMC works in different fashion and refers to a family controllers in which the control actions are calculated based on the inversion of the process model. The first proposal of IMC and its strengths are reported in series of articles by Garcia and Morari (1982, 1985a,b). The control actions are calculated by simple inversion of the process model which is carried out by a linear filter which can be fine-tuned for a trade off between performance and stability. While designing IMC enough care need to be taken to ensure the stability of resulting closed loop controller and IMC is very attractive for a process with inherent stable dynamics (Bequette, 2003). A basic platform of the IMC design for linear systems can be found in (Bequette, 2003). An extension of IMC design for nonlinear systems can be found in Economou et al. (1986). Over the years many researchers developed a wide variety of IMC design procedures for both linear and nonlinear processes, eg. (Bhat et al., 1991; Arulselvi et al., 2004; Begum et al., 2016; Besta and Chidambaram, 2017; Babuska and Verbruggen, 2003; Aydi et al., 2017; Othman et al., 2016; Azar and Serrano, 2014; Rivals and Personnaz, 2000; Brown et al., 1997; Nahas et al., 1992; Henson and Seborg, 1991; Zheng et al., 1994) to name a few. The issue of model inversion in the context of nonlinear IMC is still unexplored in Wiener type framework. Nevertheless the IMC for true nonlinear system is relatively unexplored. Ding et al. (2017) studied the trajectory-tracking problem of a hydraulic servo multi-closed-chain mechanism. The nonaffine nonlinear characteristic of the electro-hydraulic actuator and its time-varying uncertainty load resulting from the multi-closed-chain mechanism was taken into consideration for proposing a nonlinear control algorithm which is termed as the Approximate IMC (or AIMC) integrated with a position feedback control in cascade control design. Qiu (2017) proposes the composite AIMC (or CAIMC), which identifies the model and the inverse in parallel, and reduces the tracking error through the online identification. "Composite" refers to the simultaneous identifications. The constraint imposed by the stability of an n-th order model is nonconvex, and it is re-parameterized as a linear matrix inequality. The parameter identification prob-

lem with the stability constraint is reformulated as a convex programming problem. Nath et al. (2017) proposed an adaptive IMC-PI controller for a level control process where the IMC tuning parameter is varied based on a set of predefined fuzzy rules depending on the process operating conditions in terms of process error and change of error. Qiu (2017) also proposes nonlinear IMC whereby a new approach for nonlinear inversion, referred to as the structured quasi-linear parameter varying (quasi-LPV) model inverse, is developed and validated. However this nonlinear IMC is applicable only when the nonlinear system has a special structural property and has not been generalized for other uses. Clerget et al. (2017) proposed a nonlinear IMC algorithm which is a sampled nonlinear MBC with successive model inversion and bias correction. Global convergence and robustness is proved despite time-varying delays and uncertain measurements dating.

1.3 Gap areas

From the above elaborate literature survey on the pertinent issue, the following gap areas are observed.

1. The existing linear OBF models have the limitations in accurately modelling the resonating processes. Even with substantial mathematical efforts, available linear OBF models remain non parsimonious in nature and the degrees of freedom increases. There exists huge potential to unearth the full potential of Kautz modelling technique.

2. MBC of linear and/or mildly nonlinear resonating processes are still grossly unexplored due to lack of appropriate modelling techniques.

3. Even though the Wiener modeling technique is very popular in the area of system identification no efforts has been observed to use this technique in the context of nonlinear resonating systems.

4. It is observed that the highly nonlinear resonating processes such as chemical process control applications operate with a higher compromise because of

the absence of accurate nonlinear modelling technique, especially when it is required to operate the processes in high resonating zones.

5. Nonlinear IMC(NIMC), which is one of the important NMBC strategy is still unexplored in the prescriptive of Wiener modelling through optimization based model inversion.

These gap areas assist one to identify the measurable objectives of the thesis.

1.4 Objectives of the Thesis

The overall aim of the thesis is to develop a novel approach of MBC of resonating processes in the context of above key issues and study their merits. The aim can be achieved through the following measurable objectives.

1. Development of efficient linear mathematical modeling technique by using OBFs, especially Kautz functions in standard state space form. Focus will be on the identification of linear and mildly nonlinear resonating systems and other issues related to resonating systems.

2. Development of an explicit MPC algorithm by describing the required control actions with the Kautz functions. The stability margins of the proposed MPC may be analyzed by Lyapunov stability theory.

3. Development of Wiener type Kautz model using two different nonlinear mapping tools *viz,* Wavelet Network and Least Squares SVM (or LSSVM) for identification of nonlinear resonating systems. This class of models may be termed as Kautz - Wiener models.

4. It is also desired to use the developed Kautz - Wiener models in formulation of two nonlinear MBD applications, *viz.,* NMPC and NIMC.

5. Finally it is intended to prove the efficacy of the Kautz functions through various simulation case studies, *viz.,* linear mechanical oscillatory system, mildly nonlinear electro - mechanical system and highly nonlinear chemical reactors.

1.5 Outline of the Thesis

This thesis is divided into two sub fields *viz.,* linear, nonlinear system identification and MBC of resonating systems. A brief summary of each of the following chapters is furnished below.

Chapter 2 deals with identification of linear resonating systems using linear Kautz functions model. In this model, the Kautz functions are derived in discrete time state space domain in the same line of Laguerre functions in order to form a model called, *Kautz model*. The efficacy of the Kautz model is demonstrated with two case studies: (*i*) Linear oscillatory mechanical system. (*ii*) Mildly nonlinear electromechanical system.

Chapter 3 deals with Explicit MPC design for resonating linear and mildly nonlinear systems. MPC has been presented with recursive Kautz model. They have been formulated in a recursive fashion in order to compute the future incremental control effort of MPC. A complete theoretical background of the proposed controller is presented. Use of Kautz functions in the optimization procedure leads to a parsimonious representation. The stability of the developed control algorithm is proved through Lyapunov stability theory. The efficacy of the proposed MPC is evaluated through the same case studies as in Chapter 2.

A novel kind of Wiener model is developed for identification of highly nonlinear resonating systems in Chapter 4. Two types of OBF's *viz.,* Laguerre functions and Kautz functions, are employed to capture the linear dynamic part of Wiener structure while the static nonlinear mapping is described by two means, *viz.,* wavelet decomposition and least squares support vector machine. Use of OBF leads to parsimony for nonlinear model too. The superiority of the proposed Wiener model is demonstrated through two simulation case studies: (*i.*) Continuous Stirred Tank Reactor (CSTR) which is reasonably nonlinear resonating system. (*ii.*) Series CSTR (or SCSTR) where degree of non-linearity as well as resonance increases manifold.

The above nonlinear models have further been employed in the Chapter 5 for developing nonlinear MBC strategies and their closed loop control performance have

been evaluated through case studies involving same CSTR's. Two types of MBC strategies were adopted, *viz.,* NMPC and NIMC. In case of NIMC, the problem of model inversion has been addressed, first of it's kind in approach, through tactical modification of Wiener model coupled with optimization technique. Deletion of positive zeros from OBF while modifying the Wiener model is the uniqueness of this work and it ensures the stability of the controller.

Finally, based on the works furnished in the chapter 2 to chapter 5, some conclusions are drawn in the chapter 6. Based on the experience of the author while working for this thesis some future recommendations are provided.

Chapter 2

Identification of Resonating systems using Linear Kautz Model

Kautz functions were first proposed by William.H.Kautz at (Kautz, 1954). The problem of constructing an orthonormal set from a set of continuous time exponentials has elegantly solved. The key idea of that research is to determine the corresponding Laplace transform which will be very simple in structure. The analogous discrete problem is solved by (Ninness, 1996).

Kautz filters have the ability to describe any physical system which is having complex poles. Although the Kautz filters have their first inspection in the field of system approximation in $1960's$, but was left with less priority till date. The reason could be the complicated structure of the Kautz filters. However, the use of Kautz filters in modelling the resonating system will greatly increases the accuracy and the parsimonious nature.

2.1 Theoretical Development

The problem of orthogonalizing a set of discrete time exponential functions can be summarized as the following Wahlberg (1991a):

The sequence of functions $\Psi_j(z)$

$$\Psi_{2n-1}(z) = C_o^{(n)}\left\{1 - a_o^{(n)}z\right\}\Gamma^{(n)}(z) \tag{2.1}$$

$$\Psi_{2n}(z) = C_e^{(n)}\left\{1 - a_e^{(n)}z\right\}\Gamma^{(n)}(z) \tag{2.2}$$

for $\forall n = 1, 2, ...$ where

$$\Gamma^{(n)}(z) = \frac{\prod_{j=1}^{n-1}(1-\beta_j z)\left(1-\beta_j^* z\right)}{\prod_{j=1}^{n}(z-\beta_j)\left(z-\beta_j^*\right)} \tag{2.3}$$

$$\left\{1 + a_o^{(n)}a_e^{(n)}\right\}(1 + \beta_n\beta_n^*) - \left\{a_o^{(n)} + a_e^{(n)}\right\}(\beta_n + \beta_n^*) = 0$$

$$C_g^{(n)} = \sqrt{\frac{(1-\beta_n^2)(1-\beta_n^{*2})(1-\beta_n\beta_n^*)}{\left\{1 + \left(a_g^{(n)}\right)^2\right\}\{1+\beta_n\beta_n^*\} - 2a_g^{(n)}\{\beta_n + \beta_n^*\}}} \tag{2.4}$$

form an orthonormal set, *i.e.*,

$$\delta_{jl} = \frac{1}{2\pi i}\oint \Psi_j(z)\,\Psi_l\left(z^{-1}\right)\frac{dz}{z} \tag{2.5}$$

where δ_{jl} is the Kronecker delta function and $\beta_n, \beta_n^* \in \mathbb{C}$ in the region $|\beta_n| < 1$. The functions $\{\Psi_j(z), \forall j\}$, where $j = 1, 2, \cdots$ are called discrete Kautz functions. The suffix 'g' for 'C' and 'a' in Eq.2.4 collectively represents suffices 'o' and 'e', as and when appropriate. □

2.2 Kautz Representation

2.2.1 Recursive Linear Kautz functions Model

By taking the inverse $\mathcal{Z}$-transform of the Kautz functions defined in Theorem 2.1 as

$$\Psi(k) = \mathcal{Z}^{-1}\Psi(z) \tag{2.6}$$

and expressing the i^{th} pole-pairs of the Kautz model parameters as

$$h_1^{(i)} = -\left(\beta_i + \beta_i^*\right) \tag{2.7}$$

$$h_2^{(i)} = \beta_i\beta_i^* \tag{2.8}$$

the odd Kautz functions, given in Eq. 2.1, can further be derived as

$$\begin{aligned}
\Psi_{2i-1}(z) &= C_o^{(i)}\left(1 - a_o^{(i)}z\right)\Gamma^{(i)}(z) \\
&= C_o^{(i)}\left(1 - a_o^{(i)}z\right) \times \frac{\left(1-\beta_i z\right)\left(1-\beta_i^* z\right)}{\left(z-\beta_i\right)\left(z-\beta_i^*\right)}\Gamma^{(i-1)}(z) \\
&= C_o^{(i)}\left(1 - a_o^{(i)}z\right) \times \frac{1 - \left(\beta_i + \beta_i^*\right)z + \beta_i\beta_i^* z^2}{z^2 - \left(\beta_i + \beta_i^*\right)z + \beta_i\beta_i^*} \times \frac{\Psi_{2(i-1)-1}(z)}{C_o^{(i-1)}\left(1 - a_o^{(i-1)}z\right)} \\
&= \dots \\
&= p_{o,0}^{(i)} \times \frac{z^3 + p_{o,1}^{(i)}z^2 + p_{o,2}^{(i)}z + p_{o,3}^{(i)}}{z^3 - p_{o,4}^{(i)}z^2 - p_{o,5}^{(i)}z - p_{o,6}^{(i)}} \times \Psi_{2(i-1)-1}(z)
\end{aligned} \tag{2.9}$$

In a similar fashion, the even Kautz functions, given in Eq.2.2, can further be derived as

$$\Psi_{2i}(z) = p_{e,0}^{(i)} \times \frac{z^3 + p_{e,1}^{(i)}z^2 + p_{e,2}^{(i)}z + p_{e,3}^{(i)}}{z^3 - p_{e,4}^{(i)}z^2 - p_{e,5}^{(i)}z - p_{e,6}^{(i)}} \times \Psi_{2(i-1)}(z) \tag{2.10}$$

The detailed derivation of Eq. 2.9 and Eq. 2.10 are given in Appendix A. The suffices 'o' and 'e' indicate the corresponding parameters of the odd and even Kautz

functions respectively. These suffices are collectively represented as suffix 'g'

$$p_{g,0}^{(i)} = \frac{C_g^{(i)} a_g^{(i)} h_2^{(i)}}{C_g^{(i-1)} a_g^{(i-1)}} \tag{2.11}$$

$$p_{g,1}^{(i)} = \frac{h_1^{(i)}}{h_2^{(i)}} - \frac{1}{a_g^{(i)}} \tag{2.12}$$

$$p_{g,2}^{(i)} = \frac{1}{h_2^{(i)}} - \frac{h_1^{(i)}}{a_g^{(i)} h_2^{(i)}} \tag{2.13}$$

$$p_{g,3}^{(i)} = -\frac{1}{a_g^{(i)} h_2^{(i)}} \tag{2.14}$$

$$p_{g,4}^{(i)} = \frac{1}{a_g^{(i-1)}} - h_1^{(i)} \tag{2.15}$$

$$p_{g,5}^{(i)} = \frac{h_1^{(i)}}{a_g^{(i-1)}} - h_2^{(i)} \tag{2.16}$$

$$p_{g,6}^{(i)} = \frac{h_2^{(i)}}{a_g^{(i-1)}} \tag{2.17}$$

The odd Kautz functions in Eq. 2.9 are in 3^{rd} order $\mathcal{Z}$ - domain and they can be represented in discrete time domain as follows:

$$\begin{aligned}\Psi_{2i-1}(k+3) = {} & p_{o,4}^{(i)} \Psi_{2i-1}(k+2) + p_{o,5}^{(i)} \Psi_{2i-1}(k+1) + p_{o,6}^{(i)} \Psi_{2i-1}(k) \\ & + p_{o,0}^{(i)} \left\{ \Psi_{2(i-1)-1}(k+3) + p_{o,1}^{(i)} \Psi_{2(i-1)-1}(k+2) + p_{o,2}^{(i)} \right. \\ & \left. \Psi_{2(i-1)-1}(k+1) + p_{o,3}^{(i)} \Psi_{2(i-1)-1}(k) \right\}\end{aligned} \tag{2.18}$$

The general expression for the odd Kautz functions can be derived by using long division method on Eq. 2.9.

$$\begin{aligned}\Psi_{2i-1}(z) = {} & p_{o,0}^{(i)} \Psi_{2(i-1)-1}(0) z^{-1} + p_{o,0}^{(i)} \left\{ \Psi_{2(i-1)-1}(1) + \Psi_{2(i-1)-1}(0) \left(p_{o,1}^{(i)} + p_{o,4}^{(i)} \right) \right\} z^{-2} \\ & + p_{o,0}^{(i)} \left\{ \Psi_{2(i-1)-1}(2) + \Psi_{2(i-1)-1}(1) \left(p_{o,1}^{(i)} + p_{o,4}^{(i)} \right) + \Psi_{2(i-1)-1}(0) \left(p_{o,2}^{(i)} + p_{o,5}^{(i)} \right) \right. \\ & \left. + \Psi_{2(i-1)-1}(0) p_{o,4}^{(i)} \left(p_{o,1}^{(i)} + p_{o,4}^{(i)} \right) \right\} z^{-3} + \cdots\end{aligned} \tag{2.19}$$

The samples at time instants 1,2 and 3 are observed from Eq. 2.19.

$$\Psi_{2i-1}(1) = p_{o,0}^{(i)} \psi_{2(i-1)-1}(0) \tag{2.20a}$$

$$\Psi_{2i-1}(2) = p_{o,0}^{(i)} \left\{ \Psi_{2(i-1)-1}(1) + \Psi_{2(i-1)-1}(0) \left(p_{o,1}^{(i)} + p_{o,4}^{(i)} \right) \right\} \tag{2.20b}$$

$$\begin{aligned} \Psi_{2i-1}(3) = p_{o,0}^{(i)} \Big\{ & \Psi_{2(i-1)-1}(2) + \Psi_{2(i-1)-1}(1) \left(p_{o,1}^{(i)} + p_{o,4}^{(i)} \right) \\ & + \Psi_{2(i-1)-1}(0) \left(p_{o,2}^{(i)} + p_{o,5}^{(i)} \right) + \Psi_{2(i-1)-1}(0)\, p_{o,4}^{(i)} \left(p_{o,1}^{(i)} + p_{o,4}^{(i)} \right) \Big\} \end{aligned} \tag{2.20c}$$

Eqs. 2.20a–2.20c provides the necessary past values in Eq. 2.18.

For $i = 1$,

$$\begin{aligned} \Psi_1(z) &= C_o^{(1)} \left(1 - a_o^{(1)} z\right) \Gamma^{(1)}(z) \\ &= \frac{C_o^{(1)} \left(1 - a_o^{(1)} z\right)}{z^2 + h_1^{(1)} z + h_2^{(1)}} \end{aligned} \tag{2.21}$$

$$\Psi_1(k+2) = -h_1^{(1)} \Psi_1(k+1) - h_2^{(1)} \Psi_1(k) \tag{2.22}$$

and long division of Eq. 2.21 leads to the following $\mathcal{Z}$-domain form

$$\begin{aligned} \Psi_1(z) = & -C_o^{(1)} a_o^{(1)} z^{-1} + C_o^{(1)} \left\{ 1 + a_o^{(1)} h_1^{(1)} \right\} z^{-2} \\ & + C_o^{(1)} \left[a_o^{(1)} h_2^{(1)} - h_1^{(1)} \left\{ 1 + a_o^{(1)} h_1^{(1)} \right\} \right] z^{-3} + \cdots \end{aligned} \tag{2.23}$$

with

$$\Psi_1(1) = -C_o^{(1)} a_o^{(1)} \tag{2.24a}$$

$$\Psi_1(2) = C_o^{(1)} \left\{ 1 + a_o^{(1)} h_1^{(1)} \right\} \tag{2.24b}$$

$$\Psi_1(3) = C_o^{(1)} \left\{ a_o^{(1)} h_2^{(1)} - h_1^{(1)} \left(1 + a_o^{(1)} h_1^{(1)} \right) \right\} \tag{2.24c}$$

Now, from Eq. 2.22

$$\Psi_1(k+3) = -h_1^{(1)} \Psi_1(k+2) - h_2^{(1)} \Psi_1(k+1) \tag{2.25}$$

For $i = 2$, using Eq. 2.18 and Eq. 2.25

$$\Psi_3(k+3) = p_{o,0}^{(2)}\left(p_{o,1}^{(2)} - h_1^{(1)}\right)\Psi_1(k+2) + p_{o,4}^{(2)}\Psi_3(k+2) + p_{o,0}^{(2)}\left(p_{o,2}^{(2)} - h_2^{(1)}\right)$$
$$\Psi_1(k+1) + p_{o,5}^{(2)}\Psi_3(k+1) + p_{o,0}^{(2)}p_{o,3}^{(2)}\Psi_1(k) + p_{o,6}^{(2)}\Psi_3(k) \quad (2.26)$$

For $i = 3$, using Eq. 2.18 and Eq. 2.26

$$\Psi_5(k+3) = \left(\prod_{i=2}^{3} p_{o,0}^{(i)}\right)\left(p_{o,1}^{(2)} - h_1^{(1)}\right)\Psi_1(k+2) + p_{o,0}^{(3)}\left(p_{o,4}^{(2)} + p_{o,1}^{(3)}\right)\Psi_3(k+2)$$
$$+ p_{o,4}^{(3)}\Psi_5(k+2) + \left(\prod_{i=2}^{3} p_{o,0}^{(i)}\right)\left(p_{o,2}^{(2)} - h_2^{(1)}\right)\Psi_1(k+1) + p_{o,0}^{(3)}\left(p_{o,5}^{(2)} + p_{o,2}^{(3)}\right)$$
$$\times\Psi_3(k+1) + p_{o,5}^{(3)}\Psi_5(k+1) + \left(\prod_{i=2}^{3} p_{o,0}^{(i)}\right)p_{o,3}^{(2)}\Psi_1(k) + p_{o,0}^{(3)}\left(p_{o,6}^{(2)} + p_{o,3}^{(3)}\right)$$
$$\times\Psi_3(k) + p_{o,6}^{(3)}\Psi_5(k) \quad (2.27)$$

Similarly for $i = 4$, using Eq. 2.18, Eq. 2.26 and Eq. 2.27

$$\begin{aligned}\Psi_7(k+3) \;=\; & \left(\prod_{i=2}^{4} p_{o,0}^{(i)}\right)\left(p_{o,1}^{(2)} - h_1^{(1)}\right)\Psi_1(k+2) + \left(\prod_{i=3}^{4} p_{o,0}^{(i)}\right)\left(p_{o,4}^{(2)} + p_{o,1}^{(3)}\right)\\
& \times\Psi_3(k+2) + p_{o,0}^{(4)}\left(p_{o,4}^{(3)} + p_{o,1}^{(4)}\right)\Psi_5(k+2) + p_{o,4}^{(4)}\Psi_7(k+2)\\
& + \left(\prod_{i=2}^{4} p_{o,0}^{(i)}\right)\left(p_{o,2}^{(2)} - h_2^{(1)}\right) \times \Psi_1(k+1) + \left(\prod_{i=3}^{4} p_{o,0}^{(i)}\right)\left(p_{o,5}^{(2)} + p_{o,2}^{(3)}\right)\\
& \times\Psi_3(k+1) + p_{o,0}^{(4)}\left(p_{o,5}^{(3)} + p_{o,2}^{(4)}\right) \times \Psi_5(k+1) + p_{o,5}^{(4)}\Psi_7(k+1)\\
& + \left(\prod_{i=2}^{4} p_{o,0}^{(i)}\right)p_{o,3}^{(2)}\Psi_1(k) + \left(\prod_{i=3}^{4} p_{o,0}^{(i)}\right) \times \left(p_{o,6}^{(2)} + p_{o,3}^{(3)}\right)\Psi_3(k)\\
& + p_{o,0}^{(4)}\left(p_{o,6}^{(3)} + p_{o,3}^{(4)}\right)\Psi_5(k) + p_{o,6}^{(4)}\Psi_7(k) \quad (2.28)\end{aligned}$$

The Eq. 2.25, Eq. 2.26, Eq. 2.27 and Eq. 2.28 together can be written in a compact matrix form as following

$$\begin{bmatrix} \Psi_1(k+3) \\ \Psi_3(k+3) \\ \Psi_5(k+3) \\ \Psi_7(k+3) \end{bmatrix} = \begin{bmatrix} m_{11} & m_{12} & m_{13} & m_{14} \end{bmatrix} \begin{bmatrix} \Psi_1(k+2) \\ \Psi_3(k+2) \\ \Psi_5(k+2) \\ \Psi_7(k+2) \end{bmatrix} + \begin{bmatrix} m_{21} & m_{22} & m_{23} & m_{24} \end{bmatrix} \begin{bmatrix} \Psi_1(k+1) \\ \Psi_3(k+1) \\ \Psi_5(k+1) \\ \Psi_7(k+1) \end{bmatrix} + \begin{bmatrix} m_{31} & m_{32} & m_{33} & m_{34} \end{bmatrix} \begin{bmatrix} \Psi_1(k) \\ \Psi_3(k) \\ \Psi_5(k) \\ \Psi_7(k) \end{bmatrix} \tag{2.29}$$

where

$$m_{11} = \begin{bmatrix} -h_1^{(1)} \\ p_{o,0}^{(2)}\left(p_{o,1}^{(2)} - h_1^{(1)}\right) \\ \left(\prod_{i=2}^{3} p_{o,0}^{(i)}\right)\left(p_{o,1}^{(2)} - h_1^{(1)}\right) \\ \left(\prod_{i=2}^{4} p_{o,0}^{(i)}\right)\left(p_{o,1}^{(2)} - h_1^{(1)}\right) \end{bmatrix}$$

$$m_{12} = \begin{bmatrix} 0 \\ p_{o,4}^{(2)} \\ p_{o,0}^{(3)}\left(p_{o,4}^{(2)} + p_{o,1}^{(3)}\right) \\ \left(\prod_{i=3}^{4} p_{o,0}^{(i)}\right)\left(p_{o,4}^{(2)} + p_{o,1}^{(3)}\right) \end{bmatrix}$$

$$\begin{bmatrix} m_{13} & m_{14} \end{bmatrix} = \begin{bmatrix} 0 & 0 \\ 0 & 0 \\ p_{o,4}^{(3)} & 0 \\ p_{o,0}^{(4)}\left(p_{o,4}^{(3)} + p_{o,1}^{(4)}\right) & p_{o,4}^{(4)} \end{bmatrix}$$

$$m_{21} = \begin{bmatrix} -h_2^{(1)} \\ p_{o,0}^{(2)}\left(p_{o,2}^{(2)} - h_2^{(1)}\right) \\ \left(\prod_{i=2}^{3} p_{o,0}^{(i)}\right)\left(p_{o,2}^{(2)} - h_2^{(1)}\right) \\ \left(\prod_{i=2}^{4} p_{o,0}^{(i)}\right)\left(p_{o,2}^{(2)} - h_2^{(1)}\right) \end{bmatrix}$$

$$m_{22} = \begin{bmatrix} 0 \\ p_{o,5}^{(2)} \\ p_{o,0}^{(3)}\left(p_{o,5}^{(2)} + p_{o,2}^{(3)}\right) \\ \left(\prod_{i=3}^{4} p_{o,0}^{(i)}\right)\left(p_{o,5}^{(2)} + p_{o,2}^{(3)}\right) \end{bmatrix}$$

$$\begin{bmatrix} m_{23} & m_{24} \end{bmatrix} = \begin{bmatrix} 0 & 0 \\ 0 & 0 \\ p_{o,5}^{(3)} & 0 \\ p_{o,0}^{(4)}\left(p_{o,5}^{(3)} + p_{o,2}^{(4)}\right) & p_{o,5}^{(4)} \end{bmatrix}$$

$$m_{31} = \begin{bmatrix} 0 \\ p_{o,0}^{(2)} p_{o,3}^{(2)} \\ \left(\prod_{i=2}^{3} p_{o,0}^{(i)}\right) p_{o,3}^{(2)} \\ \left(\prod_{i=2}^{4} p_{o,0}^{(i)}\right) p_{o,3}^{(2)} \end{bmatrix}$$

$$m_{32} = \begin{bmatrix} 0 \\ p_{o,6}^{(2)} \\ p_{o,0}^{(3)}\left(p_{o,6}^{(2)} + p_{o,3}^{(3)}\right) \\ \left(\prod_{i=3}^{4} p_{o,0}^{(i)}\right)\left(p_{o,6}^{(2)} + p_{o,3}^{(3)}\right) \end{bmatrix}$$

$$\begin{bmatrix} m_{33} & m_{34} \end{bmatrix} = \begin{bmatrix} 0 & 0 \\ 0 & 0 \\ p_{o,6}^{(3)} & 0 \\ p_{o,0}^{(4)}\left(p_{o,6}^{(3)} + p_{o,3}^{(4)}\right) & p_{o,6}^{(4)} \end{bmatrix}$$

By analyzing the above derived matrix equality, one can easily observe that the set of Kautz functions can be represented in recursive manner that satisfies the following difference equation with initial conditions $\Psi(1)$, $\Psi(2)$ and $\Psi(3)$.

$$\begin{bmatrix} \Psi_1(k+3) \\ \Psi_3(k+3) \\ \Psi_5(k+3) \\ \Psi_7(k+3) \\ \vdots \\ \Psi_{2n-1}(k+3) \end{bmatrix} = \Omega_{2,o} \begin{bmatrix} \Psi_1(k+2) \\ \Psi_3(k+2) \\ \Psi_5(k+2) \\ \Psi_7(k+2) \\ \vdots \\ \Psi_{2n-1}(k+2) \end{bmatrix} + \Omega_{1,o} \begin{bmatrix} \Psi_1(k+1) \\ \Psi_3(k+1) \\ \Psi_5(k+1) \\ \Psi_7(k+1) \\ \vdots \\ \Psi_{2n-1}(k+1) \end{bmatrix} + \Omega_{0,o} \begin{bmatrix} \Psi_1(k) \\ \Psi_3(k) \\ \Psi_5(k) \\ \Psi_7(k) \\ \vdots \\ \Psi_{2n-1}(k) \end{bmatrix} \tag{2.30}$$

And the n^{th} rows of the matrices $\Omega_{2,o}$, $\Omega_{1,o}$and $\Omega_{0,o}$ will be

$$\Omega_{2,o}(n) = \begin{bmatrix} \left\{\prod_{i=2}^{n} p_{o,0}^{(i)}\right\}\left(p_{o,1}^{(2)} - h_1^{(1)}\right) \\ \left\{\prod_{i=3}^{n} p_{o,0}^{(i)}\right\}\left(p_{o,4}^{(2)} + p_{o,1}^{(3)}\right) \\ \left\{\prod_{i=4}^{n} p_{o,0}^{(i)}\right\}\left(p_{o,4}^{(3)} + p_{o,1}^{(4)}\right) \\ \vdots \\ \left\{\prod_{i=n-1}^{n} p_{o,0}^{(i)}\right\}\left(p_{o,4}^{(n-2)} + p_{o,1}^{(n-1)}\right) \\ p_{o,0}^{(n)}\left(p_{o,4}^{(n-1)} + p_{o,1}^{(n)}\right) \\ p_{o,4}^{(n)} \end{bmatrix}^T \tag{2.31}$$

$$\Omega_{1,o}(n) = \begin{bmatrix} \left\{\prod_{i=2}^{n} p_{o,0}^{(i)}\right\}\left(p_{o,2}^{(2)} - h_2^{(1)}\right) \\ \left\{\prod_{i=3}^{n} p_{o,0}^{(i)}\right\}\left(p_{o,5}^{(2)} + p_{o,2}^{(3)}\right) \\ \left\{\prod_{i=4}^{n} p_{o,0}^{(i)}\right\}\left(p_{o,5}^{(3)} + p_{o,2}^{(4)}\right) \\ \vdots \\ \left\{\prod_{i=n-1}^{n} p_{o,0}^{(i)}\right\}\left(p_{o,5}^{(n-2)} + p_{o,2}^{(n-1)}\right) \\ p_{o,0}^{(n)}\left(p_{o,5}^{(n-1)} + p_{o,2}^{(n)}\right) \\ p_{o,5}^{(4)} \end{bmatrix}^T \tag{2.32}$$

$$\Omega_{0,0}(n) = \begin{bmatrix} \left\{\prod_{i=2}^{n} p_{o,0}^{(i)}\right\} p_{o,3}^{(2)} \\ \left\{\prod_{i=3}^{n} p_{o,0}^{(i)}\right\}\left(p_{o,6}^{(2)} + p_{o,3}^{(3)}\right) \\ \left\{\prod_{i=4}^{n} p_{o,0}^{(i)}\right\}\left(p_{o,6}^{(3)} + p_{o,3}^{(4)}\right) \\ \vdots \\ \left\{\prod_{i=n-1}^{n} p_{o,0}^{(i)}\right\}\left(p_{o,6}^{(n-2)} + p_{o,3}^{(n-1)}\right) \\ p_{o,0}^{(n)}\left(p_{o,6}^{(n-1)} + p_{o,3}^{(n)}\right) \\ p_{o,6}^{(4)} \end{bmatrix}^T \tag{2.33}$$

Similarly, starting from Eq. 2.10 one can easily obtain similar structure for even

Kautz functions in a recursive form as,

$$\begin{bmatrix} \Psi_2(k+3) \\ \Psi_4(k+3) \\ \Psi_6(k+3) \\ \Psi_8(k+3) \\ \vdots \\ \Psi_{2n}(k+3) \end{bmatrix} = \Omega_{2,e} \begin{bmatrix} \Psi_2(k+2) \\ \Psi_4(k+2) \\ \Psi_6(k+2) \\ \Psi_8(k+2) \\ \vdots \\ \Psi_{2n}(k+2) \end{bmatrix} + \Omega_{1,e} \begin{bmatrix} \Psi_2(k+1) \\ \Psi_4(k+1) \\ \Psi_6(k+1) \\ \Psi_8(k+1) \\ \vdots \\ \Psi_{2n}(k+1) \end{bmatrix} + \Omega_{0,e} \begin{bmatrix} \Psi_2(k) \\ \Psi_4(k) \\ \Psi_6(k) \\ \Psi_8(k) \\ \vdots \\ \Psi_{2n}(k) \end{bmatrix} \tag{2.34}$$

where the n^{th} rows of the matrices $\Omega_{2,e}$, $\Omega_{1,e}$and $\Omega_{0,e}$ are

$$\Omega_{2,e}(n) = \begin{bmatrix} \left\{\prod_{i=2}^{n} p_{e,0}^{(i)}\right\}\left(p_{e,1}^{(2)} - h_1^{(1)}\right) \\ \left\{\prod_{i=3}^{n} p_{e,0}^{(i)}\right\}\left(p_{e,4}^{(2)} + p_{e,1}^{(3)}\right) \\ \left\{\prod_{i=4}^{n} p_{e,0}^{(i)}\right\}\left(p_{e,4}^{(3)} + p_{e,1}^{(4)}\right) \\ \vdots \\ \left\{\prod_{i=n-1}^{n} p_{e,0}^{(i)}\right\}\left(p_{e,4}^{(n-2)} + p_{e,1}^{(n-1)}\right) \\ p_{e,0}^{(n)}\left(p_{e,4}^{(n-1)} + p_{e,1}^{(n)}\right) \\ p_{e,4}^{(n)} \end{bmatrix}^T \tag{2.35}$$

$$\Omega_{1,e}(n) = \begin{bmatrix} \left\{\prod_{i=2}^{n} p_{e,0}^{(i)}\right\}\left(p_{e,2}^{(2)} - h_2^{(1)}\right) \\ \left\{\prod_{i=3}^{n} p_{e,0}^{(i)}\right\}\left(p_{e,5}^{(2)} + p_{e,2}^{(3)}\right) \\ \left\{\prod_{i=4}^{n} p_{e,0}^{(i)}\right\}\left(p_{e,5}^{(3)} + p_{e,2}^{(4)}\right) \\ \vdots \\ \left\{\prod_{i=n-1}^{n} p_{e,0}^{(i)}\right\}\left(p_{e,5}^{(n-2)} + p_{e,2}^{(n-1)}\right) \\ p_{e,0}^{(n)}\left(p_{e,5}^{(n-1)} + p_{e,2}^{(n)}\right) \\ p_{e,5}^{(4)} \end{bmatrix}^T \tag{2.36}$$

and

$$\Omega_{0,e}(n) = \begin{bmatrix} \left\{\prod_{i=2}^{n} p_{e,0}^{(i)}\right\} p_{e,3}^{(2)} \\ \left\{\prod_{i=3}^{n} p_{e,0}^{(i)}\right\} \left(p_{e,6}^{(2)} + p_{e,3}^{(3)}\right) \\ \left\{\prod_{i=4}^{n} p_{e,0}^{(i)}\right\} \left(p_{e,6}^{(3)} + p_{e,3}^{(4)}\right) \\ \vdots \\ \left\{\prod_{i=n-1}^{n} p_{e,0}^{(i)}\right\} \left(p_{e,6}^{(n-2)} + p_{e,3}^{(n-1)}\right) \\ p_{e,0}^{(n)} \left(p_{e,6}^{(n-1)} + p_{e,3}^{(n)}\right) \\ p_{e,6}^{(4)} \end{bmatrix}^{T} \tag{2.37}$$

Now, the Eq. 2.30 and Eq. 2.34 can be represented in a single equation as

$$\mathbf{\Psi}(k+3) = \mathbf{\Omega}_2 \mathbf{\Psi}(k+2) + \mathbf{\Omega}_1 \mathbf{\Psi}(k+1) + \mathbf{\Omega}_0 \mathbf{\Psi}(k) \tag{2.38}$$

where

$$\mathbf{\Psi}(k) = \begin{bmatrix} \Psi_1(k) \\ \Psi_2(k) \\ \Psi_3(k) \\ \vdots \\ \Psi_{2N}(k) \end{bmatrix} \tag{2.39}$$

and

$$\mathbf{\Omega}_p(2i-1, 2j-1) = \begin{cases} \Omega_{p,o}(i,j), & i = j, i \in [1\ N], j \in [1\ N] \\ \Omega_{p,o}(i,j), & i \neq j, i \in [2\ N], j =\in [1\ i] \\ 0, & Otherwise \end{cases}$$

$$\mathbf{\Omega}_p(2i, 2j) = \begin{cases} \Omega_{p,e}(i,j), & i = j, i \in [1\ N], j \in [1\ N] \\ \Omega_{p,e}(i,j), & i \neq j, i \in [2\ N], j \in [1\ i] \\ 0, & Otherwise \end{cases} \tag{2.40}$$

where $p = 0, 1, 2$. The detailed derivation of Eqs.(2.9) - (2.40) have been given in Appendix A.

2.2.2 State space representation

Let $G(z)$ be any function which is strictly proper *i.e.* $G(\infty) = 0$, analytic in $|z| > 1$, and continuous in $|z| \geq 1$. Let $\{\beta_n, \beta_n^*\} < 1$, then the pulse-transfer function can be estimated as a linear combination of OBFs (Aadaleesan et al., 2008; Saha et al., 2004; Wahlberg, 1991a). Using Kautz functions defined in Theorem 2.1

$$G(z) = \sum_{i=1}^{2N} \theta_i \Psi_i(z) \tag{2.41}$$

where input-output relation can be expressed as

$$\hat{y}(k) = \mathcal{Z}^{-1}\{G(z)u(z)\} = \Theta\ \Phi(k) \tag{2.42}$$

where

$$\Phi(k) = \begin{bmatrix} \varphi_1(k) & \varphi_2(k) & \cdots & \varphi_{2N-1}(k) & \varphi_{2N}(k) \end{bmatrix}^T \tag{2.43}$$

$$\Theta = \begin{bmatrix} \theta_1 & \theta_2 & \cdots & \theta_{2N-1} & \theta_{2N} \end{bmatrix} \tag{2.44}$$

The parameter vector Θ can be estimated using a least squares approach. The Kautz model can further be represented as the following state space realization (with shift operator q). By defining the states $x_{2n-1}(k)$ and $x_{2n}(k)$ for $\forall n = 1, 2, ...N$ as

$$x_{2n-1}(k) = \begin{cases} \dfrac{q}{q^2 + h_1^{(1)} q + h_2^{(1)}} u(k), \text{for } n = 1. \\ \dfrac{h_2^{(n-1)} q^2 + h_1^{(n-1)} q + 1}{q^2 + h_1^{(n)} q + h_2^{(n)}} x_{2n-3}(k), \forall n \geq 2 \end{cases} \tag{2.45}$$

$$x_{2n}(k) = x_{2n-1}(k-1) \tag{2.46}$$

where Kautz model parameters are

$$h_1^{(n)} = -(\beta_n + \beta_n^*) \tag{2.47}$$

$$h_2^{(n)} = \beta_n \beta_n^* \tag{2.48}$$

The components of regression vector in Eq. 2.43 are expressed as

$$\varphi_{2n-1}(k) = C_o^{(n)}\left[x_{2n}(k) - a_o^{(n)}x_{2n-1}(k)\right] \tag{2.49}$$

$$\varphi_{2n}(k) = C_e^{(n)}\left[x_{2n}(k) - a_e^{(n)}x_{2n-1}(k)\right] \tag{2.50}$$

where $C_o^{(n)}$ and $C_e^{(n)}$ are defined with the help of Eq. 2.4, Eq. 2.47 and Eq. 2.48 as

$$C_g^{(n)} = \sqrt{\frac{\left\{1 - \left(h_1^{(n)}\right)^2 + 3\left(h_2^{(n)}\right)^2\right\}\left(1 - h_2^{(n)}\right)}{\left(1 + a_g^{(n)2}\right)\left(1 + h_2^{(n)}\right) + 2a_g^{(n)}h_1^{(n)}}} \tag{2.51}$$

The states in Eq. 2.45 and Eq. 2.46 can further be arranged in vector forms as

$$\boldsymbol{x}_o(k) = \begin{bmatrix} x_1(k) & x_3(k) & x_5(k) & \ldots & x_{2N-1}(k) \end{bmatrix}^T \tag{2.52}$$

$$\begin{aligned} \boldsymbol{x}_e(k) &= \begin{bmatrix} x_2(k) & x_4(k) & x_6(k) & \ldots & x_{2N}(k) \end{bmatrix}^T \\ &= \begin{bmatrix} x_1(k-1) & x_3(k-1) & \ldots & x_{2N-1}(k-1) \end{bmatrix}^T \\ &= \boldsymbol{x}_o(k-1) \end{aligned} \tag{2.53}$$

which would yield the complete state space representation as

$$\boldsymbol{x}(k+1) = \boldsymbol{A}\boldsymbol{x}(k) + \boldsymbol{b}u(k) \tag{2.54}$$

where

$$\boldsymbol{x}(k) = \begin{bmatrix} x_1(k) & x_2(k) & \ldots & x_{2N-1}(k) & x_{2N}(k) \end{bmatrix}^T \tag{2.55}$$

and

$$\boldsymbol{A} = \begin{bmatrix} A_1 & A_2 & \cdots & A_N \end{bmatrix} \tag{2.56}$$

$$\boldsymbol{b} = \begin{bmatrix} 1 & 0 & h_2^{(1)} & 0 & \prod_{i=1}^{2} h_2^{(i)} & 0 & \prod_{i=1}^{3} h_2^{(i)} & 0 & \ldots & \prod_{i=1}^{N-1} h_2^{(i)} & 0 \end{bmatrix}^T \tag{2.57}$$

where

$$A_1 = \begin{bmatrix} -h_1^{(1)} & -h_2^{(1)} \\ 1 & 0 \\ h_1^{(1)}\left(1-h_2^{(1)}\right) & 1-\left(h_2^{(1)}\right)^2 \\ 0 & 0 \\ h_1^{(1)}h_2^{(2)}\left(1-h_2^{(1)}\right) & h_2^{(2)}\left\{1-\left(h_2^{(1)}\right)^2\right\} \\ 0 & 0 \\ h_1^{(1)}\prod_{i=2}^{3}h_2^{(i)}\left(1-h_2^{(1)}\right) & \prod_{i=2}^{3}h_2^{(i)}\left\{1-\left(h_2^{(1)}\right)^2\right\} \\ 0 & 0 \\ h_1^{(1)}\prod_{i=2}^{4}h_2^{(i)}\left(1-h_2^{(1)}\right) & \prod_{i=2}^{4}h_2^{(i)}\left\{1-\left(h_2^{(1)}\right)^2\right\} \\ 0 & 0 \\ \vdots & \vdots \\ h_1^{(1)}\prod_{i=2}^{N-1}h_2^{(i)}\left(1-h_2^{(1)}\right) & \prod_{i=2}^{N-1}h_2^{(i)}\left\{1-\left(h_2^{(1)}\right)^2\right\} \\ 0 & 0 \end{bmatrix} \tag{2.58}$$

and

$$A_2 = \begin{bmatrix} 0 & 0 \\ 0 & 0 \\ -h_1^{(2)} & -h_2^{(2)} \\ 1 & 0 \\ h_1^{(2)}\left(1-h_2^{(2)}\right) & 1-\left(h_2^{(2)}\right)^2 \\ 0 & 0 \\ h_1^{(2)}h_2^{(3)}\left(1-h_2^{(2)}\right) & h_2^{(3)}\left\{1-\left(h_2^{(2)}\right)^2\right\} \\ 0 & 0 \\ h_1^{(2)}\prod_{i=3}^{4}h_2^{(i)}\left(1-h_2^{(2)}\right) & \prod_{i=3}^{4}h_2^{(i)}\left\{1-\left(h_2^{(2)}\right)^2\right\} \\ 0 & 0 \\ \vdots & \vdots \\ h_1^{(2)}\prod_{i=3}^{N-1}h_2^{(i)}\left(1-h_2^{(2)}\right) & \prod_{i=3}^{N-1}h_2^{(i)}\left\{1-\left(h_2^{(2)}\right)^2\right\} \\ 0 & 0 \end{bmatrix} \tag{2.59}$$

and

$$A_N = \begin{bmatrix} \mathbf{0}_{10\times 1} & \mathbf{0}_{10\times 1} \\ \vdots & \vdots \\ -h_1^{(N)} & -h_2^{(N)} \\ 1 & 0 \end{bmatrix} \tag{2.60}$$

where $\mathbf{0}_{10\times 1}$ is a 10×1 zero matrix. Detailed derivation of Eqs. (2.54)−(2.60)is given in the Appendix B. The regressors in Eq. 2.49 and Eq. 2.50 can be written as

$$\boldsymbol{\varphi}_o(k) = \overline{\boldsymbol{c}}_o \circ [\boldsymbol{x}_e(k) - \overline{\boldsymbol{a}}_o \circ \boldsymbol{x}_o(k)] \tag{2.61}$$

$$\boldsymbol{\varphi}_e(k) = \overline{\boldsymbol{c}}_e \circ [\boldsymbol{x}_e(k) - \overline{\boldsymbol{a}}_e \circ \boldsymbol{x}_o(k)] \tag{2.62}$$

where $\circ$ denotes the Schur product and

$$\boldsymbol{\varphi}_o(k) = \begin{bmatrix} \varphi_1(k) & \varphi_3(k) & \varphi_5(k) & \dots & \varphi_{2N-1}(k) \end{bmatrix}^T \tag{2.63}$$

$$\boldsymbol{\varphi}_e(k) = \begin{bmatrix} \varphi_2(k) & \varphi_4(k) & \varphi_6(k) & \dots & \varphi_{2N}(k) \end{bmatrix}^T \tag{2.64}$$

$$\overline{\boldsymbol{c}}_o = \begin{bmatrix} C_o^{(1)} & C_o^{(2)} & C_o^{(3)} & \dots & C_o^{(N)} \end{bmatrix}^T \tag{2.65}$$

$$\overline{\boldsymbol{c}}_e = \begin{bmatrix} C_e^{(1)} & C_e^{(2)} & C_e^{(3)} & \dots & C_e^{(N)} \end{bmatrix}^T \tag{2.66}$$

$$\overline{\boldsymbol{a}}_o = \begin{bmatrix} a_o^{(1)} & a_o^{(2)} & a_o^{(3)} & \dots & a_o^{(N)} \end{bmatrix}^T \tag{2.67}$$

Eq. 2.63 and Eq. 2.64 can be rearranged as a single vector as following

$$\boldsymbol{\varphi}(k) = \begin{bmatrix} \varphi_1(k) & \varphi_2(k) & \dots & \varphi_{2N-1}(k) & \varphi_{2N}(k) \end{bmatrix}^T \tag{2.68}$$

For a linear model represented by Eq. 2.41, the model output can be computed as the weighted sum of the Kautz states.

$$\hat{y}(k) = c^T \varphi(k) \tag{2.69}$$

where the elements of vector c are the Kautz filters coefficients, *i.e.,*

$$c = \begin{bmatrix} c_1 & c_2 & c_3 & \dots & c_{2N} \end{bmatrix}^T$$

2.3 Numerical Examples

Two simulation case studies are presented here to show the efficacy of the proposed linear Kautz model. All the simulations were carried out using 64 bit MATLAB® (Version 10) under Windows 7 operating system in a PC with Intel(R) Core™ 2 Duo processor @2.4GHz speed.

2.3.1 Case study I: Linear oscillatory non-minimum phase system

Description of the system

A mechanical system that exhibits oscillatory and non-minimum phase characteristics(Wang, 2004) is considered in this example. The system has 2 pairs of complex conjugate poles, one pair of complex conjugate zeros and one real zero. The system shows inverse response because of the non-minimum phase characteristics.

$$G(z) = \frac{-5.798z^3 + 19.5128z^2 - 21.645z + 7.9547}{z^4 - 3.0228z^3 + 3.8632z^2 - 2.6426z + 0.8084} \tag{2.70}$$

In order to develop the linear Kautz model, the system is excited with random input signal with mean -0.22 and variance 14.738. Total 1000 input and output data of the system are recorded at a sampling period of 0.1 sec. Seventy five percent of the data has been used for training the linear Kautz model whereas rest 25% data are used for model validation purpose. The model parameters are estimated by least square estimation through the *training dataset*.

The Kautz filters poles are randomly selected as $0.5 + j0.5$ (center of the unit circle) and the number of Kautz filters states as 6. The approximation capabilities of linear Kautz model are graphically shown in Fig. 2.1 and Fig. 2.2. It's very clearly evident from Fig. 2.1 that the linear Kautz model is quit able to capture the high oscillatory response of the process by very closely following the process output and the mean square error between the process output and linear Kautz model output is as low as 0.304.

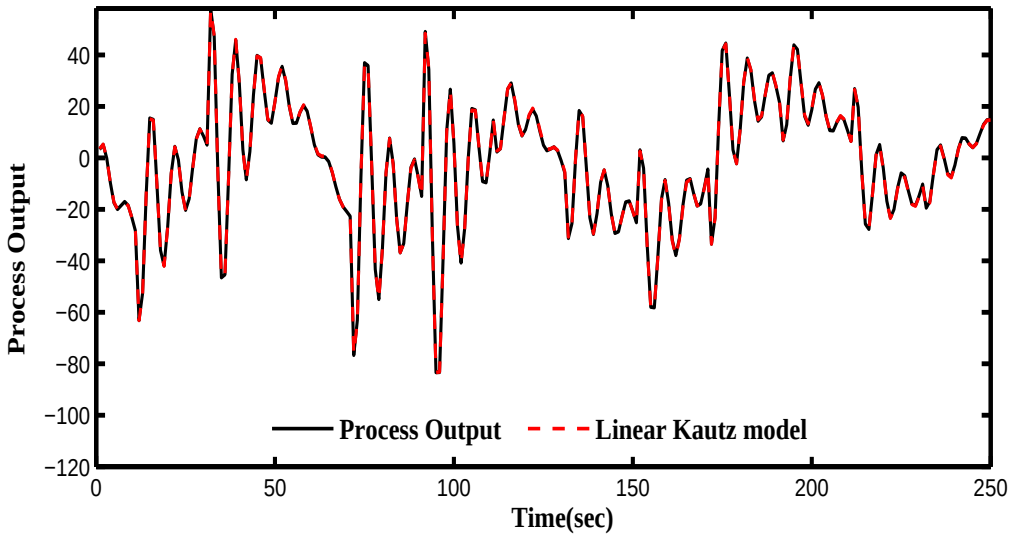

Figure 2.1: Dynamic response of linear Kautz model for highly oscillatory mechanical system

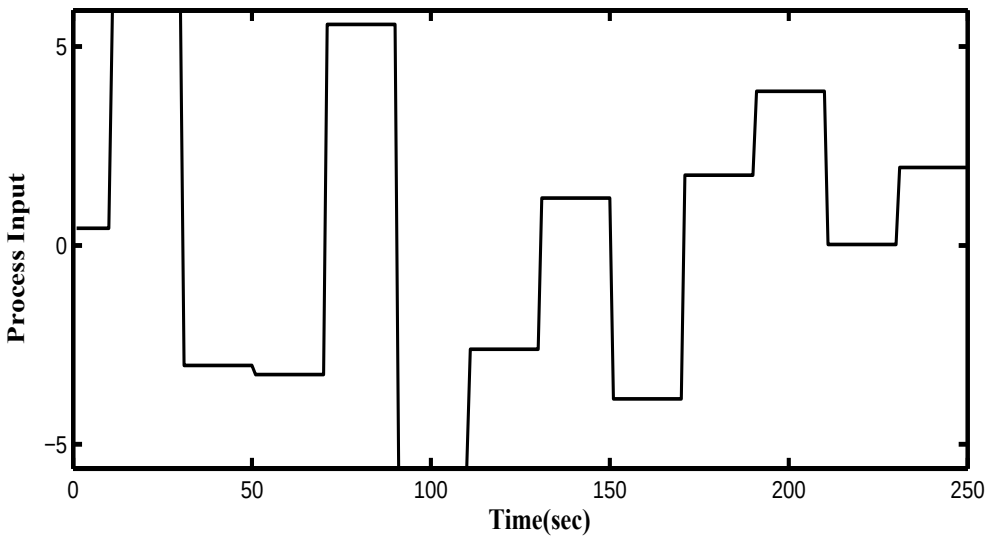

Figure 2.2: Input to linear Kautz model for highly oscillatory mechanical system

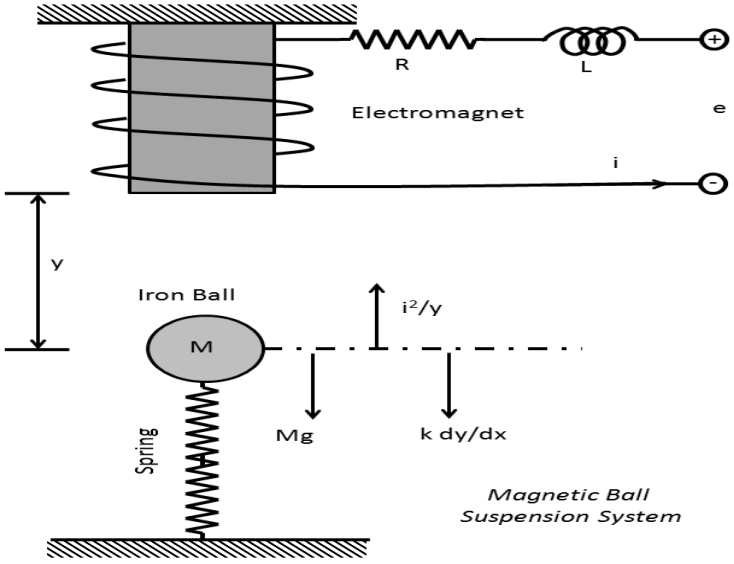

Figure 2.3: The schematic of a magnetic ball suspension system

2.3.2 Case study II: Mildly nonlinear magnetic ball suspension system

The Fig. 2.3 shows a schematic of Magnetic Ball Suspension System (MBSS). It consists of an electromagnet firmly placed at the ceiling of an encloser while an iron ball is suspended over the floor by means of a spring. The electric coil that winds the electromagnet has a resistor (R) and an inductor (L) in series. The voltage, e, supplied to the electromagnet yields a current (i) which in turn generates the magnetic field sufficient to pull the iron ball upwards. The mass of the ball is M and the spring constant is k. The distance between the ball and the electromagnet is denoted by y. The objective of the system is to control the position of the ball (y) by adjusting the input voltage (e).

The differential equations of the system are given by

$$M\frac{d^2y\left(t\right)}{dt^2}+k\frac{dy\left(t\right)}{dt}+Mg = \frac{i^2\left(t\right)}{y\left(t\right)} \tag{2.71}$$

$$L\frac{di\left(t\right)}{dt}+Ri\left(t\right) = e\left(t\right) \tag{2.72}$$

where g is the acceleration due to gravity. For all simulation studies in this paper, the following numerical values have been considered, $g = 9.8$; $M = 1$; $L = 10$; $R = 100$; $k = 1$. The nominal steady state position of the ball is 0.4939, (i.e. $y_s = 0.4939$) away from the

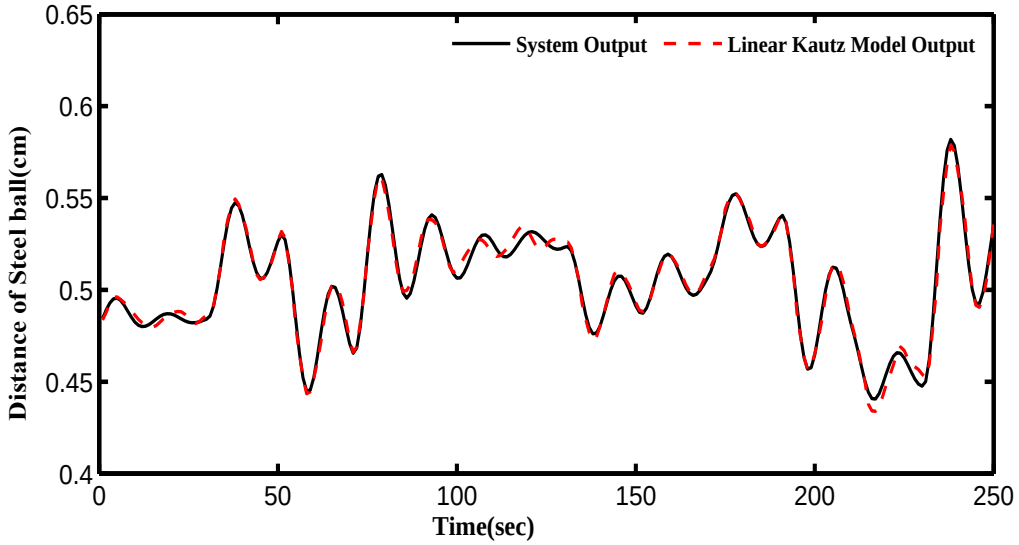

Figure 2.4: Dynamic response of linear Kautz model for MBSS

magnet; and the corresponding nominal value of input voltage and current are $e_s = 220$ and $i_s = 2.2$ respectively. The RHS expression of Eq.2.71 indicates that the process is nonlinear in nature.

The system displays reasonably oscillatory response and also shows mildly nonlinear dynamic characteristics. It is worth to examine how efficiently a linear Kautz model can approximate this system.

In order to develop the linear Kautz model, the system is excited with random input signal with mean 220.8 and variance 31.38. Total 1000 input and output data of the system is recorded at a sampling period of 0.1 sec. Seventy five percent of the data has been used for training the linear Kautz model whereas rest 25% data are used for model validation purpose. The model parameters are estimated by least square estimation through the *training dataset*.

The Kautz filters poles are randomly selected as $0.5 + j0.5$ (center of the unit circle) and the number of Kautz filters states as 6. The approximation capabilities of linear Kautz model are graphically shown in Fig. 2.4 and Fig. 2.5. It's very quit able to capture the high oscillatory response of the process by following the process output very closely and the mean square error between the process output and linear Kaut model output is as low as 0.0034.

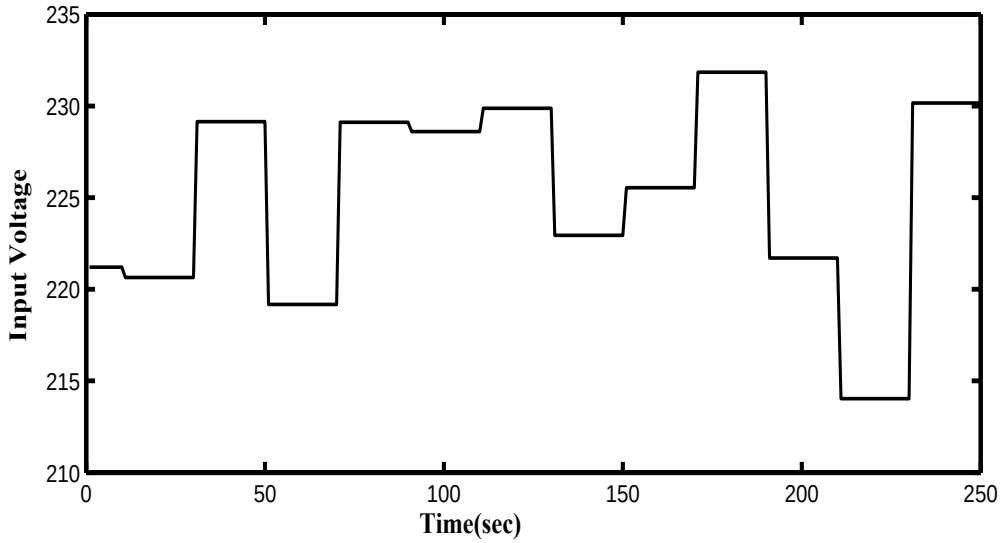

Figure 2.5: Input to linear Kautz model for MBSS

2.4 Summary

Linear Kautz model has been developed to approximate the oscillatory dynamic characteristics of physical systems. Two simulation case studies are presented to prove the efficacy of the developed model. In both the cases the linear Kautz model is quit able to capture the oscillatory dynamics with good accuracy. The Kautz filters poles are selected randomly in order to maintain the simplicity in model development. However, they could also be chosen optimally.

Chapter 3

Explicit Linear Kautz filters model for controlling Resonating Systems

An explicit linear MPC for controlling the resonating systems is formulated by extending the recursive linear Kautz functions model developed in Section 2.2.1 of Chapter 2. In the explicit MPC the incremental control action is calculated as the weighted sum of the recursive Kautz states. The stability of the proposed linear MPC in presence of input constraints is derived by adopting well known Lyapunov theory.

3.1 Theoretical developments

The Theorem related to problem of orthogonalizing a set of discrete time exponential functions can be found in section 2.1 of Chapter 2. The details of the Kautz representation and the recursive linear Kautz functions model are furnished in Section 2.2.1 of Chapter 2.

3.1.1 Control signal trajectory based on Kautz function

A set of discrete orthonormal Kautz functions is proposed in order to describe the future incremental signal for controlling the underdamped dynamics of linear/mildly nonlinear systems. The set of discrete Kautz functions $\Psi_1(k), \Psi_2(k), \cdots, \Psi_{2N}(k)$ are employed to

represent the incremental control signal as follows:

$$\Delta u(k+j) \approx \sum_{i=1}^{2N} c_i(k)\Psi_i(j) \tag{3.1}$$

where $\Delta u(k+j) = u(k+j) - u(k+j-1)$, k is the current time instant of moving horizon window, j is the future time instant, N is the number of pairs of Kautz function states required in estimation procedure and $c_i(k)$ are coefficients to be calculated. In other words, the incremental control input is approximated as weighted sum of Kautz function states. The above expression (Eq.3.1) can be viewed as a set of input signals, $\Delta u(k), \Delta u(k+1), \cdots, \Delta u(k+N_c)$ in conventional MPC design, where N_c is the control horizon.

3.1.2 State Feedback MPC using Recursive Kautz functions

The development of control algorithm is based on the state space model of the open loop process.

$$\begin{aligned} \mathbf{x}(k+1) &= \mathbf{A}\mathbf{x}(k) + \mathbf{B}u(k) \\ \mathbf{y}(k) &= \mathbf{C}\mathbf{x}(k) \end{aligned} \tag{3.2}$$

where, $\mathbf{x}(k) \in \mathbb{R}^n$ is the state vector, $u(k) \in \mathbb{R}$ is the input and $\mathbf{y}(k) \in \mathbb{R}$ is the output of the system respectively. Assume that the plant has n states. The state space form of the plant can be re-arranged in such a way that the incremental change in the input(Δu) is manipulated variable. Creating a new state vector with incremental change in states and the absolute value of the process output as $X(k) = [\Delta\mathbf{x}(k) \quad \mathbf{y}(k)]^T$, an augmented state space model can be obtained as,

$$\begin{aligned} X(k+1) &= \Lambda X(k) + \Upsilon\Delta u(k) \\ Y(k) &= \Xi X(k) \end{aligned} \tag{3.3}$$

where

$$\Lambda = \begin{bmatrix} \mathbf{A} & 0_1 \\ \mathbf{CA} & 1 \end{bmatrix} \tag{3.4}$$

$$\Upsilon = \begin{bmatrix} \mathbf{B} \\ \mathbf{CB} \end{bmatrix} \tag{3.5}$$

$$\Xi = \begin{bmatrix} 0_2 & 1 \end{bmatrix} \tag{3.6}$$

and $\Delta\mathbf{x}(k) = \mathbf{x}(k) - \mathbf{x}(k-1)$. Further $0_1, 0_2$ are zero matrices with dimensions $n \times 1$ and $1 \times n$ respectively.

The incremental control signal is represented as a linear combination of the Kautz function states.

$$\begin{aligned} \Delta u(k+j) &= \sum_{i=1}^{2N} c_i \Psi_i(j) \\ &= \mathbf{\Psi}(j)^T \eta \end{aligned} \tag{3.7}$$

where $\eta^T = \begin{bmatrix} c_1 & c_2 & c_3 & ..... & c_N \end{bmatrix}$.

The future predicted states from the augmented state space model can be estimated as

$$\begin{aligned} X(k+j/k) &= \Lambda^j X(k) + \sum_{i=0}^{j-1} \Lambda^{j-i-1} \Upsilon \Delta u(i) \\ &= \Lambda^j X(k) + \sum_{i=0}^{j-1} \Lambda^{j-i-1} \Upsilon \mathbf{\Psi}(i)^T \eta \end{aligned} \tag{3.8}$$

And the prediction for the plant output is

$$\begin{aligned} \mathbf{y}(k+j/k) &= \Xi \Lambda^j X(k) + \Xi \sum_{i=0}^{j-1} \Lambda^{j-i-1} \Upsilon \mathbf{\Psi}(i)^T \eta \\ &= \Xi \Lambda^j X(k) + \Phi(j)^T \eta \end{aligned} \tag{3.9}$$

where

$$\Phi(j)^T = \Xi \sum_{i=0}^{j-1} \Lambda^{j-i-1} \Upsilon \mathbf{\Psi}(i)^T \tag{3.10}$$

MPC is an optimization based control strategy, and the performance measure is almost always is a quadratic function. In a typical MPC algorithm, the aim is to find a set of control input sequence(s) that will guide the predicted plant output $y(k+j)$ towards the target trajectory $r(k+j)$. Suppose that future set point trajectory $r(k+j), 0 \leq j \leq N_p$ is available. Now, the idea in MPC algorithm is to define a prediction horizon(N_p) and minimize the problem with a finite horizon cost function as

$$\begin{aligned} \underset{\Delta u}{\text{minimize}} \quad & J(k) \\ \text{subject to} \quad & Eq.3.9, \quad j = 1, \ldots, N_p. \\ & \Delta u_{min} \leq \Delta u \leq \Delta u_{max} \end{aligned}$$

where,

$$\begin{aligned} J(k) &= \sum_{j=1}^{N_p} [r(k+j) - Y(k+j/k)]^T Q [r(k+j) - Y(k+j/k)] \\ &\quad + \sum_{j=0}^{N_p-1} \Delta u(k+j)^T R \Delta u(k+j) \end{aligned} \tag{3.11}$$

where $Q = Q^T > 0$ and $R = R^T > 0$. Using Eq.(3.7) in Eq.(3.11)

$$\begin{aligned} J(k) &= \sum_{j=1}^{N_p} [r(k+j) - Y(k+j/k)]^T Q [r(k+j) - Y(k+j/k)] \\ &\quad + \sum_{j=0}^{N_p-1} \eta^T \mathbf{\Psi}(j) R \mathbf{\Psi}(j)^T \eta \end{aligned} \tag{3.12}$$

By substituting Eq. 3.9 in Eq. 3.12 and without imposing any constraints on input(s). The optimal value of the cost function can be found by differentiating the cost function w.r.t η and equating it to zero.

$$\frac{\partial J}{\partial \eta} = 0$$

And the value of η at the optimum is given by

$$\begin{aligned}\eta^* &= \left\{\sum_{j=1}^{N_p}\Phi(j)Q\Phi(j)^T + \sum_{j=0}^{N_p-1}\mathbf{\Psi}(j)R\mathbf{\Psi}^T(j)\right\}^{-1} \\ &\times \sum_{j=1}^{N_p}[\Phi(j)Q\{r(k+m) - \Xi\Lambda^j X(k)\}]\end{aligned} \tag{3.13}$$

Now, the control law is realized as

$$\Delta u^*(k+j) = \mathbf{\Psi}(j)^T\eta^* \tag{3.14}$$

The change in the future control signal can be written by considering future reference trajectories to remain constant within the prediction horizon and replacing j with k in linear state feedback form as following.

$$\Delta u^*(k) = Sr(k) - K_{mpc}X(k) \tag{3.15}$$

where

$$\begin{aligned}S &= \mathbf{\Psi}(0)^T\left\{\sum_{j=1}^{N_p}\Phi(j)Q\Phi(j)^T + \sum_{j=0}^{N_p-1}\mathbf{\Psi}(j)R\mathbf{\Psi}^T(j)\right\}^{-1} \\ &\times \sum_{j=1}^{N_p}(\Phi(j)Q \\ K_{mpc} &= \mathbf{\Psi}(0)^T\left\{\sum_{j=1}^{N_p}\Phi(j)Q\Phi(j)^T + \sum_{j=0}^{N_p-1}\mathbf{\Psi}(j)R\mathbf{\Psi}^T(j)\right\}^{-1} \\ &\times \sum_{j=1}^{N_p}\Phi(j)Q\Xi\Lambda^j\end{aligned} \tag{3.16}$$

3.2 Stability analysis

Without any constraints on input, the asymptotic stability of the unconstrained MPC can be guaranteed by selecting proper values of control input weight matrix(R) or long

prediction horizon(N_p). The stability needs to be proved when the constraints are imposed on control action. Although the system we analyze is a linear system, the constraints introduce nonlinearity which makes the stability analysis more complicated. Assuming $\Delta u_{\min}$ and $\Delta u_{\max}$ are lower and upper limits on input manipulation, the constraint can be denoted as

$$\Delta u_{\min} \leq \Psi\left(j\right)^T \eta_k^* \leq \Delta u_{\max} \tag{3.17}$$

where $j = 0, 1, 2, \cdots, (M-1)$ denotes the set of future time instants at which constraints are intended to be imposed. Similarly assuming the limits on the amplitude of the maipulated variable, i.e. $u_{\min}$ and $u_{\max}$, the constraint on the amplitude can be denoted as

$$u_{\min} \leq \left\{ u_{prev} + \sum_{j=0}^{M-1} \Delta u_j \right\} \leq u_{\max} \tag{3.18}$$

or

$$u_{\min} \leq \left\{ u_{prev} + \sum_{j=0}^{M-1} \Psi\left(j\right)^T \eta_k^* \right\} \leq u_{\max} \tag{3.19}$$

where u_{prev} is the value of previous control signal. These inequality constraints are imposed on calculation of $J(k)$ in Eq. 3.12. The stability of the linear MPC in presence of constraints can be established by defining the Control Lyapunov Function (CLF) as the optimum of the cost function. Consider the CLF for regulatory response, *i.e.* for $r(.) = 0$.

$$\begin{aligned} V(k) &= \sum_{j=1}^{N_p} X(k+j/k)^T Q X(k+j/k) \\ &\quad + \sum_{j=0}^{N_p-1} \Delta u^*(k+j)^T R \Delta u^*(k+j) \end{aligned} \tag{3.20}$$

where

$$X(k+j/k) = \Lambda^j X(k) + \sum_{i=0}^{j-1} \Lambda^{j-i-1} \Upsilon \mathbf{\Psi}(i)^T \eta_k^* \tag{3.21}$$

$$\Delta u(k+j) = \mathbf{\Psi}(j)^T \eta_k^* \tag{3.22}$$

and η_k^* is the optimal coefficient vector for the CLF at sampling instant k.

[Stability of MPC] Suppose for a large value of N_p the following additional (assumptions)

constraints on terminal states and terminal incremental input hold for nominal controller $C_{mpc}(X)$.

1. $X(k+N_p+i)=0, \forall i$
2. $C_{mpc}(X(k+N_p)) \approx 0$.

Then, MPC algorithm using the aforesaid minimization problem will guarantee the asymptotic stability. □ At sampling instant $k+1$,

$$\begin{aligned} V(k+1) &= \sum_{j=1}^{N_p} X(k+j+1/k+1)^T Q X(k+j+1/k+1) \\ &\quad + \sum_{j=0}^{N_p-1} \Delta u^*(k+j+1)^T R \Delta u^*(k+j+1) \end{aligned} \tag{3.23}$$

where

$$X(k+j+1/k) = \Lambda^j X(k+1) + \sum_{i=0}^{j-1} \Lambda^{j-i-1} \Upsilon \Psi(i)^T \eta^*_{k+1} \tag{3.24}$$

$$\Delta u(k+j+1) = \Psi(j)^T \eta^*_{k+1} \tag{3.25}$$

where η^*_{k+1} is the optimal coefficient vector for the CLF at sampling instant $k+1$.

Again, a feasible solution (not optimal) can be obtained at sampling instant $k+1$ by using the one step ahead prediction resulting from the solution(η^*_k) at sampling instant k as

$$X(k+1) = \Lambda X(k) + \Upsilon \Delta u^*(k) \tag{3.26}$$

i.e, the sub-optimal solution at $k+1$ can be obtained by shifting the optimal solution at k one step forward. Therefore, the sub optimal cost is evaluated by applying input sequence $[\Psi(1)^T \eta^*_k, \Psi(2)^T \eta^*_k \cdots, \Psi(k+N_p-1)^T \eta^*_k, C_{mpc}(X(k+N_p))]$.

$$\begin{aligned} V_{sub-opt}(k+1) &= \sum_{j=1}^{N_p} [X(k+j+1/k+1)^T Q X(k+j+1/k+1)] \\ &\quad + \sum_{j=0}^{N_p-1} [\Delta u_{sub-opt}(j)^T R \Delta u_{sub-opt}(j)] \\ &= X(k+2/k+1)^T Q X(k+2/k+1) + X(k+3/k+1)^T Q X(k+3/k+1) + \cdots \end{aligned}$$

$$
\begin{aligned}
& +X(k+N_p+1/k+1)^T QX(k+N_p+1/k+1) + \Delta u^*(k+1)^T R\Delta u^*(k+1) \\
& +\Delta u^*(k+2)^T R\Delta u^*(k+2) + \cdots + C_{mpc}(X(k+N_p))^T RC_{mpc}(X(k+N_p)) \\
= \; & V(k) - X(k+1/k)^T QX(k+1/k) - \Delta u^*(k)^T R\Delta u^*(k) \\
& +X(k+N_p/k+1)^T QX(k+N_p/k+1) \\
& +C_{mpc}(X(k+N_p))^T RC_{mpc}(X(k+N_p)) \qquad (3.27)
\end{aligned}
$$

Using the assumption in Theorem 3.2,

$$V_{sub-opt}(k+1) = V(k) - X(k+1/k)^T QX(k+1/k) - \Delta u^*(k)^T R\Delta u^*(k) \quad (3.28)$$

Let us denote the optimal value of the cost function at sampling instant $k+1$ as $V(k+1)$ and any sub-optimal cost function value $V_{sub-opt}(k+1)$ should follow that $V(k+1) \leq V_{sub-opt}(k+1)$, which means

$$
\begin{aligned}
V(k+1) &\leq V_{sub-opt}(k+1) \\
&\leq V(k) - X(k+1/k)^T QX(k+1/k) - \Delta u^*(k)^T R\Delta u^*(k) \\
V(k+1) - V(k) &\leq -X(k+1/k)^T QX(k+1/k) - \Delta u^*(k)^T R\Delta u^*(k) \qquad (3.29)
\end{aligned}
$$

which implies that the Control Lyapunov Function (CLF) is a decreasing function and hence the asymptotic stability is proved. Detailed derivation of the stability is given in Appendix B.

3.3 Numerical Examples

MPC based on two OBFs, *viz.* Laguerre functions(Wang, 2004) and Kautz functions (present study) have been developed and their performances are compared through simulation studies. Two simulation case studies are presented here to show the efficacy of the proposed Kautz MPC. All the simulations were carried out using 64 bit MATLAB® (Version 10) under Windows 7 operating system in a PC with Intel(R) Core™ 2 Duo processor @2.4GHz speed.

3.3.1 Case study I: Linear oscillatory non-minimum phase system

Description of the system

For the system description the reader is advised to refer Section 2.3.1 of Chapter 2.

Unconstrained control study

With $t_d = 0$, In (Wang, 2004), the incremental control action is represented by using set of Laguerre functions with Laguerre model parameter $a = 0.9$. It needed 10 coefficients of Laguerre functions to obtain a reliable and efficient control action(Fig. 3.1 and Fig. 3.2).

The control algorithm of (Wang, 2004) was redeveloped with lesser number of Laguerre functions such as $N = 7$ and $N = 4$. The prediction horizon and control horizon of the MPC are 100 and 1 respectively. It is observed that the efficiency of the control action decreases with decreasing number of Laguerre coefficients. The response of the process becomes more oscillatory under such inefficient control action and with unacceptable overshoots. The settling time of the process becomes longer too. Controlled output under Laguerre-MPC with $N = 4$ shows 25% overshoot and settles after 160s whereas the controlled output under Laguerre-MPC with $N = 7$ settles within 100s albeit without much overshoot. The ISE values of their control performance are 9.3468 and 7.4467 respectively. On the other hand, Laguerre-MPC with $N = 10$ and Kautz-MPC show a settling time of about 25s while their controlled responses do not show any overshoot. Moreover the manipulated input of Kautz-MPC demonstrates shorter oscillations than its Laguerre counterpart. Further, the Kautz function based MPC is able to serve the purpose only with 4 Kautz states. It is observed from Fig.3.1 and Fig.3.2 that the Kautz function based MPC, with considerable less number parameters, is able to produce control performance similar to the one showed by the Laguerre-MPC with $N = 10$. The robustness of the controller is increased with a controller with less number of parameters as degrees of freedom is fewer. The ISE values of controlled responses by Kautz-MPC and Laguerre-MPC with $N = 10$ are 7.2318 and 7.3185 respectively.

With input time delay $t_d = 4$ and by keeping the all MPC tuning parameters unchanged the performance of the proposed control algorithm is shown in Fig. 3.3 and Fig. 3.4. The

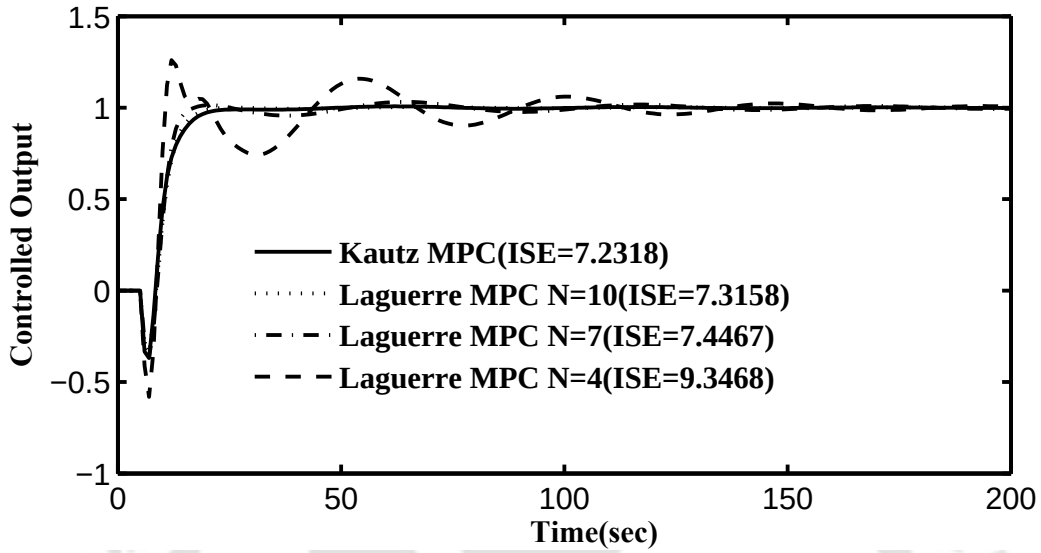

Figure 3.1: Performance of unconstrained MPC in Case Study I: Controlled output

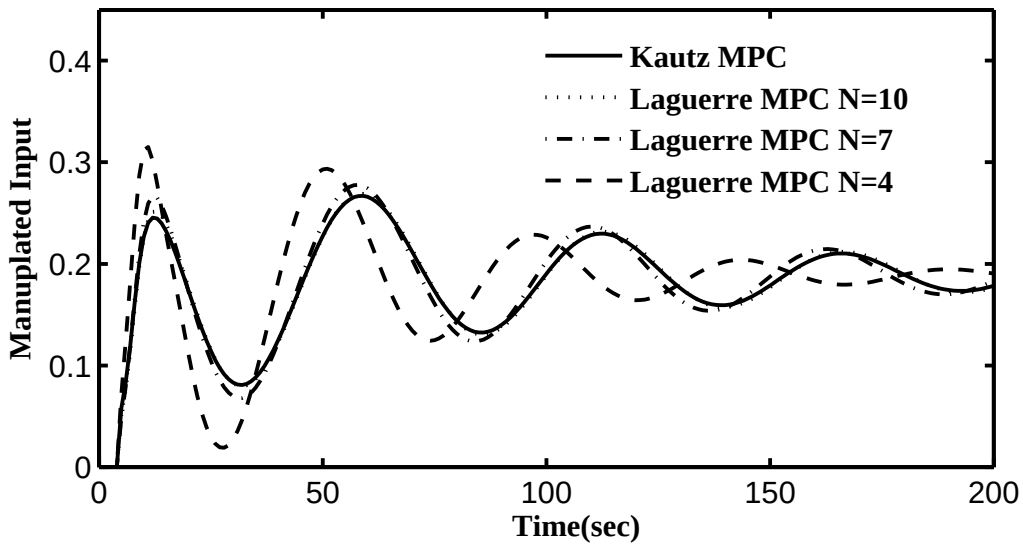

Figure 3.2: Performance of unconstrained MPC in Case Study I: Manipulated input

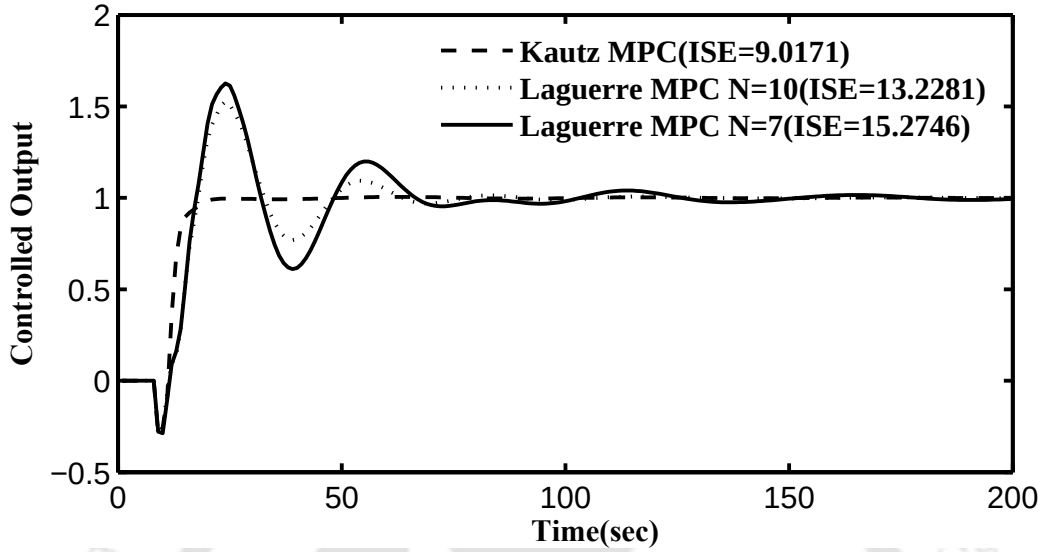

Figure 3.3: Performance of unconstrained MPC in Case Study I with $t_d = 4$: Controlled Output

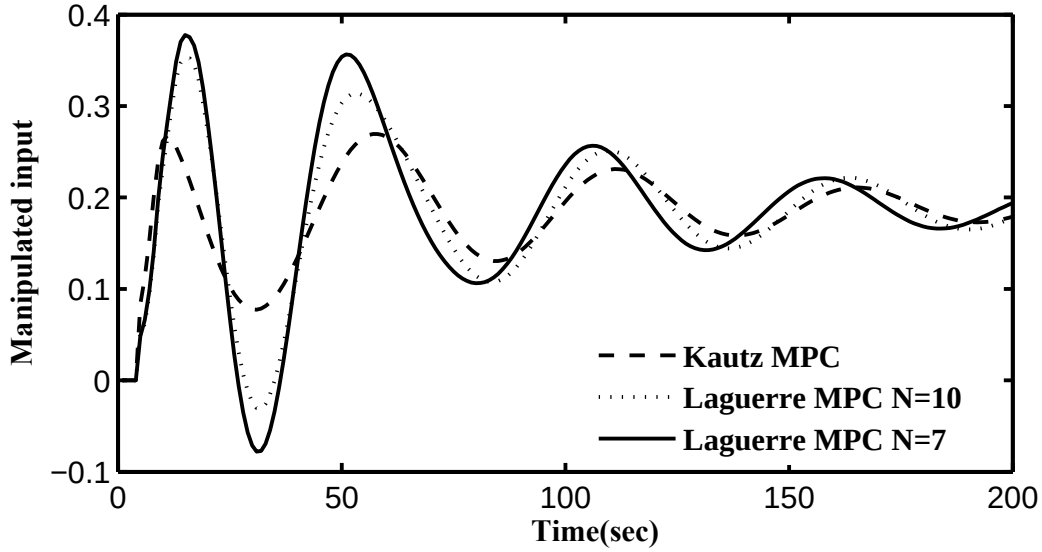

Figure 3.4: Performance of unconstrained MPC in Case Study I with $t_d = 4$: Manipulated input

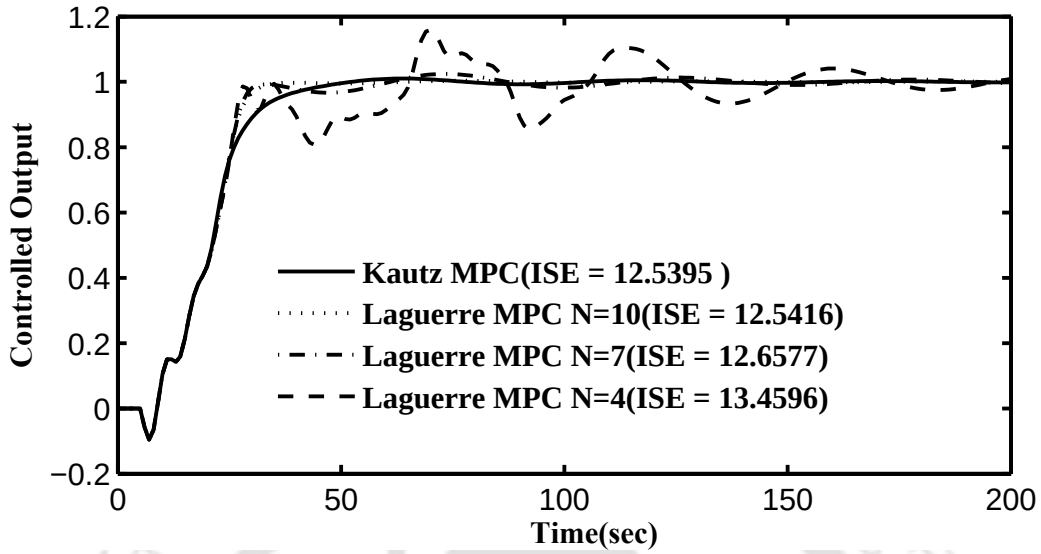

Figure 3.5: Performance of constrained MPC in Case Study I: Controlled output in presence of input constraints

closed loop response of Kautz filters based MPC is as good as that of $t_d = 0$ except the corresponding delay in the output response. Whereas, Laguarre filters based MPC shows significant distraction in the resulting control input signal and the close loop response is poor. The ISE value of controlled response in presence of time delay by Kautz-MPC and Laguerre-MPC with $N = 10$ are 9.0171 and 13.2281 respectively.

Constrained control study

When constraints are imposed on the incremental control signal in the range of $-0.01 \leq \Delta u \leq 0.01$, the Laguerre-MPC still needed 10 coefficients to offer efficient and reliable control action with Laguerre model parameter $a = 0.9$(Fig. 3.5, Fig. 3.6 and Fig. 3.7).

The prediction horizon and control horizon of the MPC are 100 and 1 respectively. The incremental control action using the Laguerre-MPC with lesser number of Laguerre functions such as $N = 7$ and $N = 4$ show oscillatory behavior. As the number of parameters in representing the future incremental control effort decreases a longer settling time is resulted. Controlled output under Laguerre-MPC with $N = 4$ produces 20% oscillations around the reference value and does not settle even after 200s while the controlled output under Laguerre-MPC with $N = 7$ settles within 180s albeit without much oscillations. The

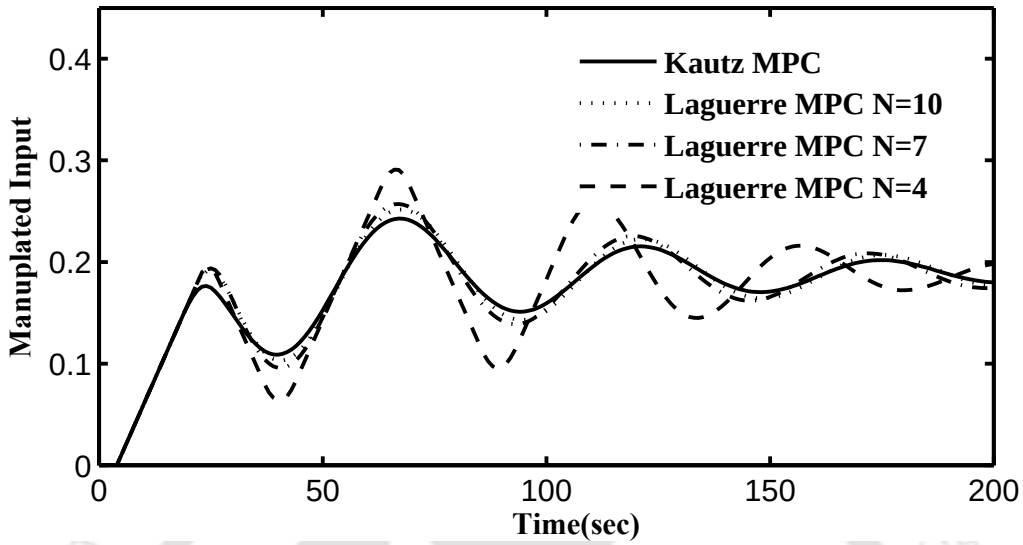

Figure 3.6: Performance of constrained MPC in Case Study I: Manipulated input in presence of input constraints

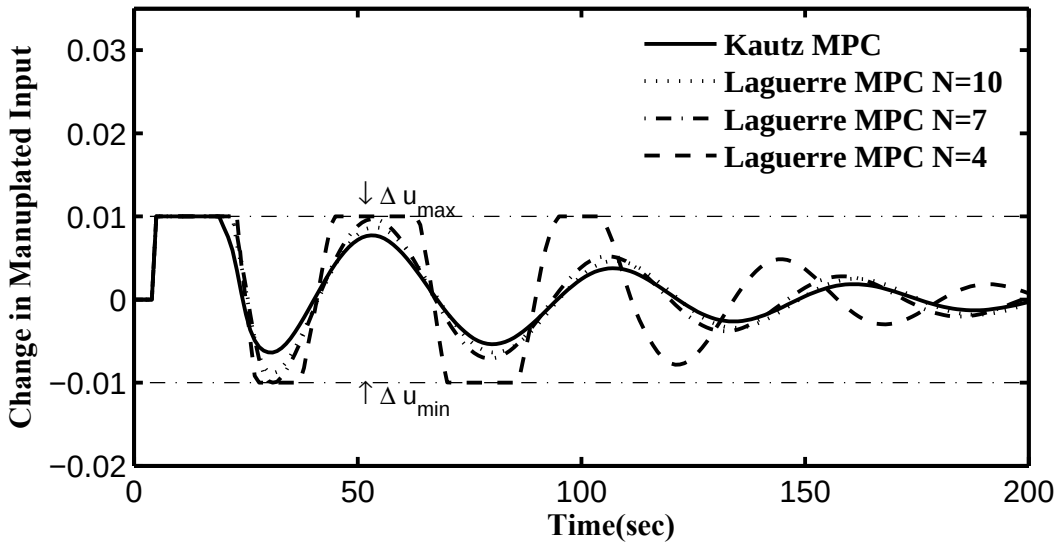

Figure 3.7: Performance of constrained MPC in Case Study I: Change in manipulated input in presence of input constraints

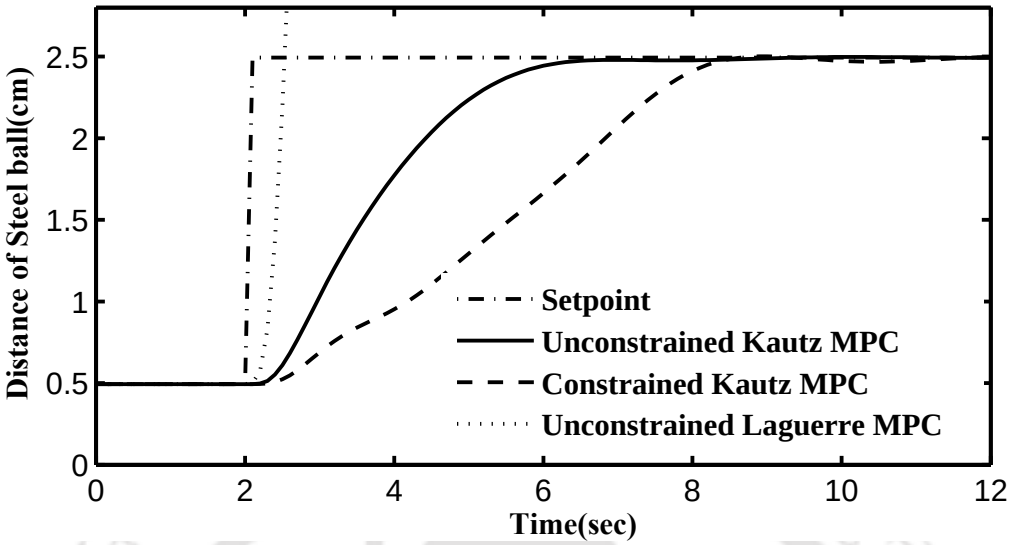

Figure 3.8: Performance of MPC in Case Study II: Controlled output

ISE values of their control performance are 13.4596 and 12.6577 respectively. On the other hand, the Kautz-MPC with 4 parameters is found to be better than Laguerre-MPC with $N = 10$ in terms of number of parameters used in optimization procedure. The setting time in both the cases is 50s. The ISE values of controlled responses by Kautz-MPC and Laguerre-MPC with $N = 10$ are 12.5395 and 12.5416 respectively.

3.3.2 Case study II: Mildly nonlinear magnetic ball suspension system

For the system description, schematic of Magnetic Ball Suspension System and mathematical modelling equations the reader is advised to refer Section 2.3.2 of Chapter 2. It is worth to examine how efficiently a linear Kautz MPC can control this process.

Linearization of the system

The system is linearized around the steady state operating point. The nonlinearity is due to the quadratic term $\frac{i^2(t)}{y(t)}$ in the Eq. 2.71. Applying truncated Taylor's series expansion in the nonlinear term, one obtains

$$\frac{i^2(t)}{y(t)} = \frac{i_s^2}{y_s} + \frac{2i_s}{y_s}(i(t) - i_s) - \frac{i_s}{y_s^2}(y(t) - y_s) \tag{3.30}$$

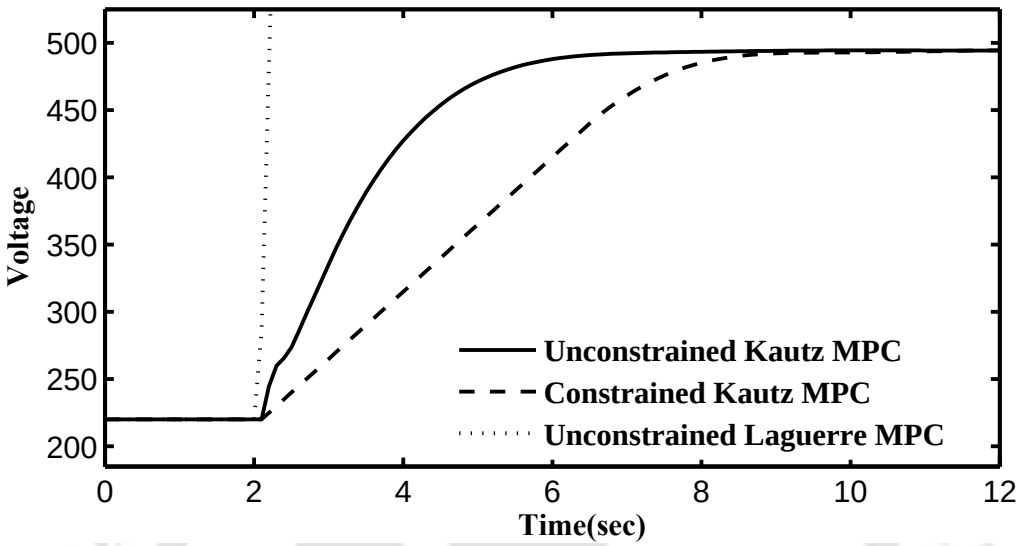

Figure 3.9: Performance of MPC in Case Study II: Manipulated input

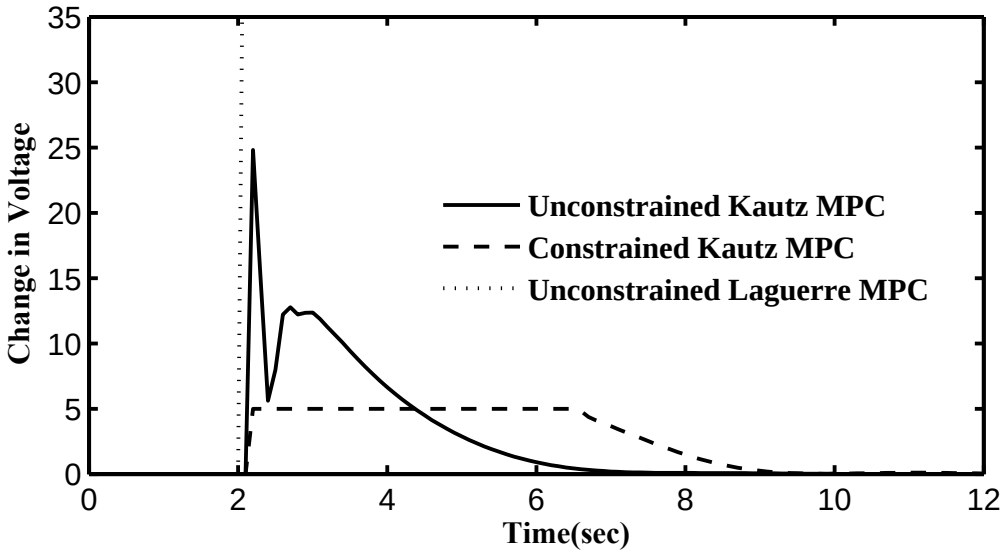

Figure 3.10: Performance of MPC in Case Study II: Change in manipulated input

Considering the deviation variables as $\bar{i}(t) = i(t) - i_s$ and $\bar{y}(t) = y(t) - y_s$. From Eq. 2.71, Eq. 2.72 and Eq. 3.30 the system can be represented in state space from as

$$\begin{aligned} \frac{dX(t)}{dt} &= AX(t) + Bu(t) \\ y(t) &= CX(t) \end{aligned} \tag{3.31}$$

where $X(t) = \begin{bmatrix} y(t) & \frac{dy(t)}{dt} & i(t) \end{bmatrix}^T$. The continuous time state space model can be represented in discrete time domain as

$$\begin{aligned} X(k+1) &= G(T_s)X(k) + H(T_s)u(k) \\ y(k) &= CX(k) \end{aligned} \tag{3.32}$$

where T_s is the sampling time, $G(T_s) = e^{AT_s}$ and $H(T_s) = (\int_0^{T_s} e^{A\lambda} d\lambda)B$. In the present study $T_s = 0.5$sec. The linearized system has one pair of complex conjugate poles and one real pole. The poles are located at $-0.4665 + 0.6236i$, $-0.4665 - 0.6236i$ and 0.0067.

Unconstrained Control study

With $t_d = 0$, the weight matrices for Kautz MPC are taken as $Q = I$ and $R = 0$. The prediction horizon and control horizon are selected as 100 and 1 respectively. From Fig. 3.8, it is inferred that the Kautz MPC with $N = 4$ is able to offer smooth and efficient control action in controlling the MBSS. The overshoots and undershoots are completely eliminated and the process variable is reaching the reference signal within 6s. The ISE value of controlled response by Kautz MPC is 46.1236. The manipulated input (voltage) and the incremental input are shown in Figs.3.9 and 3.10 respectively. A sharp rise in incremental input is observed in the initial 1 s before it subsides to zero. On the other hand, the Laguere MPC(Wang, 2004) with $N = 15$ has completely failed to control this mildly nonlinear underdamped dynamic system (Reddy and Saha, 2017a). Both the manipulated input and controlled output shoots up upon a step change in the reference signal. The rise is so sharp that no statistical analysis is possible.

With input time delay $t_d = 3$ and by keeping the all MPC tuning parameters unchanged the performance of the proposed control algorithm is shown in Fig. 3.11, Fig. 3.12 and Fig. 3.13. Although minute oscillations in both controlled output and manipulated input

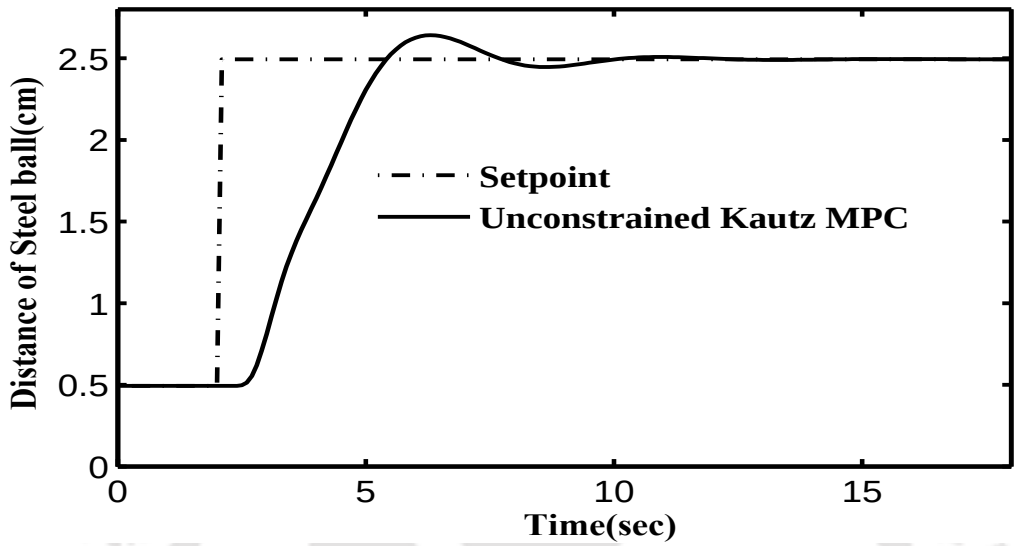

Figure 3.11: Performance of MPC in Case Study II with $t_d = 3$: Controlled output

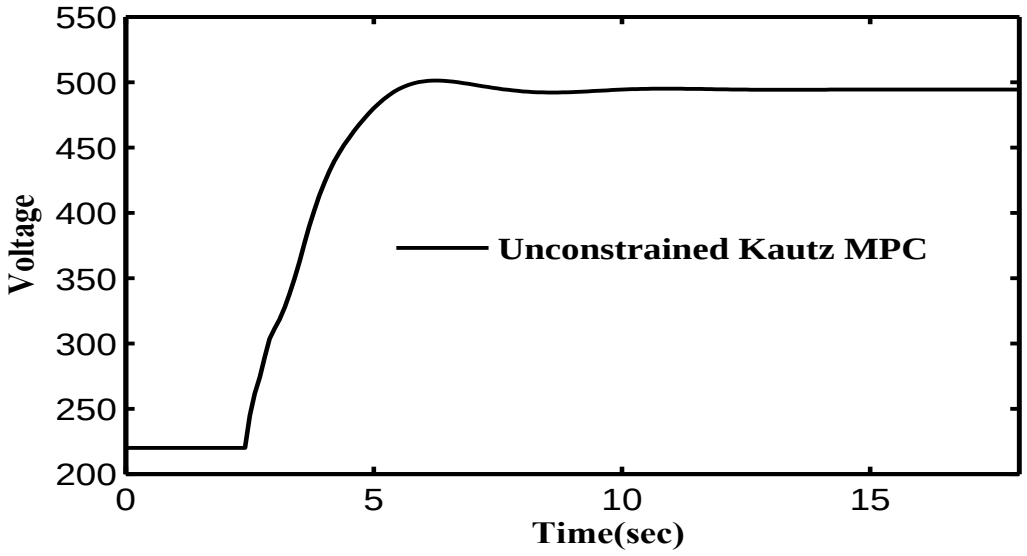

Figure 3.12: Performance of MPC in Case Study II with $t_d = 3$: Manipulated input

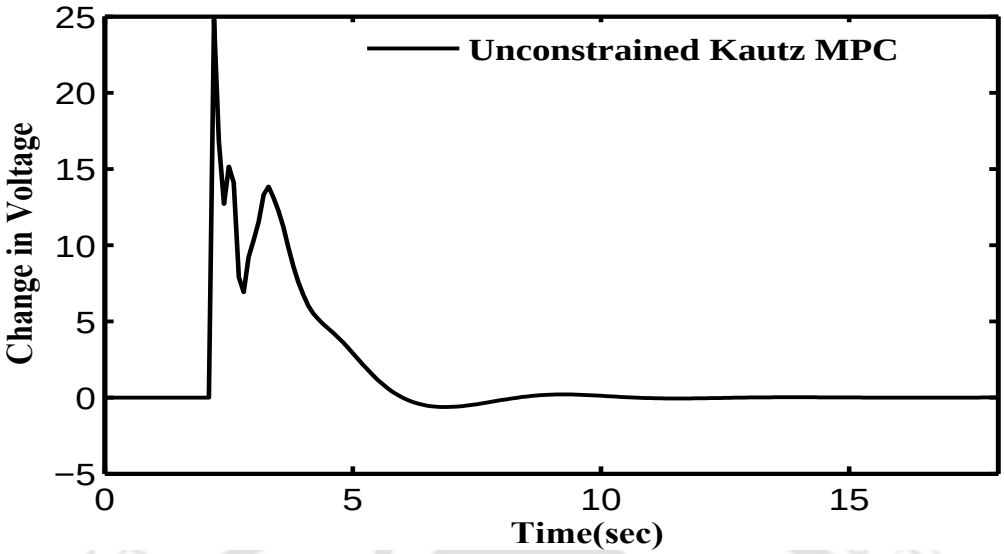

Figure 3.13: Performance of MPC in Case Study II with $t_d = 3$: Change in manipulated input

are resulted, the Kautz filters based MPC is well able to negate the effect of delay time and able to keep the system response closely to the set value. The ISE value of controlled response in presence of time delay by Kautz-MPC is 54.5142.

Constrained control study

The sharp nature of incremental manipulated input, as observed in Fig. 3.8, substantiates the need for imposing constraints on the incremental control signal ($0 \leq \Delta u \leq 5$) for Kautz MPC. The weight matrices are $Q = I$ and $R = 10$, while the prediction and control horizons (100 and 1 respectively) are left unchanged. The control action as well as the manipulated input are relatively sluggish in this case for obvious reasons, however, the Kautz MPC offers oscillation-free closed loop control even in presence of constraints and the settling time is slightly higher (9s). The ISE value of controlled response is 97.9188.

3.4 Summary

In this work, a novel MPC is developed where Kautz functions are employed for computing future incremental control signal of linear/mildly nonlinear dynamics of resonating

system(s). The performance of Kautz MPC technique has been compared with that of Laguerre MPC technique(Wang, 2004) through two case studies. In the first case study, the system is linear and resonating. The performances of Kautz MPC and Laguerre MPC are comparable in this case, however, Laguerre MPC needs more number of control parameters than Kautz MPC. In the second case study, the system is mildly nonlinear and resonating. The proposed Kautz functions based MPC is able to provide smooth and efficient control performance while the Laguerre functions based MPC has completely failed. Laguerre model deals with only real poles, whereas Kautz model deals with complex poles. Hence, Kautz model always has a clear advantage over Laguerre model in identifying/controlling an oscillatory system. Even with some limitations Laguerre function based MPC is capable of controlling a strictly linear system such as the one given in the first case study, albeit with higher number of Laguerre coefficients. The same system could be controlled by Kautz MPC with significantly less number of coefficients. It is important to note that even a mild nonlinearity cannot be handled by Laguerre MPC as shown in the case study II. This observation strongly substantiates the efficacy and applicability of Kautz functions over Laguerre functions in modelling/controlling real life processes with oscillating nature. The stability of the Kautz functions based MPC is proved when input constraints are imposed in the control action.

Chapter 4

Nonlinear Kautz Model - A Wiener type approach

The linear state space Kautz model developed in Section 2.2.2 of Chapter 2 is extended to formulate a newer kind of Wiener model, called *Kautz-Wiener model*. In the developed Kautz-Wiener model the linear dynamic part is represented by the Kautz functions model, the static nonlinear mapping described by means of wavelet network and LS-SVM.

Nonlinear function approximation using wavelet decomposition (Zhang, 1997) is gaining increasing interest in signal processing, nonlinear modeling (Zhang, 1997) and system identification (Aadaleesan et al., 2008). Any nonlinear function, $f \in \mathrm{L}^2(\mathbb{R}^n)$, can be approximated using translated and dilated versions of basis function (Zhang and Benveniste, 1992), called mother wavelet. (Zhang and Benveniste, 1992) established a connection between the single hidden layer neural network and wavelet decomposition to find the best set of translated and dilated parameters in order to approximate nonlinear functions. The superiority of wavelet decomposition in representing nonlinear mapping of Wiener model is demonstrated by (Aadaleesan et al., 2008).

Support Vector Machine (henceforth termed as SVM) is also very popular in classification and nonlinear function estimation problems. The very first version of SVMs are introduced by (Vapnik, 1998) and are based on solving quadratic optimization problem. In LSSVM, the quadratic optimization problem is solved in a high dimensional dual space as a set of linear equations (Suykens and Vandewalle, 1999). Both SVMs as well as the LSSVMs are explored in the field of system identification as reported elsewhere (Goethals

et al., 2005; Qing-chao Wang, 2011; Totterman and Toivonen, 2009). It is further desired to compare the performance of Kautz-Wiener model with another orthonormal function based Wiener model, *viz.,* Laguerre - Wiener model. A comparative study between these two orthonormal function based Wiener models would evaluate the efficacy of the Kautz modelling.

4.1 Theoretical development

The state space representation of Laguerre model is discussed elsewhere Saha (1998). However it is worthy presenting the same in the following subsection for the sake of completeness.

4.1.1 Laguerre representation

Laguerre filters establish a compromise between FIR and IIR filters (Masnadi-Shirazi and Aleshams, 2003). With the proper choice of the Laguerre pole any system can be approximated with good degree of accuracy. When the Laguerre pole takes the value of zero, it reduces to FIR filter. Laguerre -based model is thereby considered as constrained IIR, since all the poles of Laguerre filter models are equal. A brief recall of Laguerre functions based model is necessary for further derivation. Detailed information is available elsewhere (Aadaleesan et al., 2008; Saha et al., 2004). Any N^{th} order SISO process which is strictly proper *i.e.* $G(\infty) = 0$, analytic in $|z| > 1$ and continuous in $|z| \geq 1$) can be represented using Laguerre filters as:

$$G(z) = \sum_{i=1}^{N} c_i L_i(z) \tag{4.1}$$

where $c = \begin{bmatrix} c_1 & c_2 & c_3 & \cdots & c_N \end{bmatrix}^T$ vector contains the Laguerre filters. The input-output relation can be expressed using inverse $\mathcal{Z}-$transform as

$$\hat{y}(k) = \mathcal{Z}^{-1}\left[G(z)u(z)\right] = \mathcal{Z}^{-1}\left[\left\{\sum_{i=1}^{N} c_i L_i(z)\right\} u(z)\right] \tag{4.2}$$

The Laguerre filters can be expressed as

$$L_i(z) = \sqrt{(1-a_l^2)\,T}\frac{(1-a_l z)^{i-1}}{(z-a_l)^i} \tag{4.3}$$

where T is the sampling period and a_l is a filter parameter to be designed within the range $-1 < a_l < 1$. In order to ensure faster convergence, a_l is typically chosen such that $\frac{-\ln(a_l)}{T}$ is close to the dominant time constant of the process. Defining a state vector

$$L(k) = \begin{bmatrix} l_1(k) & l_2(k) & l_3(k) & \cdots & l_N(k) \end{bmatrix}^T \tag{4.4}$$

a discrete time state space representation of Laguerre model can be expressed as (Saha et al., 2004)

$$L(k+1) = \boldsymbol{A}_l L(k) + \boldsymbol{b}_l u(k) \tag{4.5}$$

where

$$\boldsymbol{A}_l = \begin{bmatrix} a_l & 0 & 0 & \cdots & 0 \\ (1-a_l^2) & a_l & 0 & \cdots & 0 \\ -a_l(1-a_l^2) & (1-a_l^2) & a_l & \cdots & 0 \\ \cdots & \cdots & \cdots & \cdots & \cdots \end{bmatrix} \tag{4.6}$$

The last row $A_{l,last}$ of the matrix $\boldsymbol{A}_l$ is

$$A_{l,last} = \begin{bmatrix} (-1)^N a_l^{N-2}(1-a_l^2) \\ (-1)^{N-1} a_l^{N-3}(1-a_l^2) \\ \vdots \\ a_l \end{bmatrix}^T \tag{4.7}$$

and

$$\boldsymbol{b}_l = \begin{bmatrix} \sqrt{(1-a_l^2)T} \\ -a_l\sqrt{(1-a_l^2)T} \\ \vdots \\ (-a_l)^{N-1}\sqrt{(1-a_l^2)T} \end{bmatrix} \tag{4.8}$$

For linear system identification, the process can be modeled as linear combination of Laguerre filters as

$$\hat{y}(k) = c^T L(k) \tag{4.9}$$

For more details on Laguerre functions refer to (Saha et al., 2004) and (Wahlberg, 1991b).

4.2 Nonlinear mapping

In order to use the OBFs in nonlinear system identification, the linear OBF models in Section 2.2.2 of Chapter 2 and Eq. 4.9 can be extended for nonlinear function approximation as shown by (Saha et al., 2004) and the resulting OBF-Wiener model takes the form of

$$\hat{y}(k) = f(\boldsymbol{\varphi}(k)) \tag{4.10}$$

where $f(\bullet) : \mathbb{R}^N \longrightarrow \mathbb{R}$ is a static nonlinear state to output mapping. Two types of nonlinear mappings have been adopted in this work *viz.* wavelet network and LS-SVM. The following subsections present brief descriptions of the said mappings.

4.2.1 Mapping with wavelet network

In wavelet transformation, a signal or a function is decomposed into its different frequency components such that each component has resolution matched to its scale. A basis function, called *wavelet*, satisfying the property of compact supportness is appropriately chosen to decompose the signal/function over dilated and translated wavelets. A "mother" wavelet is a function $\psi(x) \in \mathcal{L}^2(\mathbb{R}^n)$ with a zero average:

$$\int_{-\infty}^{+\infty} \psi(x)dx = 0.$$

It is normalised $\|\psi\| = 1$ and centered in the neighbourhood of $x = 0$. A family of time-frequency windows, "child" wavelets, can be obtained by scaling/dilating ψ by a and translating/shifting it by b: ($a \in \mathbb{R}^+$ and $b \in \mathbb{R}$)

$$\psi^{a,b}(x) = \frac{1}{\sqrt{a}}\psi\left(\frac{x-b}{a}\right).$$

Continuous wavelet transform of any function $f(x) \in \mathcal{L}^2(\mathbb{R}^n)$ is given by

$$\begin{aligned} \mathcal{W}_{a,b}\{f(x)\} &= \int_{\mathbb{R}^n} f(x)\psi^{a,b}(x)dx \\ &= \frac{1}{\sqrt{a}}\int_{-\infty}^{+\infty} f(x)\psi\left(\frac{x-b}{a}\right)dx \end{aligned} \tag{4.11}$$

which is radial and satisfies the admissibility condition, with $\hat{\psi}(\xi)$ being the Fourier transform, as

$$C_\psi = (2\pi)^n \int_0^\infty \frac{|\hat{\psi}(\xi)|^2}{\xi} d\xi < \infty \tag{4.12}$$

and the function $f(x)$ can be reconstructed back by using the inverse wavelet transform,

$$f(x) = \frac{C_\psi^{-1}}{a^{(n+1)}} \int_0^\infty \int_{\mathbb{R}^n} \frac{\mathcal{W}_{a,b}\{f(x)\}}{(\sqrt{a})^n} \psi\left(\frac{x-b}{a}\right) da\, db \tag{4.13}$$

$a \in \mathbb{R}^n$ and $b \in \mathbb{R}^+$ are the dilation and translation parameters, respectively.

In order to implement on computers, the continuous inverse wavelet transforms need to be discretized using orthogonal wavelet bases. By relaxing the orthogonality of the wavelet basis function, *wavelet frames* can be formulated with countable number of wavelet terms (a_i, b_j)

$$\left\{ \frac{1}{(\sqrt{a_i})^n} \psi_{i,j}\left(\frac{x-b_j}{a_i}\right);\ \ i,j \in \mathbb{Z}^+ \right\}$$

where $a_i = a_0^i$, $b_j = j a_0^i b_0$ with the scalar parameters a_0 and b_0 which define the step sizes of dilation and translation discretisation, respectively (typically, $a_0 = 2$ and $b_0 = 1$).

A family of functions $\{\psi_i\}_{i \in I}$ in Hilbert space $\mathcal{H}$ is called a frame if there exist $0 < \Theta \leq \Phi < \infty$ so that, for all f in $\mathcal{H}$,

$$\Theta \leq \frac{\sum_{i \in I} |\langle f,\ \psi_i \rangle|^2}{\|f\|^2} \leq \Phi \tag{4.14}$$

where Θ and Φ are the frame bounds (Daubechies, 1992).

The wavelet frames correspond to a family of dilated and translated wavelets. Reconstruction of $f(x)$ is possible using wavelet frames as

$$f(x) = \sum_i \sum_j \frac{w_i}{(\sqrt{a_i})^n} \psi_{i,j}\left(\frac{x-b_j}{a_i}\right) \tag{4.15}$$

As proposed in (Zhang and Benveniste, 1992), Eq. 4.15 could be viewed as one-hidden-layer neural network. By optimally choosing the parameters w_i, a_i and b_j in Eq.4.15, with $\psi_{i,j}(\cdot)$ as the hidden layer activation function and a linear function in the output layer, the construction becomes similar to that of neural networks, called *wavelet network*. This method is used for static nonlinear function approximation. Although wavelet series is an infinite series, all the wavelet functions will not have data within their support (Zhang and Benveniste, 1992). However, only a finite wavelet functions is enough to map the data of finite domain such as,

$$\Psi = \left\{ \psi_{i,j} : (i,j) \in \bigcup_{q=1}^{Q} I_q \right\} \tag{4.16}$$

where I_q are the index set of wavelet functions, whose supports lie within the given data set. All the OBF states are fed as input to all the wavelet functions. The wavelet coefficients, which are originally the inner product of the states and the wavelet functions, are equivalent to the hidden-to-output layer weight in neural networks. The optimal choice of the parameters could be obtained by training wavelet network using algorithms like backpropagation.

4.2.2 Mapping with LS-SVM

Formulations of SVMs are exercised within the context of convex optimization (Falck et al., 2012). Given any input-output measurements $\{x(k), y(k)\}_{k=1}^{N}$ of the function to be approximated, the nonlinear function can be approximated in the following form by using SVMs

$$\hat{y}(k) = f\{x(k)\} = \boldsymbol{w}^T \boldsymbol{g}\{x(k)\} + b_{bias} + e(k) \tag{4.17}$$

where $\boldsymbol{w}^T \in \mathbb{R}^{nh}$, $\boldsymbol{g}(.) : \mathbb{R}^n \to \mathbb{R}^{nh}$ a mapping to a high dimensional future space, and b_{bias} is bias constant.

The function estimation is achieved by minimizing the estimation error at any sampling instant k is $e(k) = y(k) - \hat{y}(k)$. The estimation error is minimized and the unknowns $\boldsymbol{w}$ and b_{bias} are determined by solving a convex optimization (typically quadratic programming)

problem in the primal space which is formulated as

$$\min_{\boldsymbol{w},b_{bias},e} J_P\left(\boldsymbol{w},b_{bias},e\right)=\frac{1}{2}\boldsymbol{w}^T\boldsymbol{w}+\gamma\frac{1}{2}\sum_{k=1}^{N}\left\{e\left(k\right)\right\}^2 \tag{4.18}$$

$$\text{s.t.}\quad y\left(k\right)=\boldsymbol{w}^T\boldsymbol{g}\left\{x\left(k\right)\right\}+b_{bias}+e\left(k\right),\forall k \tag{4.19}$$

where $\gamma\in\mathbb{R}^+$ is the regularization constant that decides a compromise between the smoothness of the solution and the data fitting.
The Lagrangian for this problem is

$$L(\boldsymbol{w},b_{bias},e;\boldsymbol{\alpha})=\frac{1}{2}\boldsymbol{w}^T\boldsymbol{w}+\gamma\frac{1}{2}\sum_{k=1}^{N}(e(k))^2-\sum_{k=1}^{N}\alpha_k(\boldsymbol{w}^T\boldsymbol{g}(x(k))+b_{bias}+e(k)-y(k))$$

where α_k are Lagrange multipliers.

Lemma 1 *Elimination of the $\boldsymbol{w}$ and e will lead to a solution as a set of linear equations and solution to Eq. 4.18 is a dual of the optimization problem (Goethals et al., 2005).*

$$\begin{bmatrix} 0 & \mathbf{1}_v^T \\ \mathbf{1}_v & \left(\Omega+\frac{I}{\gamma}\right)\end{bmatrix}\begin{bmatrix} b_{bias} \\ \alpha\end{bmatrix}=\begin{bmatrix} 0 \\ \mathbf{y}\end{bmatrix} \tag{4.20}$$

where

$$\Omega_{ij}\equiv K\left\{x\left(i\right),x\left(j\right)\right\}=\mathbf{g}\left\{x\left(i\right)\right\}^T\mathbf{g}\left\{x\left(j\right)\right\}$$
$$\mathbf{y}=\begin{bmatrix} y\left(1\right) & y\left(2\right) & \cdots & y\left(N\right)\end{bmatrix}^T$$
$$\alpha=\begin{bmatrix} \alpha_1 & \alpha_2 & \cdots & \alpha_N\end{bmatrix}^T$$
$$\mathbf{1}_v=\begin{bmatrix} 1 & 1 & \cdots & 1\end{bmatrix}^T$$

To calculate the elements in Eq. 4.20, it is not necessary to define $\boldsymbol{g}(.)$ explicitly and it is enough to calculate the inner product of a positive kernel.

The LS-SVMs model is expressed in dual form as

$$\hat{y}(x_{new}(k)) = \sum_{k=1}^{N} \alpha_k K(x_{new}(k), x(k)) + b_{bias} \tag{4.21}$$

4.3 Development of OBF-Wiener Models

The nonlinear mappings as described in sections 4.2.1 and 4.2.2 are augmented to the linear OBF representation of process in order to develop the OBF-Wiener nonlinear models. The following subsections present the combinatorial Wiener models with different linear OBF network and nonlinear mapping.

4.3.1 Kautz-Wavelet Wiener model

In the Kautz-wavelet Wiener model, the Wavelet Neural Network (henceforth termed as WNN) is mapped by using the data set $(\boldsymbol{\varphi}(k), y(k))$ according to Eq. 4.15. And the resulting Wiener model takes the form as

$$\hat{y}(k) = \sum_{i=1}^{N} W_{a,b}^{i} \sum_{j \in \mathbb{Q}} a_{i,j}^{-n/2} \psi\left(\frac{\boldsymbol{\varphi}_{i,j} - b_{i,j}}{a_{i,j}}\right) + \boldsymbol{c}\boldsymbol{\varphi}(k) + d$$

where $\mathbb{Q}$ is an index set of wavelet functions, whose support lie within the data set and $\theta : \{W_{a,b}^{i}, a_i, b_i\}$ is the set of wavelet network parameters.

The parameters of Kautz filters are generally chosen from the open loop response of the process (Wahlberg, 1991a). (Wahlberg, 1991a), suggested that if the parameters of Kautz filters are chosen in such a way that the normalized resonant frequency of Kautz model is equal to the resonant frequency of the true system, then the resulting approximation would be accurate. Optimum selection of the Kautz parameters is adopted by (da Rosa et al., 2009). In the present work, the Kautz parameters are selected for the open loop response of the process. And the parameters of Wavelet network are estimated by adopting the back propagation algorithm proposed by (Zhang and Benveniste, 1992). The Network parameters are optimally chosen by minimizing the following performance index.

$$J(k, \theta) = \frac{1}{N} \sum_{k=1}^{N} e(k)^2 \leq \epsilon \tag{4.22}$$

Where $e(k) = y(k) - \hat{y}(k, \theta)$ and ϵ is a network performance tolerance, $y(k)$ is the actual process output. In the present study, "Maxican hat function" ((Zhang, 1997))

$$\psi(x) = (n - ||x||^2)e^{\frac{-||x||^2}{2}}, \quad ||x||^2 = x^T x \tag{4.23}$$

is used as mother wavelet, where n is the dimension of the input space of the network. The resulting Wiener model is referred as Kautz-Wavelet model.

4.3.2 Kautz-LSSVM Wiener model

In Kautz-Least Squares Support Vector Machines Wiener model, LS-SVMs forms the static nonlinear mapping. The LS-SVMs mapping can be developed using the data set $(\boldsymbol{\varphi}(k), y(k))$ according to Eq. 4.21.

In the present study, a radial basis function (RBF) is adopted as a kernel function and is given as

$$K(\boldsymbol{\varphi}(i), \boldsymbol{\varphi}(j)) = exp\left(\frac{-\|\boldsymbol{\varphi}(i) - \boldsymbol{\varphi}(j)\|_2^2}{\sigma^2}\right) \tag{4.24}$$

where $\sigma \in \mathbb{R}^+$ is the kernel bandwidth.

The resulting LSSVMs function mapping at any new data point $\boldsymbol{\varphi}_\star$ becomes

$$\hat{y}(\boldsymbol{\varphi}_\star) = \sum_{k=1}^{N} \alpha_k \mathbf{K}(\boldsymbol{\varphi}(k), \boldsymbol{\varphi}_\star) + b_{bias} \tag{4.25}$$

where $\boldsymbol{\alpha}$ and b_{bias} are the solution of linear system of equations in Eq. 4.20. The parameters γ and σ^2 depend on the nature of the data that are problem specific. A cross validation technique as proposed by (Totterman and Toivonen, 2009) is adopted in this work. The LSSVMs parameters (γ and σ^2) are selected based on the performance of the model for an independent testing input data set. Variance Accounted For (henceforth termed as VAF) (Mahmoodi et al., 2009; Wang and Zhang, 2011) criteria is used to compare the performance of the model, which is expressed as,

$$VAF = max\left\{1, \frac{variance\{y - \hat{y}\}}{y}, 0\right\} \times 100 \tag{4.26}$$

where y is the real process output and $\hat{y}$ denotes the model output.

4.3.3 Laguerre-Wavelet Wiener model

In the Laguerre-Wavelet wiener model, the Laguerre states are updated following Eq. 5.11 and the Wavelet Neural Network(WNN) can be mapped by using the data set $(L(k), y(k))$ according to Eq. 4.15. And the resulting Wiener model takes the form as proposed by (Aadaleesan et al., 2008).

$$\hat{y}(k) = f(L(k), \theta) + \boldsymbol{c}L(k) + d \tag{4.27}$$

$$= \sum_{i=1}^{N} W_{s,t}^{i} \sum_{j \in \mathbb{Q}} s_{i,j}^{-n/2} \psi(\frac{L_{i,j} - t_{i,j}}{s_{i,j}}) + \boldsymbol{c}L(k) + d \tag{4.28}$$

Where $\mathbb{Q}$ is an index set of wavelet functions, whose support lie within the data set and $\theta : \{W's, s's, t's\}$ is the set of wavelet network parameters.

4.3.4 Laguerre-LSSVM Wiener model

In the Laguerre-LSSVM Wiener model, the Laguerre states are updated following Eq. 5.11 and the LSSVMs static nonlinear mapping can be obtained by using the data set $(L(k), y(k))$ according to Eq. 4.21. And the resulting Wiener model takes the form as proposed by (Wang and Zhang, 2011).

$$\hat{y}(L_\star) = \sum_{k=1}^{N} \alpha_k \mathbf{K}(L(k), L_\star) + b_{bias} \tag{4.29}$$

4.4 Numerical Examples

The performance of the Kautz-Wiener models has been demonstrated through two simulation case studies *viz.* one single CSTR and two series connected CSTRs. Performance of Kautz filters based nonlinear models has been compared with that of already popular Laguerre filters based nonlinear models. All the simulations were carried out using 64 bit MATLAB® (Version 10) under Windows 7 operating system in a PC with Intel(R) Core™ 2 Duo processor @2.4GHz speed.

In order to develop the Kautz-Wiener models, the nonlinear processes are simulated by solving the nonlinear first principles models numerically and the resulting nonlinear differential equations are solved using ODE45 solver in MATLAB® (version 10) to obtain

the true states of the process.

4.4.1 Case study I: Continuous Stirred Tank Reactor

CSTR is a highly nonlinear and resonating process which is regularly used in chemical process industry. The degree of nonlinearity seldom depends upon several factors such as number of reactants used, order of the reaction, reversibility factor *etc.* However, in this case study we have used fewer complexities. We take a process in which a single reactant undergoes irreversible and exothermic reaction. Coolant is flown around the reactor through a cooling jacket. The mechanistic model of the CSTR is given by the following differential equations(Huang et al., 2000).

$$\frac{dC(t)}{dt} = \frac{q(t)}{V}\{C_0(t) - C(t)\} - k_0 C(t) exp\left\{\frac{-E}{RT(t)}\right\} \tag{4.30}$$

$$\frac{dT(t)}{dt} = \frac{q(t)}{V}\{T_0(t) - T(t)\} - \frac{-\Delta H k_0 C(t)}{\rho c_p} exp\left\{\frac{-E}{RT(t)}\right\} + \frac{\rho_c C_{pc}}{\rho C_p V} q_c(t)\left[1 - exp\left\{\frac{-hA}{q_c(t)\rho c_p}\right\}\right]\{T_0(t) - T(t)\} \tag{4.31}$$

The state variables *viz.* concentration and temperature of the contents inside the reactor are potential output variables to be controlled, whereas the flow rate of the coolant

Table 4.1: Case Study I − Nominal operating conditions of CSTR

Process variable/parameter	Nominal value	
Flow rate of coolant(q_c)	103	L min^{-1}
Measured Product Concentration(C)	0.0989	mol L^{-1}
Reactor temperature(T)	438.7763	K
Process flow rate(q)	100	L min^{-1}
Feed concentration(C_{A0})	1	mol L^{-1}
Feed temperature(T_0)	350	K
Inlet coolant temperature(T_{c0})	350	K
CSTR volume(V)	100	L
Heat transfer term (hA)	7×10^5	cal min^{-1} K^{-1}
Reaction rate constant(k_0)	7.2×10^{10}	min^{-1}
Activation energy term(E/R)	1×10^4	K
Heat of reaction($-\Delta H$)	-2×10^5	cal mol^{-1}
Liquid density(ρ, ρ_c)	1×10^3	g L^{-1}
Specific heats(C_p, C_{pc})	1	cal g^{-1} K^{-1}

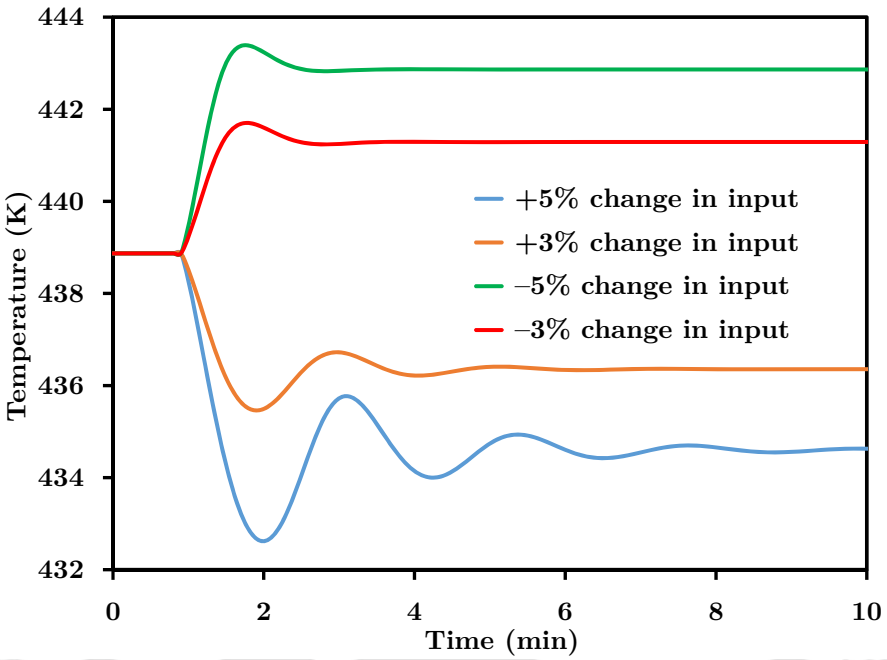

Figure 4.1: Case Study I – Open-loop response of CSTR by administering step change in flow rate of coolant

can be manipulated in order to achieve the desired control action. Nominal values(Prakash and Srinivasan, 2009) of these outputs and input as well as other parameters of the Eqs. (4.30) and (4.31) are given in Table 4.1. The flow rate of coolant has been subjected to a step change of ±3% to ±5%. The results, *i.e.* the open-loop response of the CSTR process, are shown in Fig.4.1. It demonstrates resonating dynamics around the nominal operating point. The process variable, in particular, shows severe resonating characteristics when the input changes are administered in the range of 103 − 108.6 L min^{-1}.

In order to generate the data for OBF-Wiener model, the process is excited at 2 min interval with random perturbation in flow rate of the coolant around the nominal value with mean 103.4637 L min^{-1} and variance 12.9318 L min^{-1}. Both input (flow rate of the coolant) and the output (*i.e.* reactor temperature) are recorded at a sampling period $T_s = 0.1$ min. Seventy five percent of the data has been used for training the OBF-Wiener model whereas rest 25% data are used for model validation purpose. The model parameters are estimated by training the model through the *training dataset*.

An initial estimate of the OBF filter poles can be obtained from the time domain specifications of the process. The value of the pole is thereby fine-tuned in order to get

faster convergence of the model. In case of Kautz-Wiener model, the filters parameters are chosen as $N = 2$ and $\beta = 0.85 + 0.3i$, whereas in Laguerre-Wiener model filter parameters are chosen as $N = 8$ and $p = 0.9$.

Wavelet network parameters are obtained by using the back propagation algorithm(Zhang and Benveniste, 1992; Aadaleesan et al., 2008). The performance index criteria for both the OBF-Wiener models has been set at $\epsilon < 0.001$ (Aadaleesan et al., 2008). Training of the Kautz-Wavelet model was converged within 46.15 s, whereas Laguerre-Wavelet model took 135.73 s to converge.

The LSSVMs mapping parameters γ and σ^2 are tuned by trial and error method. Different combinations of γ and σ^2 are tested and their performance indices namely *Variance Accounted For* (henceforth termed as VAF(Mahmoodi et al., 2009)) are recorded. The Kautz-LSSVM model with various combinations of γ and σ^2 are tabulated in Table 4.2. The best combination of the parameters are found to be $\gamma = 10$ and $\sigma^2 = 4$. The procedure is repeated for Laguerre-LSSVMs model (Wang and Zhang, 2011) and results are shown in Table 4.3. The best combination is found at $\gamma = 4$ and $\sigma^2 = 50$. Training of the Kautz-LSSVM model was complete in 10.5 s, whereas Laguerre-LSSVM model took 15 s to get trained.

Figs. 4.2 and 4.3 demonstrate the comparative performances of all the OBF-Wiener models discussed as above. The *validation dataset* has been used for this purpose. All the OBF-Wiener models were subjected to similar input perturbation (within the range of $103 - 109$ L min^{-1}) as recorded in the validation dataset and their outputs are compared with the process output recorded in the same validation dataset. The outputs of Laguerre-Wiener models shows higher deviations from the actual process output than that of the Kautz-Wiener models. The Kautz models are able to estimate the nonlinear resonating dynamics very accurately and follow the process output very closely (Reddy and Saha, 2017b). The performance is so close that a major portion of the Kautz model output gets hidden behind the actual process output as evident in the Fig. 4.2. The ISE values of plant/model mismatch of all four identification techniques are reported in Table 4.4. The ISE values of Kautz-Wiener models are considerably less than that of Laguerre-Wiener models. Kautz filters are by nature characterized by complex conjugate poles. As a result the Wiener models based on Kautz filters lead to more parsimonious representation in modelling the nonlinear resonating processes and the model training takes very less time.

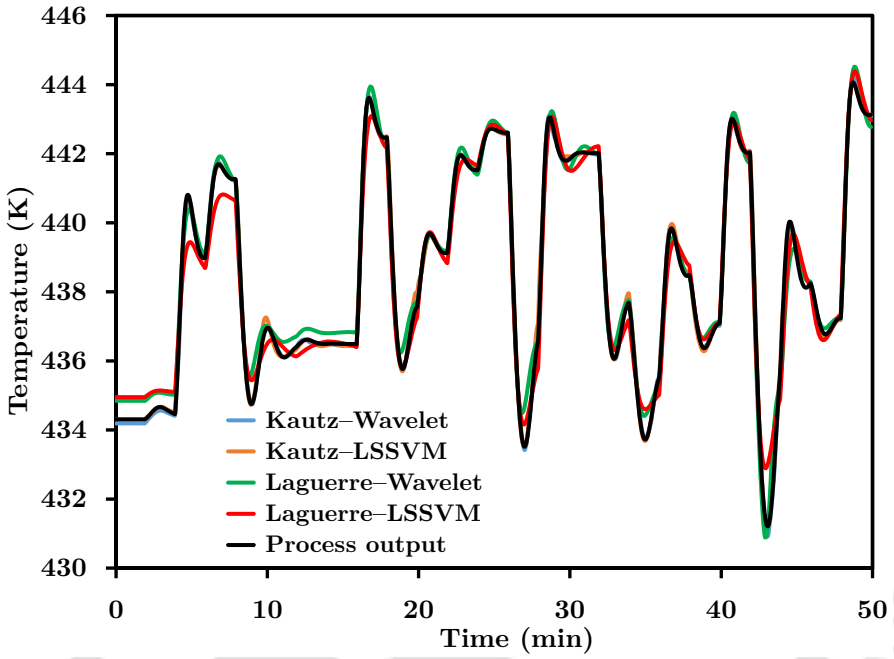

Figure 4.2: Case Study I – Comparison of performance of all OBF-Wiener models in system identification of CSTR process

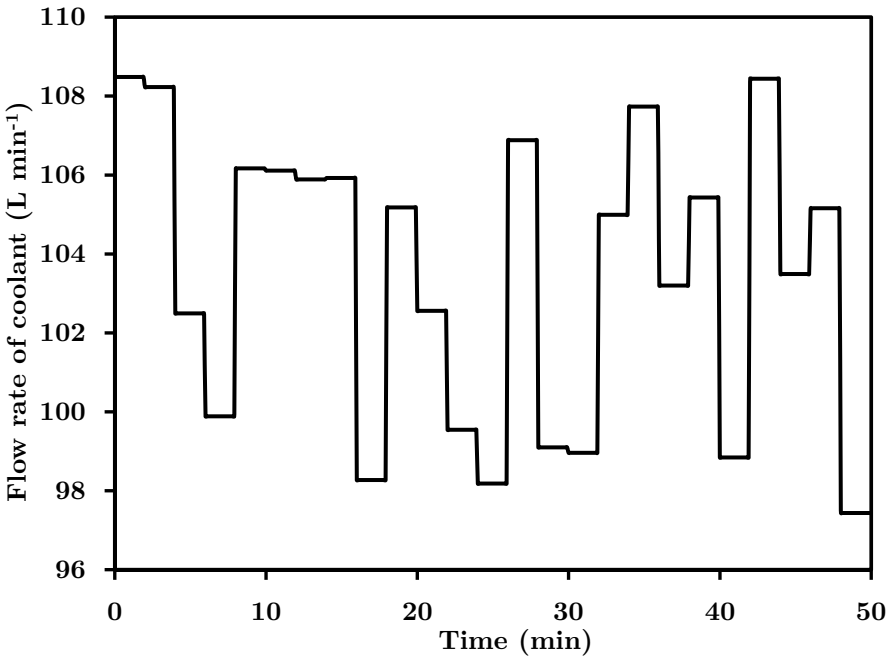

Figure 4.3: Case Study I – Random excitation in process input for generating process output data for model validation (as shown in Fig.4.2)

On the other hand, the Laguerre filters are typically fit for the systems having real poles. As a result, the convergence of Laguerre-Wiener models is very time consuming and their performance suffers too.

Table 4.2: Case Study I – List of VAFs for various combinations of γ and σ^2 while training Kautz-LSSVMs model

$\gamma(\sigma^2 = 4)$	VAF	$\sigma^2(\gamma = 10)$	VAF
1	99.6076	1	99.5256
10	99.6955	4	99.6950
50	99.682	50	99.4791
100	99.679	100	99.2147
200	99.678	200	99.0095

Among the two types of nonlinear mapping, wavelet offers better accuracy than LSSVM. It is to be noted that the wavelet type Wiener models are trained by using network based optimization technique (derivative free) in order to choose the optimum values of wavelet network parameters of the Wiener models, whereas LSSVM parameters (α 's & b_{bias}) are estimated by solving a set of linear algebraic equations; and the hidden layer activation function parameters (radial basis function in this case) are chosen by *trial and error* method for better (not necessarily the optimum) performance of the model. Hence both the OBF-wavelet Wiener models outperform the OBF-LSSVM Wiener models.

4.4.2 Case study II: Series connected Continuous Stirred Tank Reactor

In this case study, the process consists of two constant volume reactors which are connected in series. An exothermic and irreversible chemical reaction takes place in both the reac-

Table 4.3: Case Study I – List of VAFs for various combinations of γ and σ^2 while training Laguerre-LSSVMs model

$\gamma(\sigma^2 = 50)$	VAF	$\sigma^2(\gamma = 4)$	VAF
1	94.1051	10	91.2501
2	96.4008	20	93.8500
3	97.0012	30	96.3684
4	98.3887	40	97.0016
5	96.8056	50	98.3887
6	95.1357	60	97.4625

Table 4.4: Case Study I − ISE values of plant/model mismatch of all four OBF-Wiener models

Identification Technique	ISE value of plant/model mismatch
Kautz-WNN	6.4108
Kautz-LSSVMs	11.1215
Laguerre-WNN	75.136
Laguerre -LSSVMs	105.1231

tors. The output stream from the first reactor is fed into the second as an input stream. Both reactors share the same coolant flow and its temperature is assumed to be constant throughout the cooling jacket. The mechanistic model of the process is described by the following four nonlinear differential equations (Henson and Seborg, 1990). The process constants and nominal operating values are given in Table 4.5. As evident in the above nonlinear differential equations (Eq. (4.32) to Eq. (4.35)) the effluent concentration from the second reactor C_{A2} is affected by flow rate of coolant indirectly through C_{A1}, T_1 and T_2 (3^{rd} order dependence), that too through exponential terms.

$$\frac{dC_{A1}}{dt} = \frac{q}{V_1}(C_{Af} - C_{A1}) - k_0 C_{A1} e^{-\frac{E}{RT_1}} \tag{4.32}$$

$$\begin{aligned}\frac{dT_1}{dt} &= \frac{q}{V_1}(T_f - T_1) + \frac{(-\Delta H)k_0 C_{A1}}{\rho C_p} e^{-\frac{E}{RT_1}} \\ &\quad + \frac{\rho_c C_{pc}}{\rho C_p V_1} q_c \left\{1 - e^{-\frac{hA_1}{q_c \rho_c C_{pc}}}\right\} (T_{cf} - T_1)\end{aligned} \tag{4.33}$$

$$\frac{dC_{A2}}{dt} = \frac{q}{V_2}(C_{A1} - C_{A2}) - k_0 C_{A2} e^{-\frac{E}{RT_2}} \tag{4.34}$$

$$\begin{aligned}\frac{dT_2}{dt} &= \frac{q}{V_2}(T_1 - T_2) + \frac{(-\Delta H)k_0 C_{A2}}{\rho C_p} e^{-\frac{E}{RT_2}} \\ &\quad + \frac{\rho_c C_{pc}}{\rho C_p V_2} q_c \left\{1 - e^{-\frac{hA_2}{q_c \rho_c C_{pc}}}\right\} \\ &\quad \times \left\{T_1 - T_2 + e^{-\frac{hA_1}{q_c \rho_c C_{pc}}} (T_{cf} - T_1)\right\}\end{aligned} \tag{4.35}$$

This can be regarded as highly nonlinear relationship between C_{A2} and coolant flowrate (q_c). The flow rate of coolant has been subjected to a step change of ±3% to ±5%. The results, *i.e.* the open-loop response of the CSTR process (C_{A2}), are shown in Fig.4.4. One can easily notice that the process is highly resonating and exhibits high static nonlinearity. The process variable, in particular, shows severe resonating characteristics when the input changes are administered in the range of +5%.

Table 4.5: Case Study II − Nominal operating conditions of series connected CSTR

Process variable/parameter	Nominal value	
Concentration of product in reactor 1 (C_{A1})	0.1099	mol L^{-1}
Concentration of product in reactor 2 (C_{A2})	0.0076	mol L^{-1}
Temperature inside reactor 1 (T_1)	436.549	K
Temperature inside reactor 2 (T_1)	446.4024	K
Process flow rate(q)	100	L min^{-1}
Flow rate of coolant(q_c)	106	L min^{-1}
Reaction rate constant(k_0)	7.2×10^{10}	min^{-1}
Feed concentration(C_{Af})	1	mol L^{-1}
Activation energy term(E/R)	1×10^4	K
Feed temperature(T_f)	350	K
Heat of reaction ($-\Delta H$)	4.78×10^4	J mol^{-1}
Inlet temperature of coolant (T_{cf})	350	K
Liquid density(ρ, ρ_c)	1000	g L^{-1}
Volume of CSTRs (V_1, V_2)	100	L
Specific heats (C_p, C_{pc})	0.239	J g^{-1} K^{-1}
Heat transfer term (hA_1, hA_2)	1.67×10^5	J min^{-1} K^{-1}

In order to generate the data for OBF-Wiener model, the process is excited at 2 min interval with random perturbation in flow rate of the coolant around the nominal value with mean 106.1 L min^{-1} and variance 6.9318 L min^{-1}. Both input (flow rate of the coolant) and the output (*i.e.* C_{A2}) are recorded at a sampling period $T_s = 0.1$ min. Seventy five percent of the data has been used for training the OBF-Wiener model whereas rest 25% data are used for model validation purpose. The model parameters are estimated by training the model through the *training dataset*.

An initial estimate of the OBF filter poles can be obtained from the time domain specifications of the process. The value of the pole is thereby fine-tuned in order to get faster convergence of the model. In case of Kautz-Wiener model, the filters parameters are chosen as $N = 2$ and $\beta = 0.85 + 0.3i$. On the other hand, no realistic value of filter parameters could yield a reasonable Laguerre-Wiener.

Wavelet network parameters are obtained by using the back propagation algorithm(Zhang and Benveniste, 1992; Aadaleesan et al., 2008). The performance index criteria for both the Kautz-Wiener models has been set at $\epsilon < 0.001$ (Aadaleesan et al., 2008). Training of the Kautz-Wavelet model was converged within 47.61 s.

The LSSVMs mapping parameters γ and σ^2 are tuned by trial and error method.

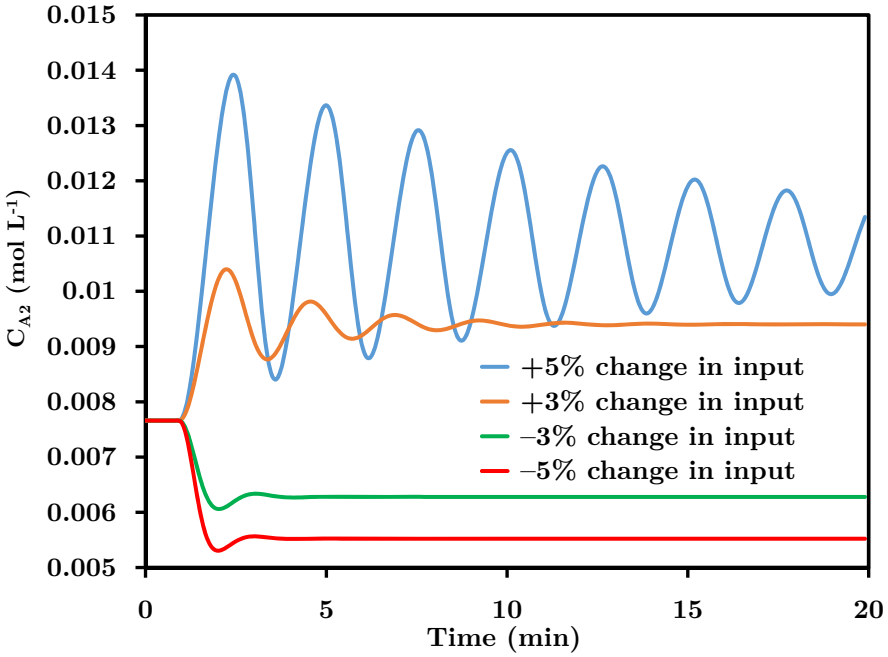

Figure 4.4: Case Study II − Open-loop response of series connected CSTR process by administering step change in flow rate of coolant

Different combinations of γ and σ^2 are tested and their performance indices VAFs are recorded. The Kautz-LSSVM model with various combinations of γ and σ^2 are tabulated in Table 4.6. The best combination of the parameters are found to be $\gamma = 200$ and $\sigma^2 = 4$. Training of the Kautz-LSSVM model was complete in 12.08 s.

Figs. 4.5 and 4.6 demonstrate the comparative performances of two Kautz-Wiener models discussed as above. The *validation dataset* has been used for this purpose. Both the Kautz-Wiener models were subjected to similar input perturbation (within the range of $102 - 109$ L min^{-1}) as recorded in the validation dataset and their outputs are compared with the process output recorded in the same validation dataset. Both the models perform almost equally well because both of them are able to estimate the nonlinear resonating dynamics very accurately and follow the process output very closely, nevertheless, the Kautz-wavelet model is marginally better Reddy and Saha (2017b). The performance is so close that a major portion of the model outputs get hidden behind the actual process output as evident in the Fig. 4.5. The ISE values of plant/model mismatch while modelling with Kautz-WNN and Kautz-LSSVM are 3.3110×10^{-6} and 3.4237×10^{-6}, respectively. The ISE value of Kautz-WNN model is marginally less than that of Kautz-LSSVM model.

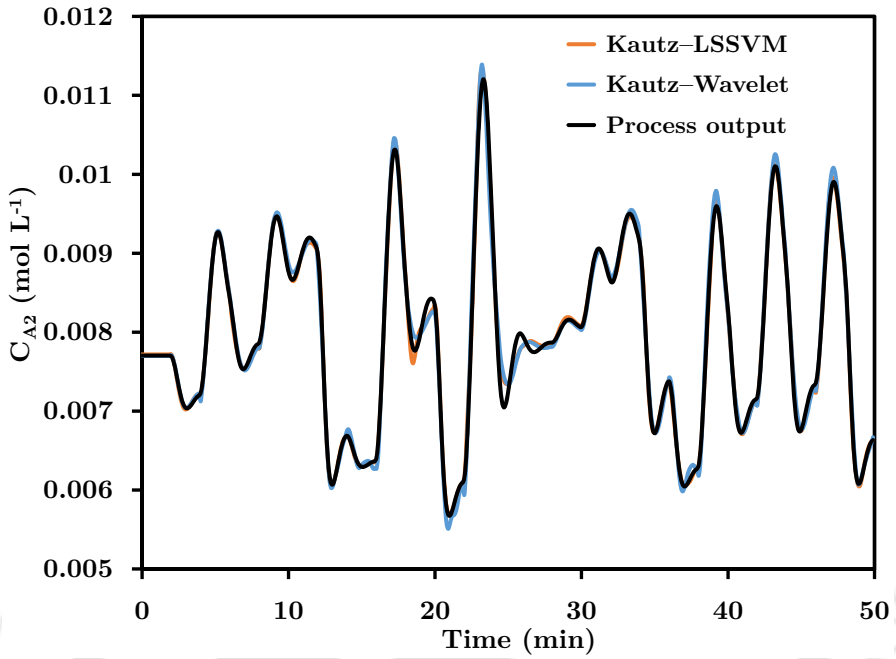

Figure 4.5: Case Study II – Comparison of performance of two Kautz-Wiener models in system identification of series connected CSTR process

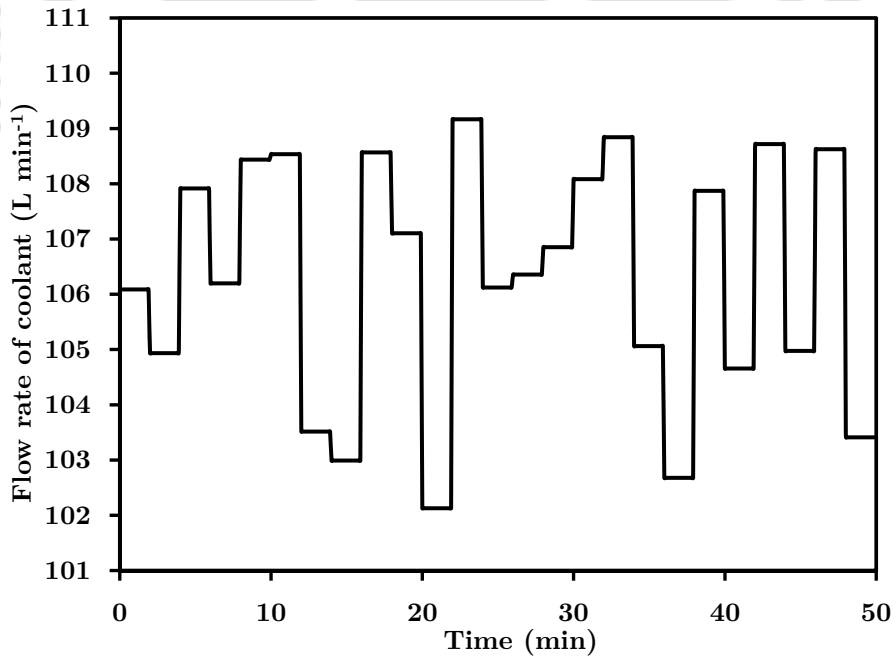

Figure 4.6: Case Study II – Random excitation in process input for generating process output data for model validation (as shown in Fig.4.5)

Table 4.6: Case Study II − List of VAFs for various combinations of γ and σ^2 while training Kautz-LSSVMs model

$\gamma(\sigma^2 = 4)$	VAF	$\sigma^2(\gamma = 10)$	VAF
1	99.120	1	99.2
10	99.4174	4	99.5081
100	99.5010	50	99.36
200	99.5081	100	99.2
250	99.502	250	99.6

In general, Laguerre-Wiener models fail to achieve any presentable results. Laguerre-wavelet model is unable to converge to the given performance index even after several hours of simulation time. Similarly the Laguerre-LSSVMs model is unable to achieve good model performance even with very high number Laguerre states. The efficacy of Kautz model is clearly evident in this case study as the natural characterization of Kautz filters by complex conjugate poles makes a Kautz model efficient in identifying resonating characteristics. Lack of such characterization, especially in acute nonlinear condition, leads to inappropriateness of the Laguerre filters in such situation.

Both static nonlinear mappings work almost equally well for Kautz model. The LSSVM model parameters might perhaps have attained optimilaity even with *trial and error* method in this case study (Reddy and Saha, 2017b).

4.4.3 Summary

A novel OBF-Wiener modelling technique, *viz.* Kautz-Wiener model, is developed for identification of the nonlinear resonating systems. The Kautz filters are derived in more generalized and standard state space form to express the linear dynamic part. Wavelet decomposition and LSSVMs are used to describe the static nonlinear mapping of the Wiener model. In the identification algorithm the Kautz parameters are chosen from open loop response of the process. Two case studies, *viz.* single CSTR and two series-connected CSTRs, have been conducted in order to evaluate the performance of the models. Both case studies substantiate the accuracy of the Kautz-Wiener models in approximating the nonlinear resonating dynamics. The efficacy of Kautz-Wiener modelling is further substantiated by comparing its peformance with that of another OBF-Wiener model, Laguerre-Wiener model. In the case study with single CSTR, the Laguerre-Wiener models are somehow

able to estimate the resonating systems, though the degrees of freedom is higher than that of Kautz-Wiener model; and the Laguerre-Wiener model is non-parsimonious too. On the other hand, the case study with series-connected CSTR clearly demonstrates the superiority of Kautz-Wiener models in dealing higher degree nonlinear resonating systems. Laguerre-Wiener model completely fails in this case. In both the case studies, the Kautz-Wiener modelling technique offers good accuracy in identification of the resonating system with parsimonious model representation, which can further be used in model based control applications.

Chapter 5

Nonlinear Model Based Control of Resonating Systems using Kautz-Wiener models

5.1 Design of model based controllers

Design of linear MPC is quite standard procedure and is available in textbooks (Wang, 2009; Rawlings and Mayne, 2009). The control law is derived by optimizing the performance objective for minimum control effort and/or maximum robustness. In almost all cases the control law is obtained as single equation to be solved (Saha, 1998). Design of NMPC, on the other hand, is rather computationally extensive as one needs to resort to an appropriate optimization algorithm to arrive at the desired control action (Saha et al., 2004). Similarly design of linear IMC is straightforward too and available in the textbooks (Bequette, 2003; Ogunnaike and Ray, 1994), however, NIMC works in a different fashion where the inverse of the model is rather difficult to compute. In this section procedures are given for developing OBF-Wiener based NMPC and NIMC.

5.2 Nonlinear MPC using OBF-Wiener models

The goal of NMPC is to obtain a set (control horizon,N_c) of future control efforts by minimizing a predefined objective function at each and every sampling instant over a finite moving horizon called prediction horizon(N_p). The optimization problem is solved on-line, by comparing the process output which is predicted by the OBF-Wiener model with actual output of the process.

In the proposed OBF-Wiener model based NMPC the N_p steps ahead predicted model output can be obtained as.

$$\begin{aligned} \boldsymbol{x}(k+j+1/k) = \boldsymbol{A}\boldsymbol{x}(k+j/k) + \boldsymbol{b}u(k+j)\cdots \\ \cdots, \forall j = 1, \cdots, N_p - 1 \end{aligned} \tag{5.1}$$

The process output is predicted using state to output mapping as following

$$\hat{y}(k) = \Psi(x(k)) \tag{5.2}$$

In order to account for the plant-model mismatch and unmeasured disturbances the corrected prediction of the model over the prediction horizon(N_p) can be calculated as (Saha et al., 2004).

$$y_c(k+j/k) = \hat{y}(k+j/k) + d(k/k), \forall j = 1, \cdots, N_p - 1 \tag{5.3}$$

$$d(k/k) = y(k) - \hat{y}(k/k-1) \tag{5.4}$$

where $y(k)$ is measured plant output at k^{th} sampling instant and $\hat{y}(k/k-1)$ is the model output at k^{th} sampling instant using input sequence upto time $k-1$.

Now, for a given reference trajectory $y_r(k+i/k)$, $j = 1, \cdots, N_p$, the nonlinear model predictive control design can be formulated by solving the following optimization problem:

$$\begin{aligned} \min_{\substack{\Delta u(k/k),\cdots \\ ,\Delta u(k+N_c-1/k)}} J = & \sum_{j=1}^{N_p} E(k+j/k)^T W_E E(k+j/k) \\ & + \sum_{j=0}^{N_c-1} \Delta u(k+j)^T W_{\Delta u} \Delta u(k+j) \end{aligned} \tag{5.5}$$

Where

$$E(k+j/k) = y_r(k+j/k) - y_c(k+j/k)$$
$$\Delta u(k+j) = u(k+j) - u(k+j-1) \tag{5.6}$$

The resulting nonlinear optimization problem can be solved by using any standard optimization algorithm.

5.3 Nonlinear IMC using OBF-Wiener models

In this section, design strategy of IMC has been extended to its nonlinear version. The NIMC uses OBF-Wiener model as an integral component for generating a control law. The crucial part of this technique is inversion of the nonlinear model. Since model inversion in nonlinear domain is not an easy task optimization technique has been adopted for this job.

Design of IMC requires isolation of non-invertible components of a model (positive zeros and dead time) while model inversion is carried out (Bequette, 2003). This is to avoid creation of any unstable poles in the closed loop system while designing the IMC. Similar strategy has been adopted for NIMC too. In a more conservative approach OBF-Wiener model is modified by isolating all the zeros irrespetive of its potential to bring in instability.

The modified OBF-Wiener model along with an optimizer forms the NIMC block as shown in Fig. 5.1. A decision variable $\Delta u_{guess}(k)$ is passed through the modified OBF-Wiener model and its output, $\hat{y}(k)$, is compared with the modified setpoint, $\hat{r}(k)$ *i.e.* setpoint $r(k)$ minus the process-model mismatch $d(k)$. The optimizer minimizes the error, $e(k) = \hat{r}(k) - \hat{y}(k)$, as

$$\min_{\Delta u(k)} J = e(k) \tag{5.7}$$

in order to find the best value of the decision variable *a.k.a* manipulated input, $\Delta u(k)$.

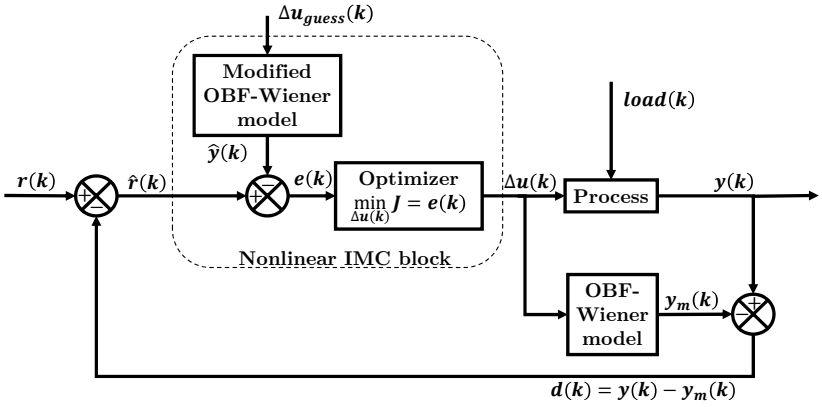

Figure 5.1: Schematic of nonlinear IMC strategy

The input-output relation out of a modified OBF-Wiener model can be expressed as

$$\hat{y}(k) = \begin{cases} f(\hat{\Phi}(k)) & \text{for Kautz-Wiener model} \\ f(\hat{L}(k)) & \text{for Laguerre-Wiener model} \end{cases} \tag{5.8}$$

where $\hat{\Phi}(k)$ and $\hat{L}(k)$ are the regressor vectors and $f(\bullet) : \mathbb{R}^N \longrightarrow \mathbb{R}$ is a static nonlinear state to output mapping, same as the one evaluated while developing original OBF-Wiener model. Two types of nonlinear mappings have been adopted in this work *viz.* wavelet network and least square-support vector machine, along with all the model parameters as calculated in Chapter 4.

5.3.1 Modified Kautz-Wiener model for NIMC

A keen look into the expressions of the Kautz filters given in the Theorem 2.1 of Chapter 2 one can easily observe that the zeros of the Kautz filters are exactly equal to reciprocal of the poles. The Kautz models generally ensure stability at least in the sense of bounded input bounded output (BIBO) stability by properly selecting the poles (β_i, β_i^*) of the Kautz filters within the unit circle. However the same pairs of (β_i, β_i^*) would lead to zeros which are outside unit circle. Inversion of Kautz filters and design of IMC thereby would surely lead to an unstable closed loop control actions. Hence the problem with *unstable zeros* of the Kautz filters is overcome by knocking off this portion completely and recreate a modified model with all the poles intact and all the zeros knocked off.

5.3.2 Modified Laguerre-Wiener model for NIMC

In a similar fashion to Kautz filters, a modified form of i^{th} Laguerre filter is derived by discarding the positive zeros as the following

$$\hat{L}_i(z) = \frac{T\sqrt{1-a_l^2}}{(z-a_l)^i} \tag{5.9}$$

where a_l is the filter parameter while T is the sampling period. Defining a state vector

$$\hat{L}(k) = \begin{bmatrix} \hat{l}_1(k) & \hat{l}_2(k) & \hat{l}_3(k) & \cdots & \hat{l}_N(k) \end{bmatrix}^T \tag{5.10}$$

a discrete time state space representation of Laguerre functions can be found as (Saha et al., 2004)

$$\hat{L}(k+1) = \hat{\boldsymbol{A}}_l \hat{L}(k) + \hat{\boldsymbol{b}}_l u(k) \tag{5.11}$$

where

$$\hat{\boldsymbol{A}}_l = \begin{bmatrix} a_l & 0 & 0 & 0 & 0 \\ 1 & a_l & 0 & 0 & 0 \\ 0 & 1 & a_l & 0 & 0 \\ \vdots & \vdots & \vdots & \vdots & \vdots \\ 0 & 0 & \cdots & 1 & a_l \end{bmatrix}$$

$$\hat{\boldsymbol{b}}_l = \begin{bmatrix} \sqrt{(1-a_l^2)T} & 0 & ... & 0 \end{bmatrix}^T$$

Regressor in Eq. 5.10 is used in Eq. 5.8 to yield modified Laguerre-Wiener model.

5.4 Numerical Examples

Both the case studies involve CSTRs which are highly nonlinear and resonating processes. The reactant undergoes irreversible and exothermic reaction. Huang et al. (2000) presented the mechanistic models for both cases which were simulated in Chapter 4 to generate *plant data* and further used those plant data to develop four OBF-Wiener models. The present case studies employ these OBF-Wiener models in order to design model based controllers that can be used for closed-loop control study by simulating on the same mechanistic

Table 5.1: List of various controllers and their acronyms

Controllers	Description
MPC-Kautz-Wavelet	: NMPC based on Kautz-Wavelet type Wiener model
MPC-Kautz-LSSVM	: NMPC based on Kautz-LSSVM type Wiener model
MPC-Laguerre-Wavelet	: NMPC based on Laguerre-Wavelet type Wiener model
MPC-Laguerre-LSSVM	: NMPC based on Laguerre-LSSVM type Wiener model
IMC-Kautz-Wavelet	: NIMC based on Kautz-Wavelet type Wiener model
IMC-Kautz-LSSVM	: NIMC based on Kautz-LSSVM type Wiener model
IMC-Laguerre-Wavelet	: NIMC based on Laguerre-Wavelet type Wiener model
IMC-Laguerre-LSSVM	: NIMC based on Laguerre-LSSVM type Wiener model
MPCs-Kautz-Wiener	: collective reference to MPC-Kautz-Wavelet and MPC-Kautz-LSSVM
MPCs-Laguerre-Wiener	: collective reference to MPC-Laguerre-Wavelet and MPC-Laguerre-LSSVM
IMCs-Kautz-Wiener	: collective reference to IMC-Kautz-Wavelet and IMC-Kautz-LSSVM
IMCs-Laguerre-Wiener	: collective reference to IMC-Laguerre-Wavelet and IMC-Laguerre-LSSVM
NMPCs	: collective reference to MPCs-Kautz-Wiener and MPCs-Laguerre-Wiener
NIMCs	: collective reference to IMCs-Kautz-Wiener and IMCs-Laguerre-Wiener

models of Huang et al. (Huang et al., 2000). The reader is advised to refer to Chapter 4 in order to get complete information on the process description and model parameters of all four OBF-Wiener models.

Altogether 8 types of model based controllers have been employed in the case studies. They are listed in Table 5.1 along with their acronyms. A comparative study of performances of these controllers have been presented. All the simulations have been performed using 64 bit MATLAB® (Version 10) under Windows 7 operating system in a PC with Intel(R) Core™ 2 Duo processor @2.4 GHz speed.

5.4.1 Case study I : Model based control of CSTR

In this case study, the temperature of the reactor needs to be regulated by manipulating the flow rate of coolant. Nominal temperature of the reactor is set at 438.78 K while nominal flow rate of coolant at steady state is 103 L min^{-1}. Data are sampled at an interval of 0.1 min.

Servo control problem

A series of step changes have been introduced on the setpoint, each for 10 min duration on either side of the nominal operating point. Two consecutive step changes, each of -2 K, followed by two more changes of 6 K and -2 K respectively were introduced on the nominal operating temperature. The reader may refer to Chapter 4 to understand that

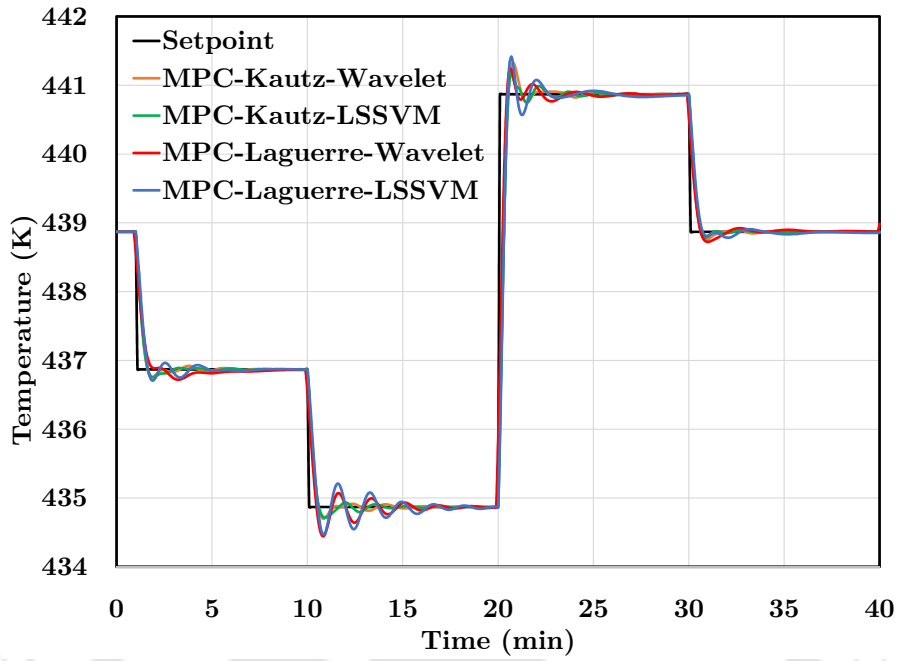

Figure 5.2: Servo control of CSTR using OBF-Wiener model based MPC: Controlled output

positive deviation from nominal operating point leads to a zone (hereafter referred to as *low-resonance zone*) where resonance is not severe. Both Kautz model and Laguerre model perform equally good in the low-resonance zone. On the other hand negative deviation from nominal operating point leads to a severely resonating zone (hereafter referred to as *high-resonance zone*). Kautz model outperforms Laguerre model in the high-resonance zone. Nevertheless, nonlinear model based controllers are designed based on all these models developed in Chapter 4.

Prediction horizon (N_p) and control horizon (N_c) of all the NMPCs are chosen as 5 and 1 respectively, whereas error weight matrix (W_E) and input weight matrix ($W_{\Delta u}$) are selected as 5 and 0 respectively. Simulation has been carried out on CSTR process for closed loop control with the NMPCs. The results have been graphically represented through Fig.5.2 and Fig.5.3. The quantitative analysis of the performance in terms of sum of squared error (hereafter referred as SSE) between setpoint and controlled output has been tabulated in Table 5.2.

All four NMPCs are able to control the temperature with varied range of efficiency. As expected Chapter 4, MPCs-Kautz-Wiener perform better than the MPCs-Laguerre-

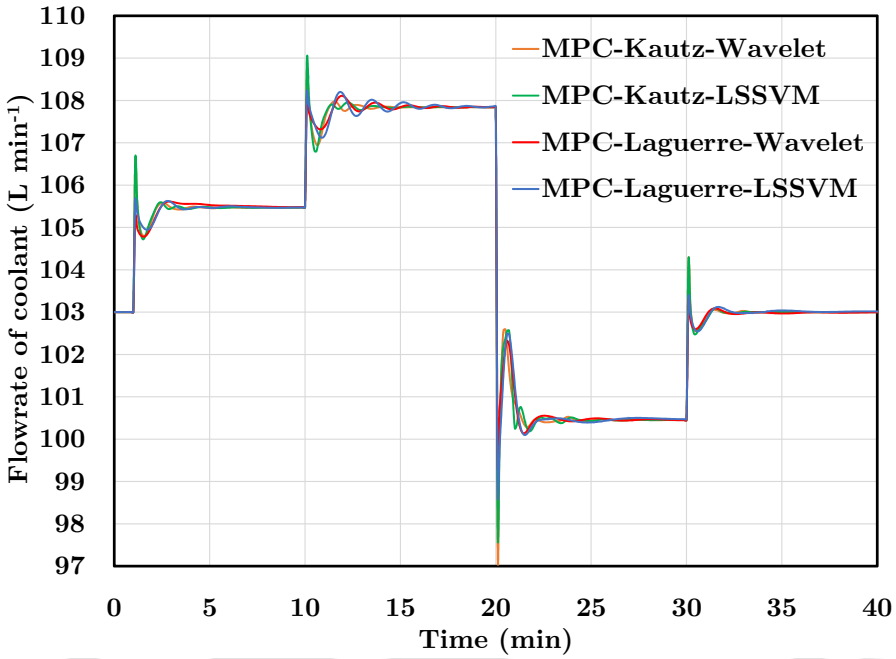

Figure 5.3: Servo control of CSTR using OBF-Wiener model based MPC: Manipulated input

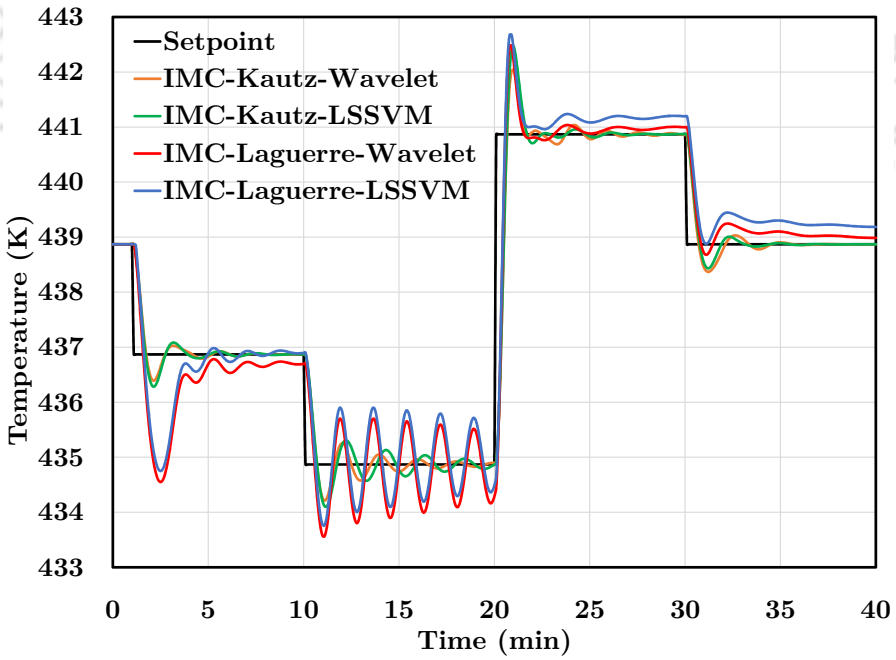

Figure 5.4: Servo control of CSTR using OBF-Wiener model based IMC: Controlled output

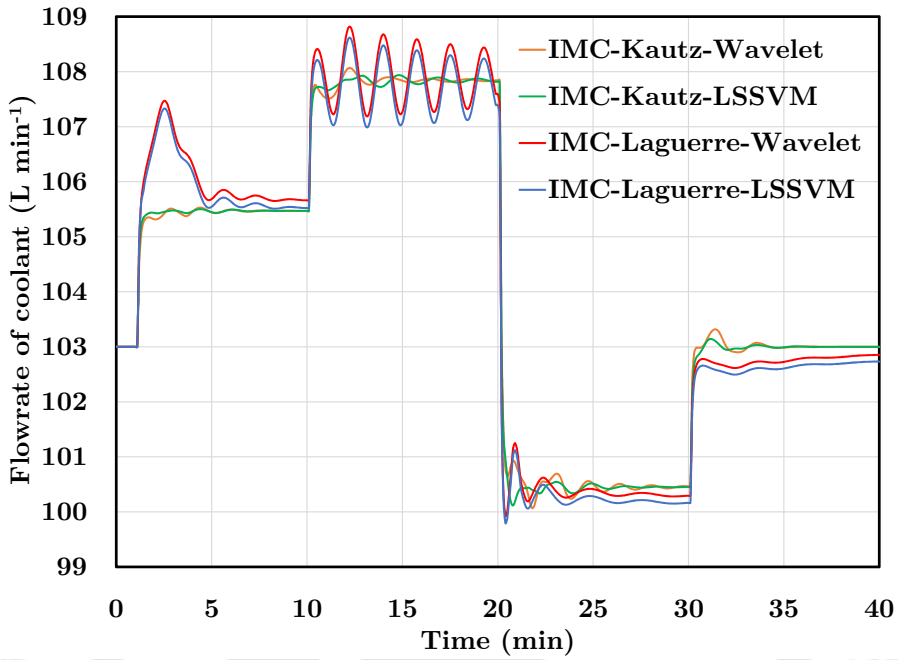

Figure 5.5: Servo control of CSTR using OBF-Wiener model based IMC: Manipulated input

Wiener when setpoint deviates to high-resonance zone. The SSE values, as computed for MPCs-Laguerre-Wiener, are almost 1.5 times that of MPCs-Kautz-Wiener. On the other hand, performances of all four NMPCs are comparable in low-resonance zone. It is further observed that oscillations are less when setpoint changes are small (near nominal operating point) and more when setpoints changes are large (away from nominal operating point). MPCs-Laguerre-Wiener yield higher oscillations as compared to that by MPCs-Kautz-Wiener (Reddy and Saha, 2017c). MPC-Kautz-Wavelet is found to be the best among the four NMPCs. The computational time for each iteration of MPC-Kautz-Wavelet algorithm is in the range of 0.0034 - 0.096 s, which is sufficiently less than chosen sampling interval.

The rate of flow of coolant experiences slightly higher manipulation by MPCs-Kautz-Wiener as shown in Fig.5.3.

The efficacy of Kautz model for resonating system is clearly manifested when NIMCs are designed and implemented in this case study. The series of step changes on setpoint, which was incorporated while studying NMPCs, has been repeated while studying NIMCs too. Simulation has been carried out on CSTR process for closed loop control with the NIMCs. The results have been graphically represented through Fig.5.4 and Fig.5.5. The

Table 5.2: Performances of model based controllers in controlling CSTR against setpoint changes

Controllers	SSE within the respective time window (min)			
	$1 < \text{time} < 10$	$10 < \text{time} < 20$	$20 < \text{time} < 30$	$30 < \text{time} < 40$
MPC-Kautz-Wavelet	4.7290	4.6963	40.7532	4.4894
MPC-Kautz-LSSVM	4.7990	5.6963	41.8292	4.5289
MPC-Laguerre-Wavelet	7.6049	7.2026	49.0715	6.1527
MPC-Laguerre-LSSVM	7.9607	7.4171	49.9938	6.6100
IMC-Kautz-Wavelet	13.3117	14.8352	106.8201	12.5037
IMC-Kautz-LSSVM	13.5025	17.1904	111.3451	12.6290
IMC-Laguerre-Wavelet	70.3210	46.9930	111.6922	17.3823
IMC-Laguerre-LSSVM	71.9160	47.8204	112.0117	30.3646

quantitative analysis of the performance in terms of SSE between setpoint and controlled output has been tabulated in Table 5.2.

The IMCs-Kautz-Wiener clearly outperform the IMCs-Laguerre-Wiener when setpoint deviates to high-resonance zone. IMCs-Laguerre-Wiener yield overtly oscillatory response coupled with huge overshoots/ undershoots, and the closed loop response settles with offsets. The SSE values, as computed for IMCs-Laguerre-Wiener, are $3-5$ times that of IMCs-Kautz-Wiener. On the other hand, performances of all four NIMCs are somewhat comparable in low-resonance zone, nonetheless superiority of IMCs-Kautz-Wiener is clearly visible in this zone too. The rate of flow of coolant experiences huge oscillatory manipulation by IMCs-Laguerre-Wiener a observed in Fig.5.5.

Regulatory control problem

A series of load changes are introduced in feed flow rate (in the range of 2-5 L min^{-1}) and feed temperature (in the range of 3-8 K) as shown in Fig.5.6 in order to evaluate the robustness of the model based controllers. The load changes were inducted both singly as well as together.

Performance of regulatory control using OBF-Wiener model based MPC, while the CSTR is disturbed with load changes on feed flow rate, has been shown in Fig.5.7. The output profile, *i.e.* the temperature of the reactor, does not fluctuate beyond $\pm$2K, while the input manipulation is never needed beyond 5 L min^{-1}. MPCs-Kautz-Wiener are better performing than MPCs-Laguerre-Wiener. Supre-macy of Kautz-Wiener models over Laguerre-Wiener models is more prominent in their application on NIMCs (Fig.5.8). The

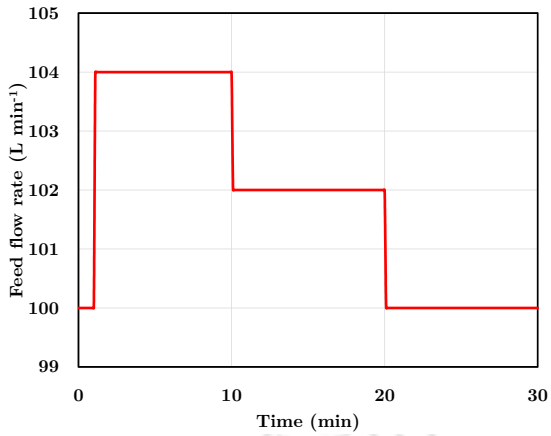

(a) Disturbances in feed flow rate

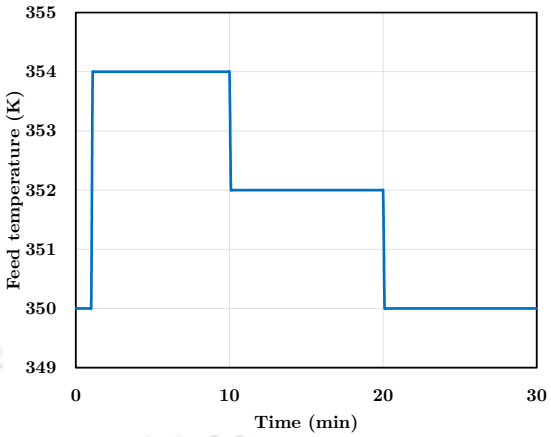

(b) Disturbances in feed temperature

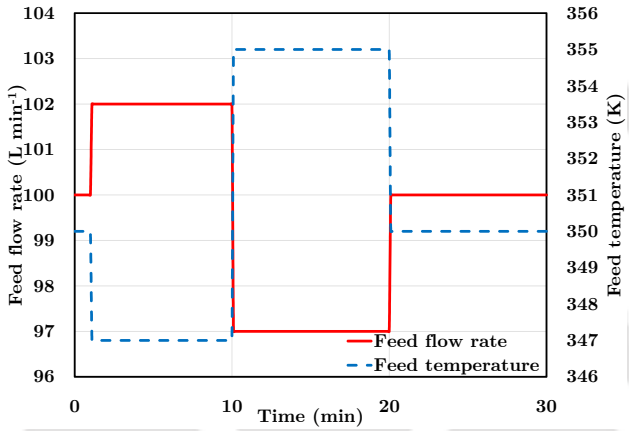

(c) Simultaneous disturbances in feed flow rate and feed temperature

Figure 5.6: Various load changes introduced in CSTR while studying regulatory control actions

IMCs-Kautz-Wiener clearly outperform the IMCs-Laguerre-Wiener. Especially when the load pushes the process towards high-resonance zone, the SSE values computed for the IMCs-Laguerre-Wiener show a value which is on an average 5-6 times higher than that of IMCs-Kautz-Wiener (Table 5.3).

Performance of regulatory control using OBF-Wiener model based IMC, while the CSTR is disturbed with load changes on feed temeprature, has been shown in Fig.5.9. The temperature of the reactor, does not fluctuate beyond ±3K, while the input manipulation is never needed beyond 8 L min^{-1}. MPCs-Kautz-Wiener are better performing than MPCs-Laguerre-Wiener. Especially MPC-Laguerre-LSSVM performs worse than the all other controllers. The SSE value computed for MPC-Laguerre-LSSVM is 3 times that of other

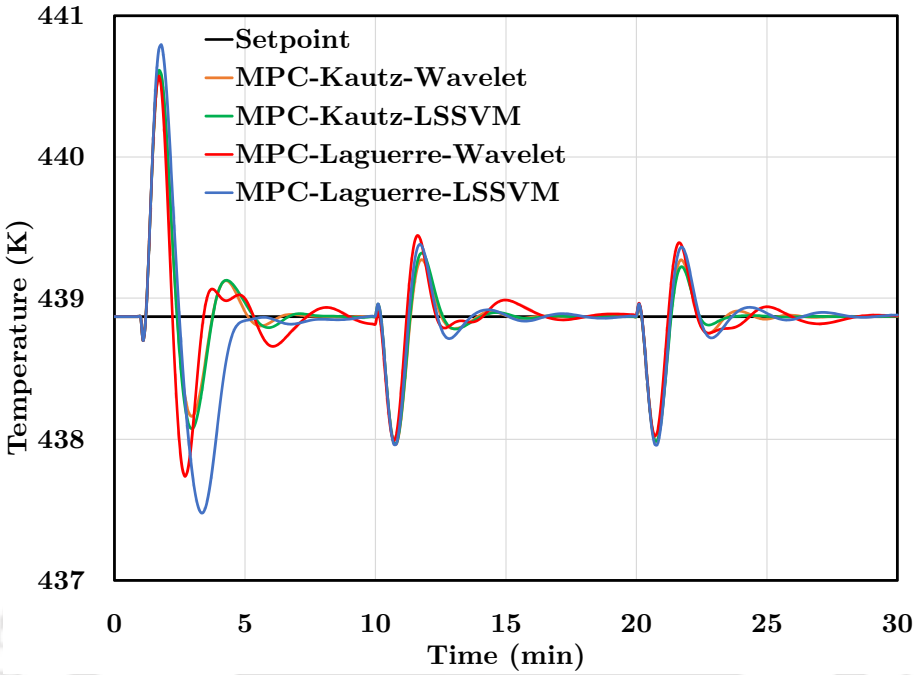

(a) Controlled output

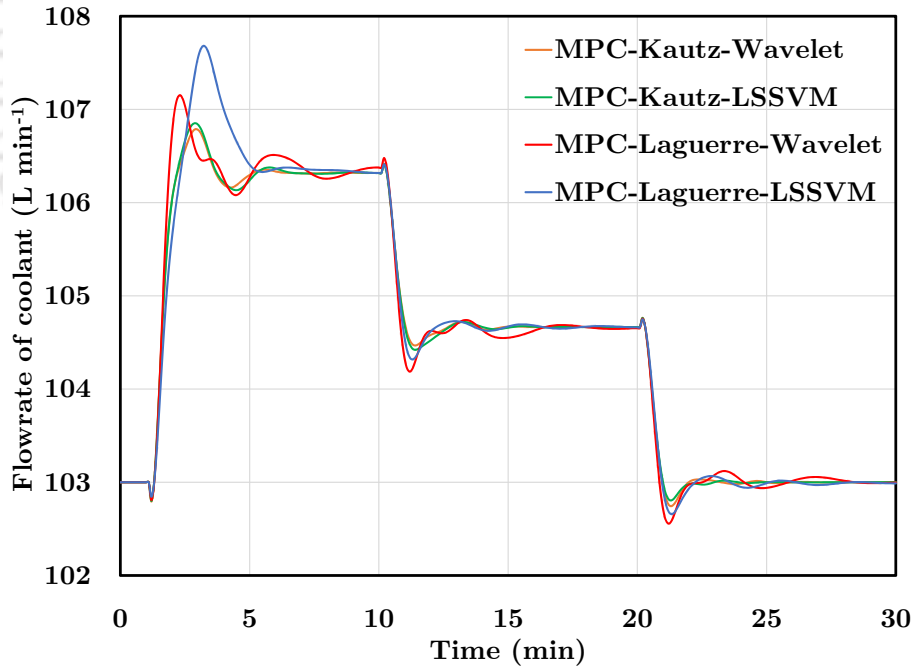

(b) Manipulated input

Figure 5.7: Regulatory control of CSTR using OBF-Wiener model based MPC: while disturbing the feed flow rate

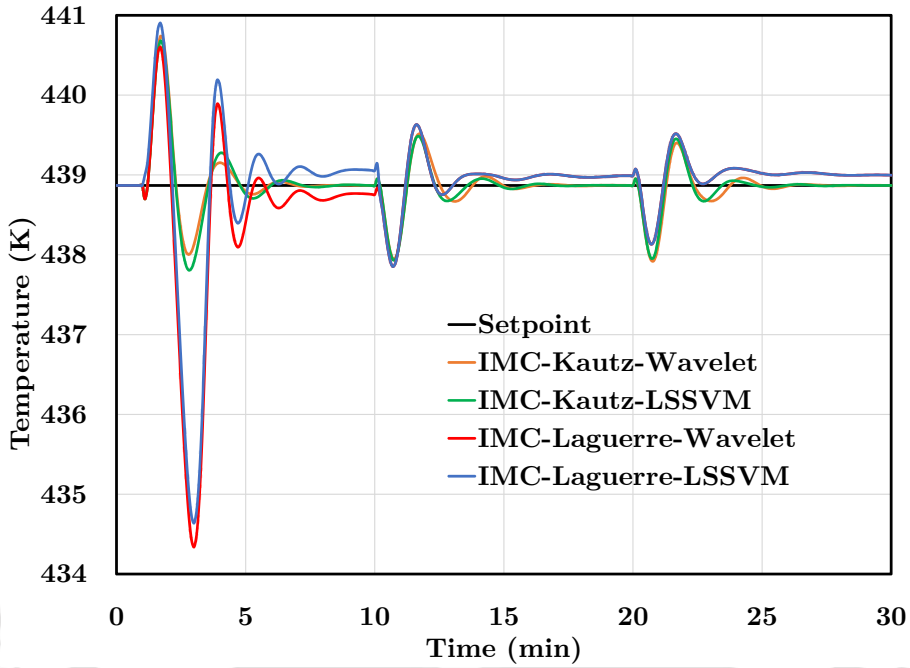

(a) Controlled output

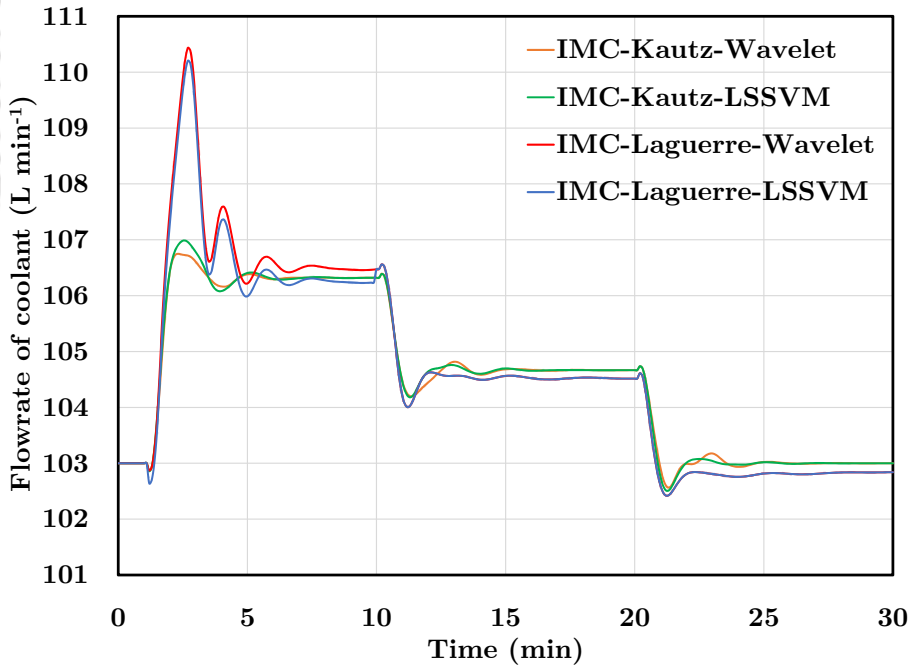

(b) Manipulated input

Figure 5.8: Regulatory control of CSTR using OBF-Wiener model based IMC: while disturbing the feed flow rate

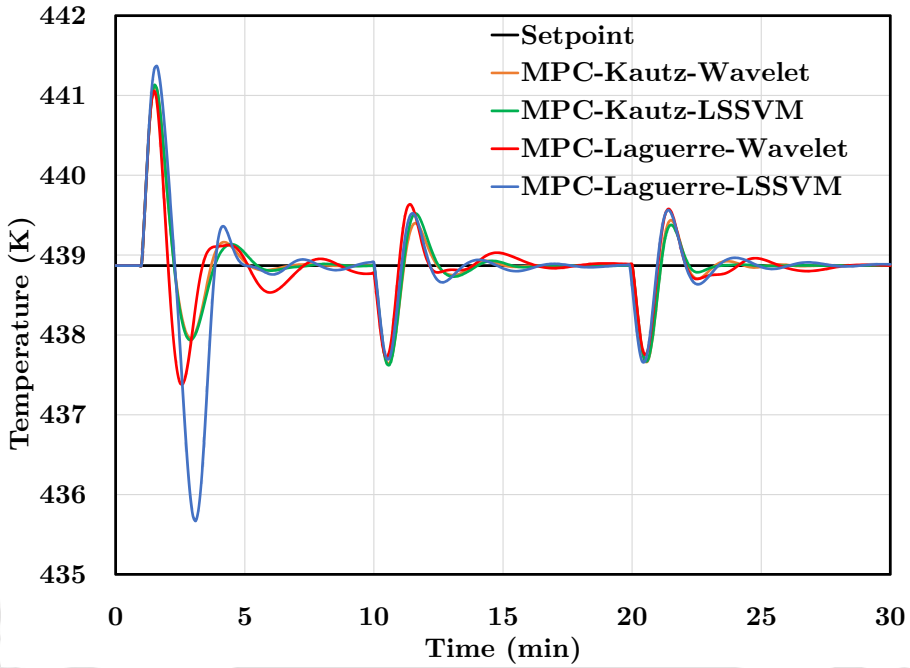

(a) Controlled output

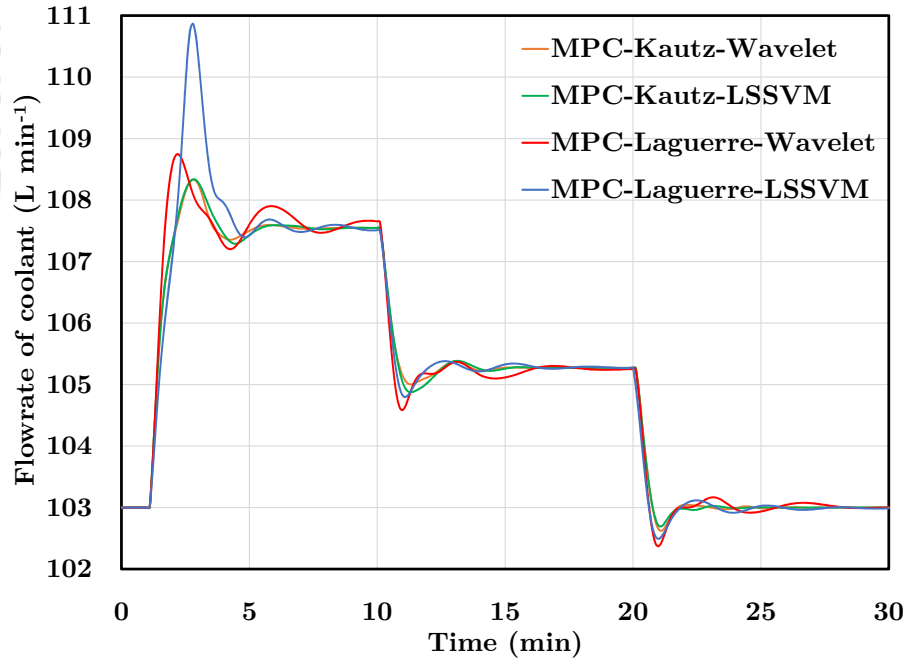

(b) Manipulated input

Figure 5.9: Regulatory control of CSTR using OBF-Wiener model based MPC: while disturbing the feed temperature

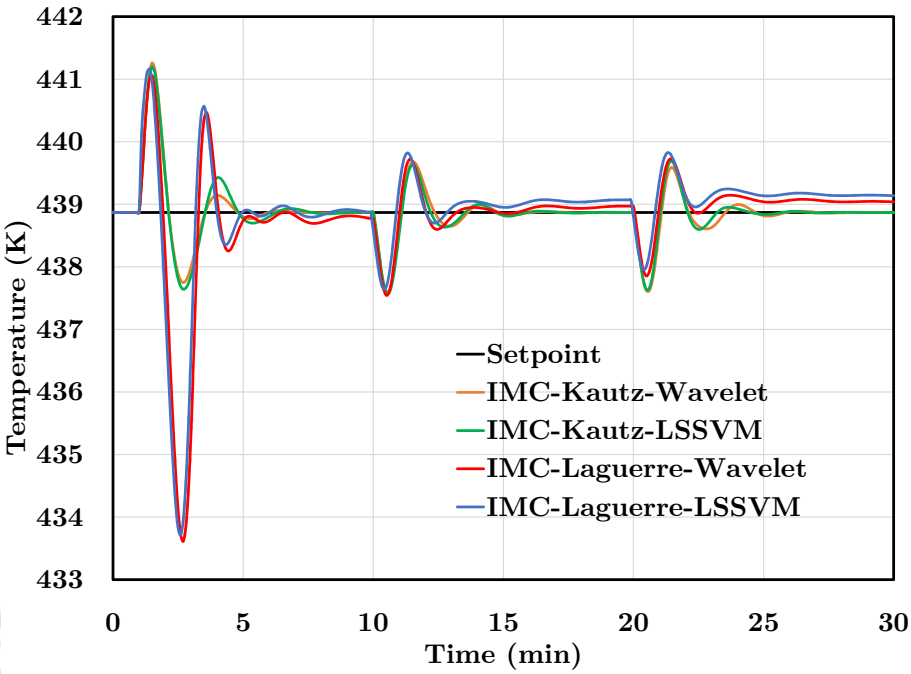

(a) Controlled output

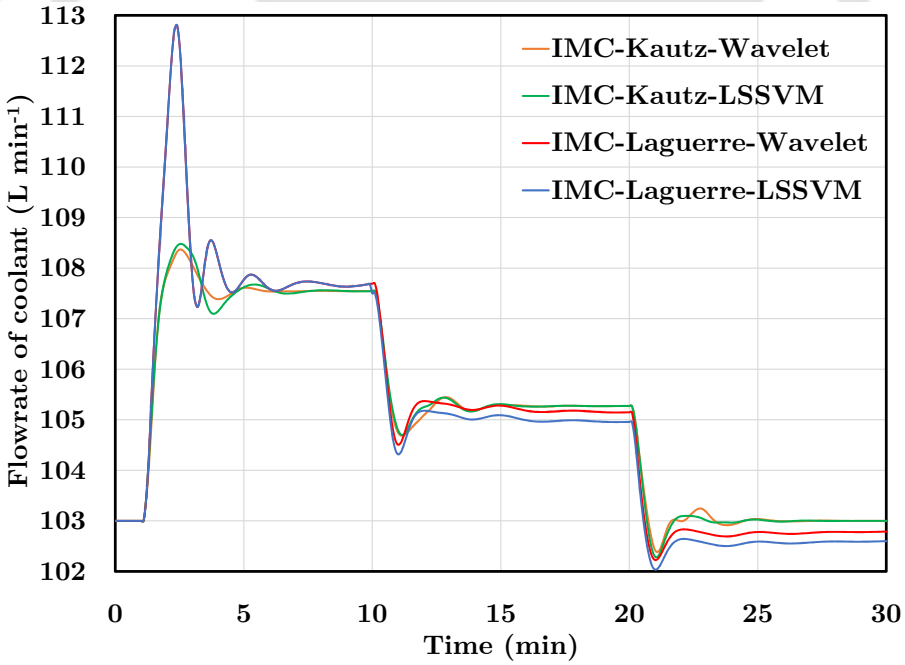

(b) Manipulated input

Figure 5.10: Regulatory control of CSTR using OBF-Wiener model based IMC: while disturbing the feed temperature

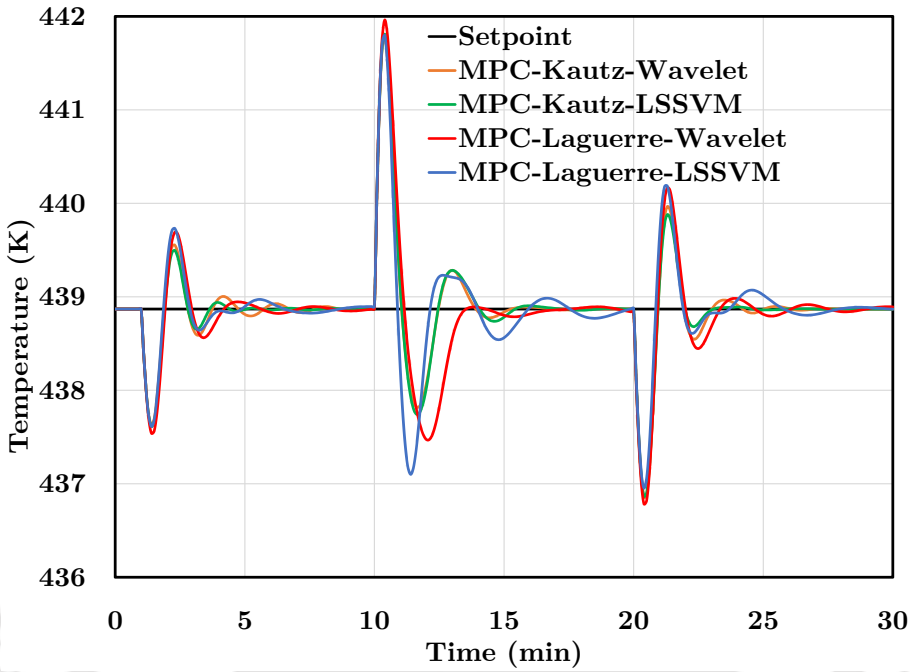

(a) Controlled output

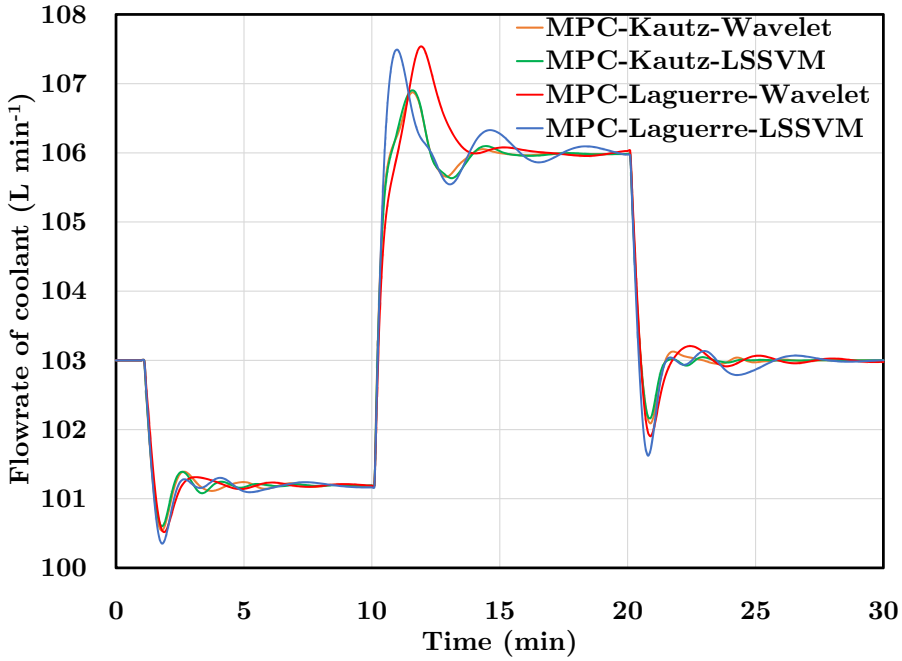

(b) Manipulated input

Figure 5.11: Regulatory control of CSTR using OBF-Wiener model based MPC: while disturbing both feed flow rate and feed temperature

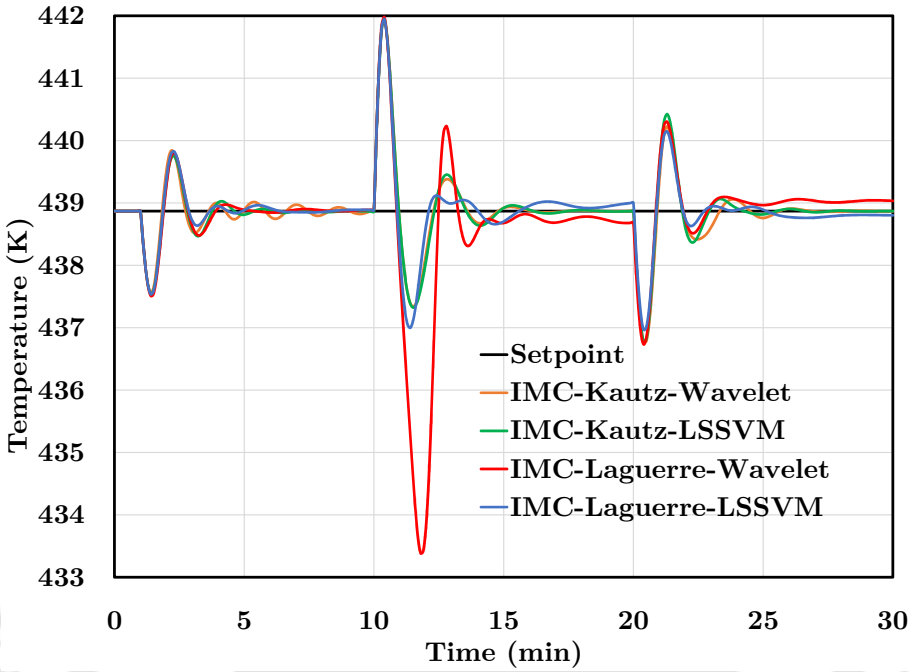

(a) Controlled output

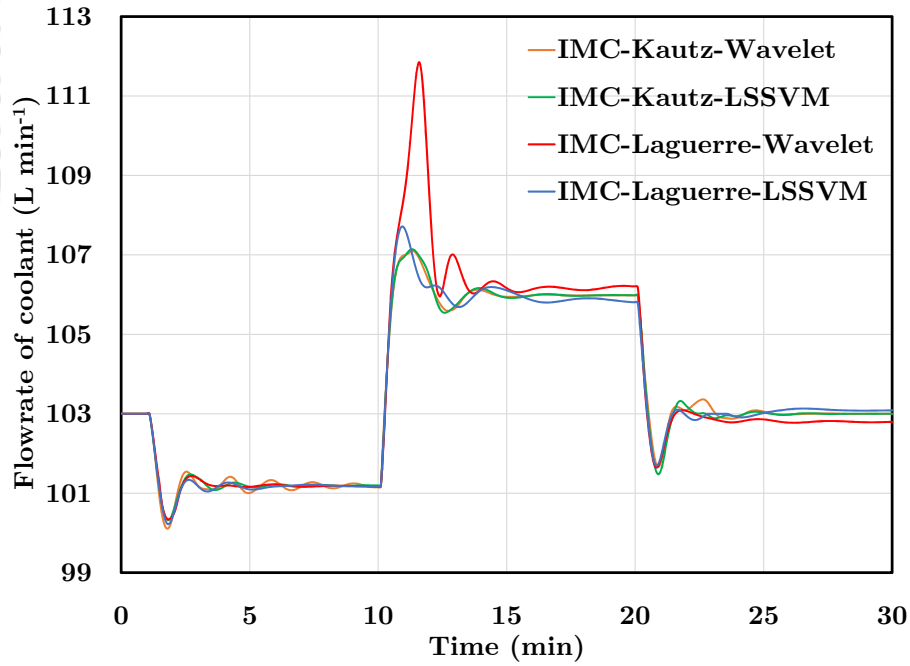

(b) Manipulated input

Figure 5.12: Regulatory control of CSTR using OBF-Wiener model based IMC: while disturbing both feed flow rate and feed temperature

Table 5.3: Performances of model based controllers in controlling CSTR against load changes in feed flow rate

Controllers	SSE within the respective time window (min)		
	$1 < \text{time} < 10$	$10 < \text{time} < 20$	$20 < \text{time} < 30$
MPC-Kautz-Wavelet	19.9564	5.3454	4.7828
MPC-Kautz-LSSVM	21.1991	5.2110	4.9770
MPC-Laguerre-Wavelet	21.6180	5.5556	5.0481
MPC-Laguerre-LSSVM	39.7405	5.7332	5.7597
IMC-Kautz-Wavelet	22.4759	6.5916	6.1057
IMC-Kautz-LSSVM	24.4954	7.0124	6.4059
IMC-Laguerre-Wavelet	160.2241	8.9403	6.6070
IMC-Laguerre-LSSVM	150.6571	9.0532	6.6070

Table 5.4: Performances of model based controllers in controlling CSTR against load changes in feed temperature

Controllers	SSE within the respective time window (min)		
	$1 < \text{time} < 10$	$10 < \text{time} < 20$	$20 < \text{time} < 30$
MPC-Kautz-Wavelet	34.839	10.0021	8.8731
MPC-Kautz-LSSVM	35.7757	11.1573	9.3437
MPC-Laguerre-Wavelet	38.3917	9.6747	8.7948
MPC-Laguerre-LSSVM	110.0633	9.6747	10.3873
IMC-Kautz-Wavelet	37.766	12.1012	11.2749
IMC-Kautz-LSSVM	40.2972	12.3519	11.3439
IMC-Laguerre-Wavelet	201.3101	12.9100	11.6219
IMC-Laguerre-LSSVM	208.8363	14.9672	18.2668

controllers. Supremacy of Kautz-Wiener models over Laguerre-Wiener models is further established in their application on NIMCs (Fig.5.10). The IMCs-Kautz-Wiener clearly outperform both the IMCs-Laguerre-Wiener. The SSE value computed for the IMCs-Laguerre-Wiener at the high-resonance zone is on an average 4 times higher than that of IMCs-Kautz-Wiener (Table 5.4). The control effort in case of IMCs-Laguerre-Wiener is enormous too.

The controllers become fragile when load changes are activated on both feed flow rate and its temperature at a higher order, while combined load changes at a lower range does not offer any significant results to draw conclusive argument. However, IMC-Laguerre-wavelet shows poor performance in this case too (Figs. 5.11 and 5.12).

5.4.2 Case study II : Model based control of a series connected CSTR

In this case study, the concentration of the product from second reactor needs to be regulated by manipulating the flow rate of coolant. Nominal concentration of the product from the second reactor is set at 0.0076 mol L^{-1} while nominal flow rate of coolant at steady state is 106 L min^{-1}. Data are sampled at an interval of 0.1 min. As observed in Chapter 4, the Laguerre-Wiener model completely fails in identifying this process due to its overtly complex and oscillatory nature and thus it is not possible to design Laguerre-Wiener model based controllers for this case study. In other words, only Kautz-Wiener model based controllers are studied in this case study.

Servo control problem

A series of step changes have been introduced on the setpoint on either side of the nominal operating point. Three consecutive step changes of magnitude 0.0002 mol L^{-1}, -0.0004 mol L^{-1} and 0.0002 mol L^{-1} respectively were introduced on the nominal operating concentration. The reader may refer to Chapter 4 to understand that positive deviation from nominal operating point leads to high-resonance zone. Prediction horizon (N_p) and control horizon (N_c) of all the NMPCs are chosen as 10 and 1 respectively, whereas error weight matrix (W_E) and input weight matrix ($W_{\Delta u}$) are selected as 10 and 0 respectively. Simulation has been carried out on series connected CSTR process for closed loop control with the MPCs-Kautz-Wiener. The results have been graphically represented through Fig.5.13 and Fig.5.14. The quantitative analysis of the performance in terms of SSE between setpoint and controlled output has been tabulated in Table 5.5.

All four model based controllers are able to control the concentration (C_{A2}) with varied range of efficiency. However, it has been observed MPCs perform better than IMCs. The overshoot of output profile, while regulated by MPC, is smaller and the output comes to steady state faster (within 6 min) as observed in Fig.5.13 and Fig.5.14. On the other hand IMC regulated output profiles show higher oscillation and oveshoots; and the response time is almost double (Fig.5.15 and Fig.5.16). The SSE values, as computed for IMCs-Kautz-Wiener, are almost 1.5 times that of MPCs-Kautz-Wiener, as observed in Table 5.5. The input manipulation is however quite steep in case of MPCs-Kautz-Wiener.

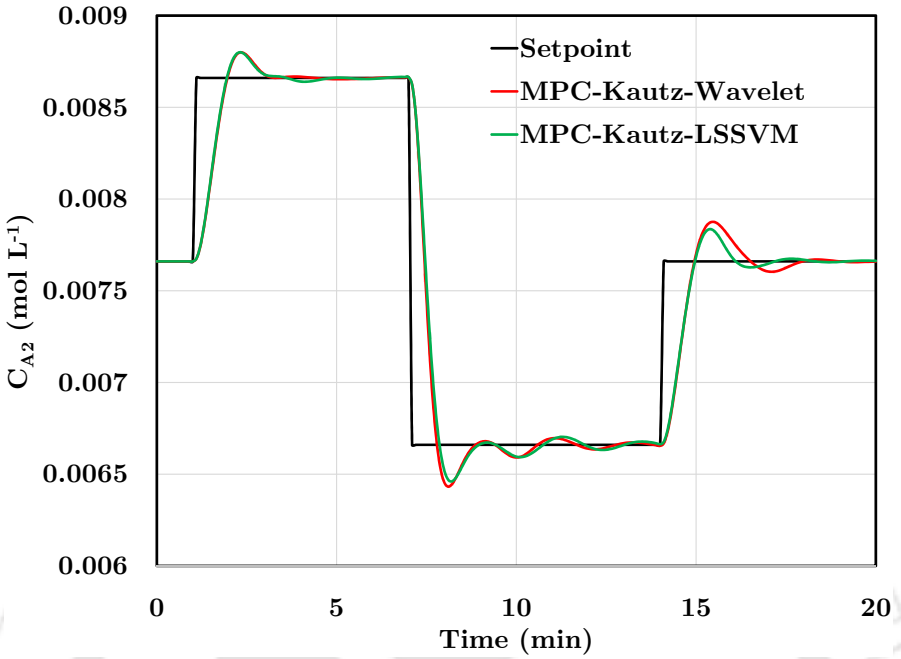

Figure 5.13: Servo control of series-connected CSTRs using OBF-Wiener model based MPC: Controlled output

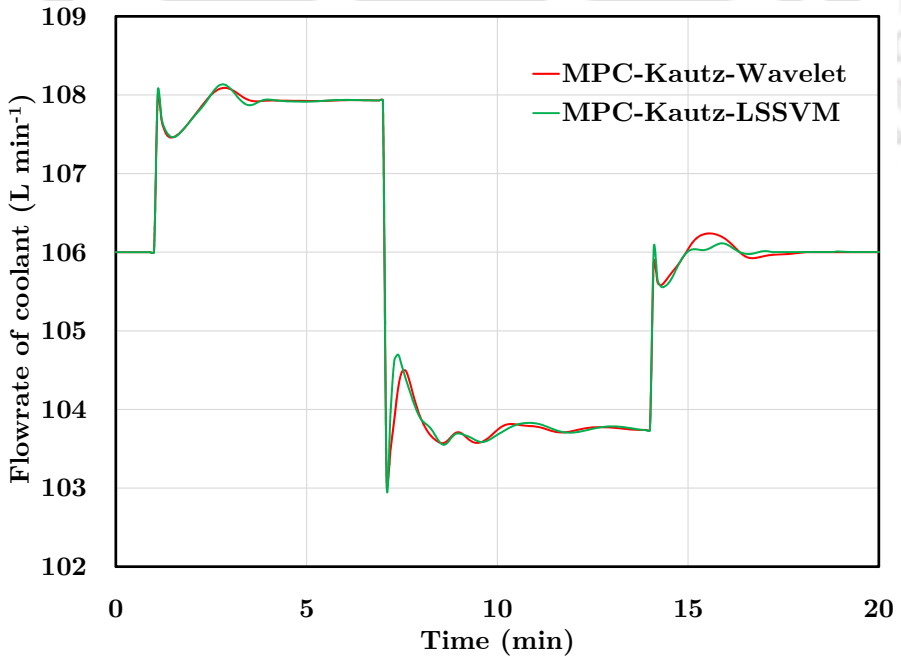

Figure 5.14: Servo control of series-connected CSTRs using OBF-Wiener model based MPC: Manipulated input

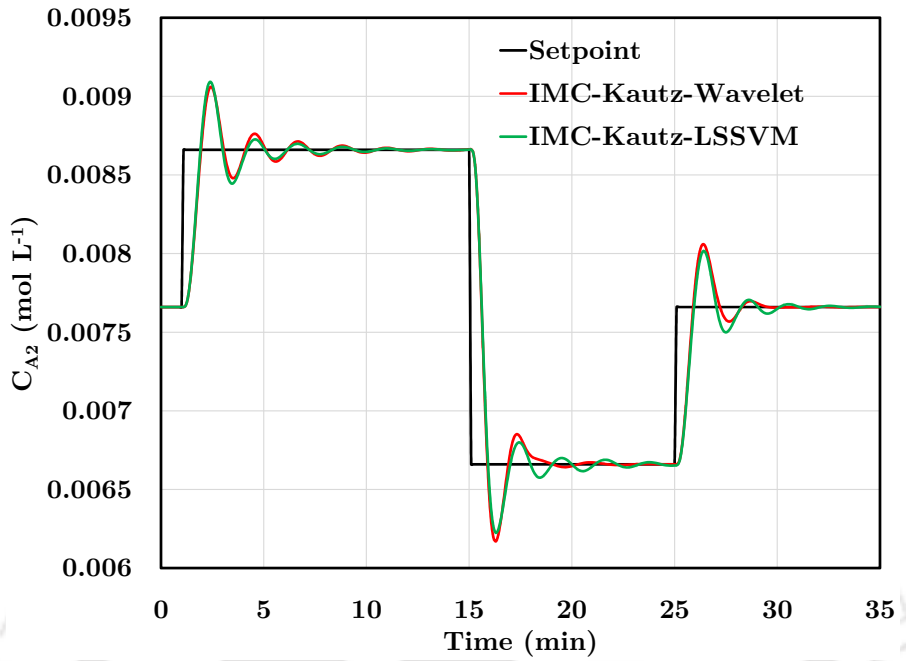

Figure 5.15: Servo control of series-connected CSTRs using OBF-Wiener model based IMC: Controlled output

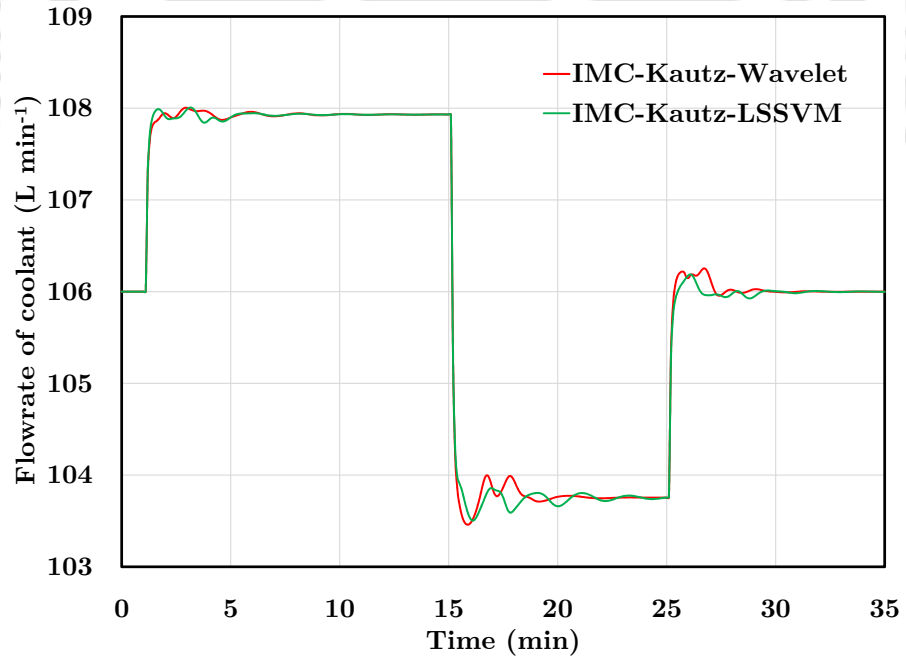

Figure 5.16: Servo control of series-connected CSTRs using OBF-Wiener model based IMC: Manipulated input

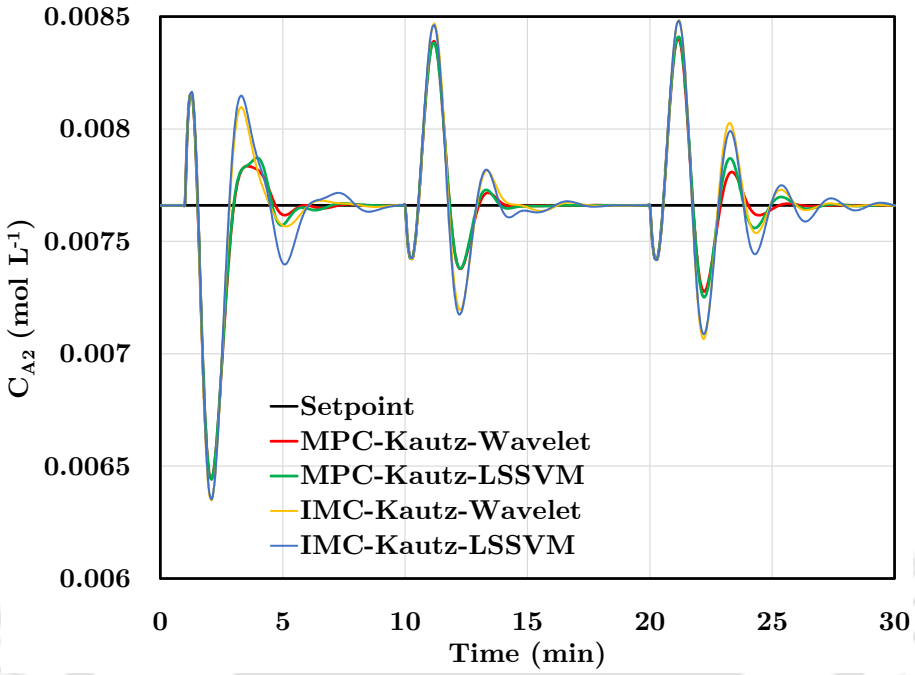

(a) Controlled output

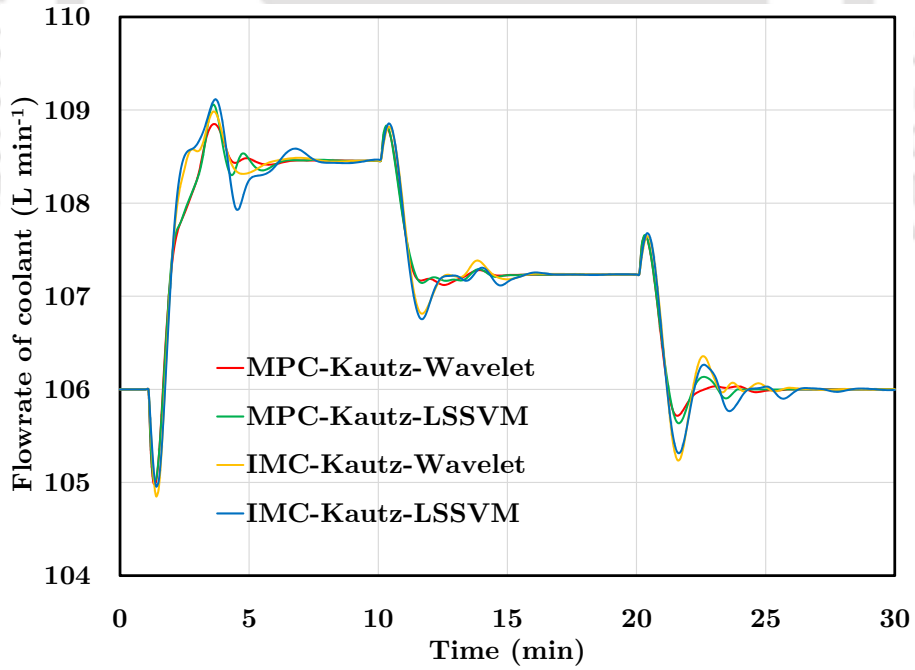

(b) Manipulated input

Figure 5.17: Regulatory control of series-connected CSTRs using OBF-Wiener model based controllers: while disturbing the feed flow rate

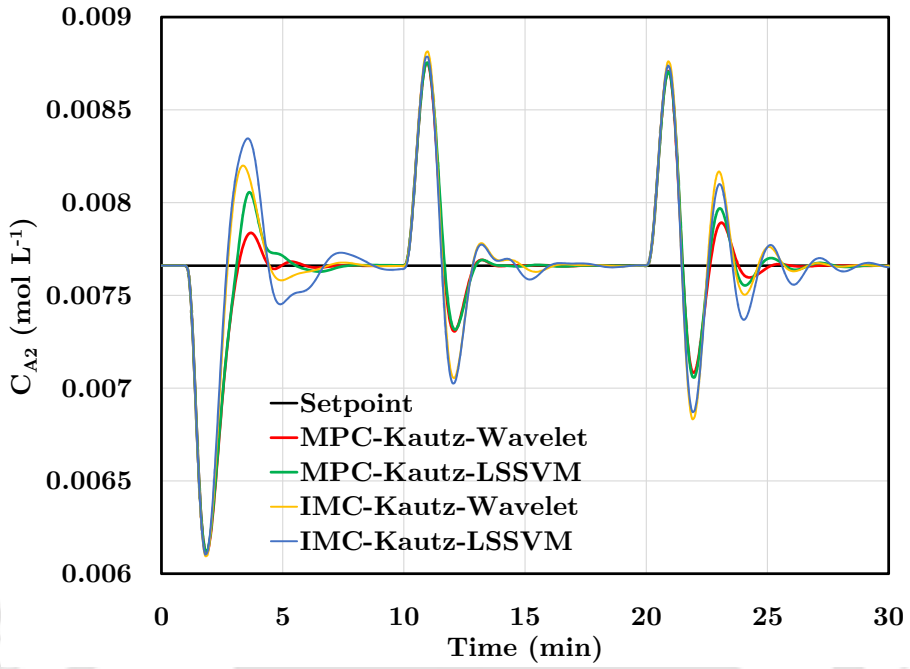

(a) Controlled output

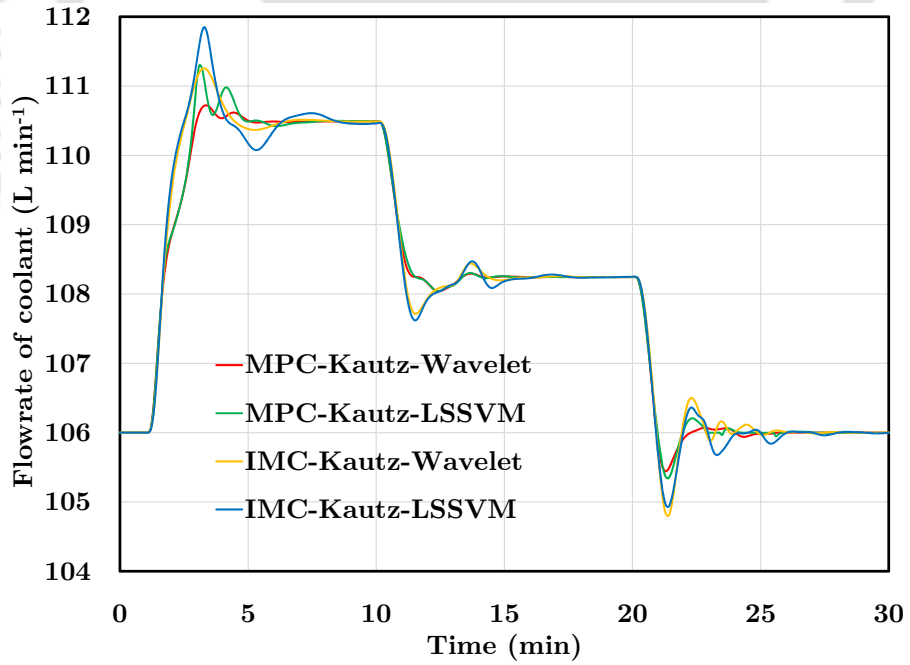

(b) Manipulated input

Figure 5.18: Regulatory control of series-connected CSTRs using OBF-Wiener model based controllers: while disturbing the feed temperature

Table 5.5: Performances (SSE values) of model based controllers in controlling series-connected CSTRs

Controllers	Servo action	Regulatory action	
		load changes in feed flowrate	load changes in feed temperature
MPC-Kautz-Wavelet	1.9643×10^{-5}	1.8751×10^{-5}	3.6613×10^{-5}
MPC-Kautz-LSSVM	1.9851×10^{-5}	1.9103×10^{-5}	3.7739×10^{-5}
IMC-Kautz-Wavelet	3.0570×10^{-5}	2.4528×10^{-5}	4.2936×10^{-5}
IMC-Kautz-LSSVM	3.0619×10^{-5}	2.5117×10^{-5}	4.3738×10^{-5}

Regulatory control problem

Performance of regulatory control using MPCs-Kautz-Wiener, while the series connected CSTR is disturbed with load changes on feed flow rate, has been shown in Fig.5.17. The output profile, *i.e.* C_{A2}, does not fluctuate beyond ± 0.0015 mol L^{-1}, while the input manipulation is never needed beyond 4 L min^{-1}. Supremacy of MPCs-Kautz-Wiener models over IMCs–Kautz-Wiener is also observed when load changes on feed temperature are incorporated (Fig.5.18). The SSE values computed for the IMCs-Kautz-Wiener show a value which is on an average 1.2-1.5 times higher than that of MPCs-Kautz-Wiener (Table 5.5). Similarly Fig.5.19 indicates the performance of the controllers when both the load changes are acted together. In all cases, it is consistently observed that the performances of MPCs-Kautz-Wiener and IMCs-Kautz-Wiener are comparable when the process output is pushed far away from the nominal operating point, while MPCs-Kautz-Wiener perform marginally better than IMCs-Kautz-Wiener when the process operates close to its nominal operating point (Reddy and Saha, 2017c). The computational time for each iteration of MPCs-Kautz-wavelet algorithm is in the range of 0.0034 - 0.099 s and the mean value of optimization problem computational times is 0.0146 s, whereas, for MPCs-Kautz-LSSVM, the values are 0.02-0.69s and 0.189 s respectively.

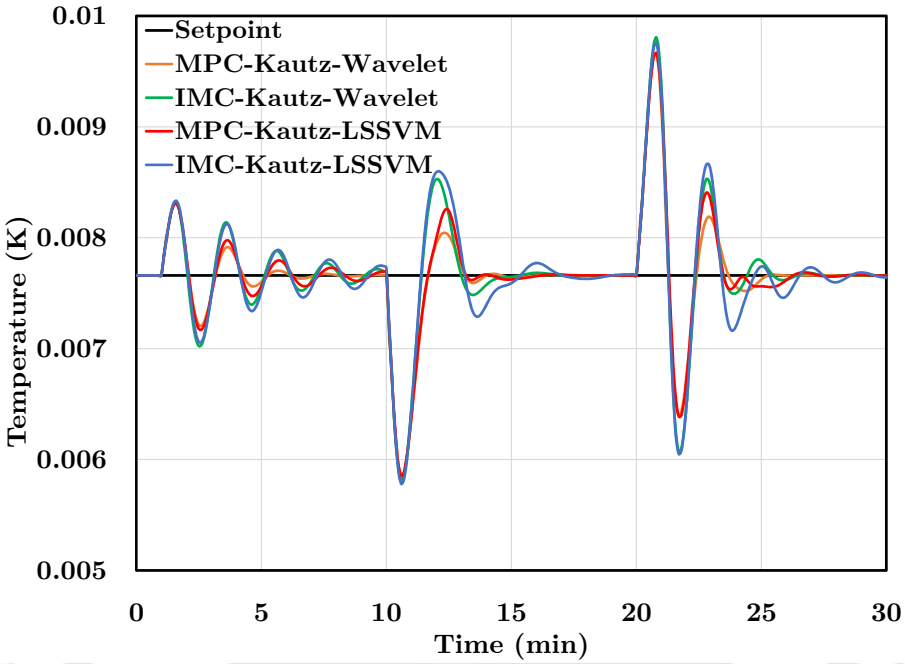

(a) Controlled output

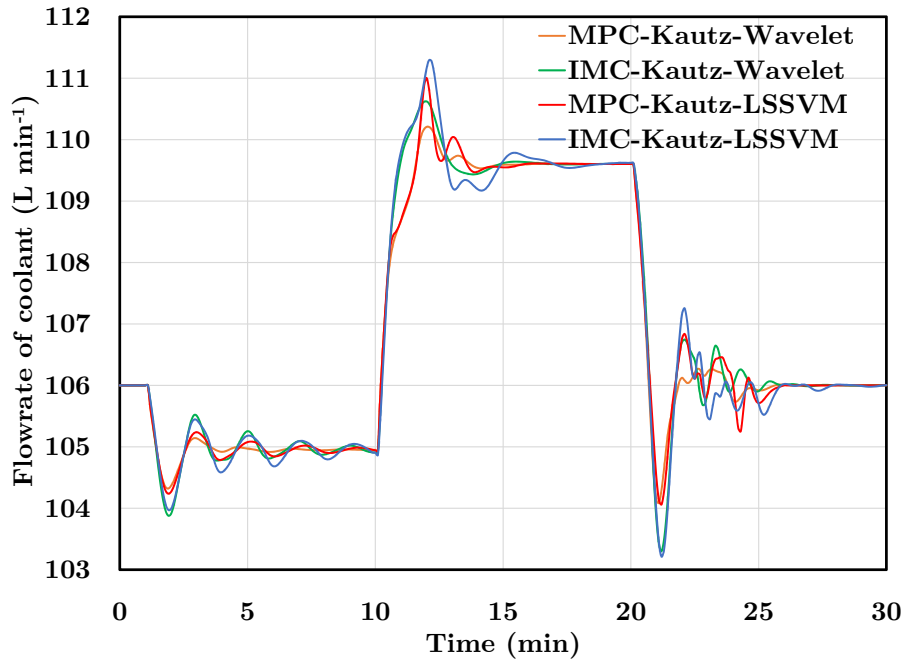

(b) Manipulated input

Figure 5.19: Regulatory control of series-connected CSTRs using Kautz-Wiener model based controllers: while disturbing both feed flow rate and feed temperature

5.5 Summary

A novel kind of design technique for nonlinear IMC has been introduced. Four OBF-Wiener models, *viz.* Kautz-wavelet, Kautz-LSSVM, Laguerre-wavelet and Laguerre-LSSVM, described in the chapter 4 of this thesis, are employed to design model based controllers, viz. MPC and IMC. Eight such combination of controllers have been developed and they are employed in closed loop control study for nonlinear resonating CSTR systems, both in servo as well as regulatory problems. The simulation results show that the Kautz-model based controllers clearly outperform the Laguerre model based controllers in all categories. The simulation time taken by Kautz model based controllers are less than that of Laguerre model based controllers.

Chapter 6

Conclusions & Future Directions

From the present work on nonlinear system identification and MBC of resonating systems the following conclusions are drawn.

1. The new kind of linear system identification technique introduced in this thesis is able to approximate linear/mildly nonlinear resonating dynamic systems. The efficacy of this model is demonstrated through simulation case studies and they are found to be able to model the processes with high accuracy.

2. The linear MPC, developed from the Kautz model is able to control the resonating systems and the stability of the controller has been established through Lyapunov stability criteria. The performance of Kautz-MPC technique is better than that of Laguerre-MPC technique proposed by Wang (2004). Even with some limitations Laguerre function based MPC is capable of controlling a strictly linear resonanting system, albeit with higher number of Laguerre coefficients. The same system could be controlled by Kautz-MPC with significantly less number of coefficients. Further, even a mild nonlinearity cannot be handled by Laguerre-MPC as shown in the case study of magnetic ball suspension system.

3. The nonlinear Kautz-Wiener models developed in this work using wavelet network and LSSVM are very efficient in identifying the dynamics of highly nonlinear systems such as CSTR. They remain equally efficient when the degree of nonlinearity is manifold in case of series connected CSTRs.

4. Although both Kautz-Wiener and Laguerre-Wiener are OBF based models, Kautz-Wiener models outperform the Laguerre-Wiener models due to its capability of capturing resonating characteristics. This issue is clearly evident in simulation results of series connected CSTRs.

5. Among the eight cases of closed loop studies that have been performed through simulation of CSTR and series connected CSTRs, both in servo and regulatory problems, Kautz-Wiener based MBCs perform better than Laguerre-Wiener based MBCs. Lagurre-Wiener based controllers yield higher oscillatory response in case of controlling single CSTR. They yield offset too. On the other hand they completely fail in case of series connected CSTRs due to failure in capturing the process dynamics which is primarily nonlinear and resonating. The simulation time taken by Kautz model based controllers are less than that taken by Laguerre model based controllers.

6. Wavelet network based MBCs yield better control performance than LSSVM based MBCs, whereas performances of MPCs and IMCs are quite comparable.

7. The nonlinear IMC design technique through deletion of positive zeros followed by model inversion(through optimization) is indeed a novel approach of its kind and it ensures the BIBO stability in the closed loop operation.

There are still some unresolved issues in connection with the contents of this thesis, which are briefly described below.

- The Kautz-Wiener models have been developed for a SISO system. This could be extended for a $n \times m$-MIMO system as m-MISO model, where m represents the number of outputs and n the number of inputs of the MIMO system. The real bottleneck found in extending the Kautz-Wiener models to non-square MIMO systems is the right technique to find the optimal values of the Kautz function parameters.

- The Kautz models can be extended for representing other classes of nonlinear process using Hammerstein and/or Hammerstein-Wiener type structures.

- The robustness issues of optimization based NIMC design can be explored by suitable numerical methods.
- An experimental validation of the developed models and the corresponding MBCs.

An interested researcher may venture into the above issues while performing research in the related area.

Visible Research Output

- Referred Journals
  - **Reddy R.B.,** and P. Saha (2017)., "Model based control of resonating processes ", *Robotics & Automation Engineering Journal*, **1**(4):555566.
  - **Reddy R.B.,** and P.Saha(2016)., "Modelling and control of resonating processes:Part I - System identification using orthogonal basis function ",*International Journal of Dynamics and Control*,**5**(4),pp.1222-1236.
  - **Reddy R.B.,** and P.Saha(2016)., "Modelling and control of resonating processes:Part II - Model based control using orthogonal basis function based Wiener models". *International Journal of Dynamics and Control*,**5**(4),pp.1237-1251.
  - **Reddy R.B.,** and P.Saha(2016)., "Kautz Filters based Model Predictive Control for Resonating Systems", *International Journal of Dynamics and Control*,**5**(3),pp.477-495.
  - Misra S., **R. Reddy** and P. Saha(2015)., " Model predictive Control for resonating Systems using Kautz model", *International Journal of Automation and Computing*, **13**(5), pp. 501-515.
- Conferences
  - **Reddy R.B.** and P.Saha(2012). "Real time model predictive control of a four tank interacting storage system", 11^{th} International Symposium on Process Systems Engineering, July 15-19, 2012, Singapore.

REFERENCES

Aadaleesan, P., Miglan, N., Sharma, R., and Saha, P. (2008). Nonlinear system identification using wiener type laguerre - wavelet network model. *Chemical Engineering Science*, 63(15):3932 – 3941.

Abdollahzade, M. and Kazemi, R. (2015). A developed local polynomial neuro-fuzzy model for nonlinear system identification. *International Journal on Artificial Intelligence Tools*, 24(03):1550004–1–1550004–20.

Afram, A., Janabi-Sharifi, F., Fung, A. S., and Raahemifar, K. (2017). Artificial neural network (ann) based model predictive control (mpc) and optimization of hvac systems: A state of the art review and case study of a residential hvac system. *Energy and Buildings*, 141:96 – 113.

Al Seyab, R. K. and Cao, Y. (2006). Nonlinear model predictive control for the ALSTOM gasifier. *Journal of Process Control*, 16(8):795–808.

Alci, M. and Asyali, M. H. (2009). Nonlinear system identification via Laguerre network based fuzzy systems. *Fuzzy Sets and Systems*, 160(24):3518 – 3529.

Arasu, S. K., Panda, A., and Prakash, J. (2016). Experimental validation of a nonlinear model based control scheme on the variable area tank process. *IFAC-PapersOnLine*, 49(1):30 – 34. 4th IFAC Conference on Advances in Control and Optimization of Dynamical Systems ACODS 2016.

Arulselvi, S., Uma, G., and Chidambaram, M. (2004). Design of pid controller for boost converter with rhs zero. In *Power Electronics and Motion Control Conference, 2004. IPEMC 2004. The 4th International*, volume 2, pages 532–537. IEEE.

Atuonwu, J., Cao, Y., Rangaiah, G., and Tadé, M. (2010). Identification and predictive control of a multistage evaporator. *Control Engineering Practice*, 18(12):1418 – 1428.

Aydi, A., Djemel, M., and Chtourou, M. (2017). Two fuzzy internal model control methods for nonlinear uncertain systems. *International Journal of Intelligent Computing and Cybernetics*, 10(2):223–240.

Azar, A. T. and Serrano, F. E. (2014). Robust imc–pid tuning for cascade control systems with gain and phase margin specifications. *Neural Computing and Applications*, 25(5):983–995.

Babuska, R. and Verbruggen, H. (2003). Neuro-fuzzy methods for nonlinear system identification. *Annual Reviews in Control*, 27(1):73–85.

Begum, K. G., Radhakrishnan, T., Rao, A. S., and Chidambaram, M. (2016). IMC based PID controller tuning of series cascade unstable systems. *IFAC-PapersOnLine*, 49(1):795 – 800. 4th IFAC Conference on Advances in Control and Optimization of Dynamical Systems ACODS 2016.

Benlahrache, M. A., Othman, S., and Sheibat-Othman, N. (2016). Fault tolerant control of wind turbine using laguerre and kautz mpc for compensation. In *Control Conference (ECC), 2016 European*, pages 1909–1914. IEEE.

Bequette, B. (2003). *Process Control: Modeling, Design, and Simulation*. Prentice-Hall International Series in the Physical and Chemi. Prentice Hall PTR.

Besta, C. and Chidambaram, M. (2017). Improved decentralized controllers for stable systems by imc method. *Indian Chemical Engineer*, pages 1–20.

Bhat, J., Madhavan, K., and Chidambaram, M. (1991). Multivariable global input/output linearized internal model control of a semibatch reactor. *Industrial & Engineering Chemistry Research*, 30(7):1541–1547.

Billings, S. A. and Fakhouri, S. Y. (1982). Identification of systems containing linear dynamics and static nonlinear elements. *Automatica*, 18(1):15–26.

Bloemen, H. H. J., Chou, C. T., van den Boom, T. J. J., Verdult, V., Verhaegen, M., and Backx, T. C. (2001a). Wiener model identification and predictive control for dual composition control of a distillation column. *Journal of Process Control*, 11(6):601–620.

Bloemen, H. H. J., Chou, C. T., van den Boom, T. J. J., Verdult, V., Verhaegen, M., and Backx, T. C. (2001b). Wiener model identification and predictive control for dual composition control of a distillation column. *Journal of Process Control*, 11(6):601–620.

Boutayeb, M. and Darouach, M. (1995). Recursive identification method for MISO Wiener - Hammerstein model. *IEEE Transactions on Automatic Control*, 40:287–291.

Bouzrara, K., Garna, T., Ragot, J., and Messaoud, H. (2012). Decomposition of an ARX model on Laguerre orthonormal bases. *ISA Transactions*, 51(6):848 – 860.

Brown, M., Lightbody, G., and Irwin, G. (1997). Nonlinear internal model control using local model networks. *Control Theory and Applications, IEE Proceedings* -, 144(6):505–514.

Cai, Y., Wang, H., Ye, X., and Fan, Q. (2013). A multiple-kernel lssvr method for separable nonlinear system identification. *Control Theory and Technology*, 11(4):651–655.

Cao, Y. (2005). A formulation of nonlinear model predictive control using automatic differentiation. *Journal of Process Control*, 15(8):851 – 858.

Cao, Y. and Chen, W.-H. (2014). Variable sampling-time nonlinear model predictive control of satellites using magneto-torquers. *Systems Science & Control Engineering*, 2(1):593–601.

Chen, S. and Billings, S. A. (1992). Neural networks for nonlinear system modeling and identification. *International Journal of Control*, 56(2):319–346.

Chen, T. and Ljung, L. (2015). Regularized system identification using orthonormal basis functions. In *Control Conference (ECC), 2015 European*, pages 1291–1296.

Chen, W.-H. and Cao, Y. (2012). Stability analysis of constrained nonlinear model predictive control with terminal weighting. *Asian Journal of Control*, 14(5):1374–1381.

Cheng, C., Peng, Z., Zhang, W., and Meng, G. (2017). Volterra-series-based nonlinear system modeling and its engineering applications: A state-of-the-art review. *Mechanical Systems and Signal Processing*, 87:340–364.

Cheng, L., Liu, W., Hou, Z. G., Yu, J., and Tan, M. (2015). Neural-network-based nonlinear model predictive control for piezoelectric actuators. *IEEE Transactions on Industrial Electronics*, 62(12):7717–7727.

Chou, H.-T. (2017). Orthogonal basis functions in discrete-time electromagnetics and their implementation to compute the matrix-type utd transition function for pec wedge diffractions. *IEEE Transactions on Antennas and Propagation*, 65(2):741–750.

Clerget, C.-H., Grimaldi, J.-P., Chèbre, M., and Petit, N. (2017). An example of robust internal model control under variable and uncertain delay.

Cutler, C. R. and Ramaker, B. L. (1980). Dynamic matrix control - a computer control algorithm. In *Proceedings of the Joint Automatic Contrl Conference*.

da Rosa, A., Campello, R., and Amaral, W. (2009). Exact search directions for optimization of linear and nonlinear models based on generalized orthonormal functions. *IEEE Transactions on Automatic Control*, 54(12):2757–2772.

Daubechies, I. (1992). *Ten Lectures on Wavelets*. Society of Industrial and Applied Mathematics, Philadelphia.

Dijoux, E., Steiner, N. Y., Benne, M., Péra, M.-C., and Pérez, B. G. (2017). A review of fault tolerant control strategies applied to proton exchange membrane fuel cell systems. *Journal of Power Sources*, 359:119 – 133.

Ding, F., Liu, X., and Liu, M. (2016). The recursive least squares identification algorithm for a class of wiener nonlinear systems. *Journal of the Franklin Institute*, 353(7):1518 – 1526.

Ding, W.-h., Deng, H., Xia, Y.-m., and Duan, X.-g. (2017). Tracking control of electro-hydraulic servo multi-closed-chain mechanisms with the use of an approximate nonlinear internal model. *Control Engineering Practice*, 58:225–241.

Economou, C. G., Morari, M., and Palsson, B. O. (1986). Internal model control: extension to nonlinear system. *Industrial & Engineering Chemistry Process Design and Development*, 25(2):403–411.

Falck, T., Dreesen, P., Brabanter, K. D., Pelckmans, K., Moor, B. D., and Suykens, J. A. (2012). Least-squares support vector machines for the identification of Wiener-Hammerstein systems. *Control Engineering Practice*, 20(11):1165 – 1174.

Forlenza, G. P., Deshpande, S., Ly, T. T., Howsmon, D. P., Cameron, F., Baysal, N., Mauritzen, E., Marcal, T., Towers, L., Bequette, B. W., Huyett, L. M., Pinsker, J. E., Gondhalekar, R., Doyle, F. J., Maahs, D. M., Buckingham, B. A., and Dassau, E. (2017). Application of zone model predictive control artificial pancreas during extended use of infusion set and sensor: A randomized crossover-controlled home-use trial. *Diabetes Care*.

Garcia, C. E. and Morari, M. (1982). Internal model control. a unifying review and some new results. *Industrial & Engineering Chemistry Process Design and Development*, 21(2):308–323.

Garcia, C. E. and Morari, M. (1985a). Internal model control. 2. design procedure for multivariable systems. *Industrial & Engineering Chemistry Process Design and Development*, 24(2):472–484.

Garcia, C. E. and Morari, M. (1985b). Internal model control. 3. multivariable control law computation and tuning guidelines. *Industrial & Engineering Chemistry Process Design and Development*, 24(2):484–494.

Garna, T., Bouzrara, K., Ragot, J., and Messaoud, H. (2013a). Nonlinear system modeling based on bilinear laguerre orthonormal bases. {*ISA*} *Transactions*, 52(3):301 – 317.

Garna, T., Bouzrara, K., Ragot, J., and Messaoud, H. (2013b). Nonlinear system modeling based on bilinear Laguerre orthonormal bases. *ISA Transactions*, 52(3):301 – 317.

Goethals, I., Pelckmans, K., Suykens, J. A., and Moor, B. D. (2005). Identification of MIMO Hammerstein models using least squares support vector machines. *Automatica*, 41(7):1263 – 1272.

Han, H. and Qiao, J. (2014). Nonlinear model-predictive control for industrial processes: An application to wastewater treatment process. *IEEE Transactions on Industrial Electronics*, 61(4):1970–1982.

He, W., Qian, F., and Cao, J. (2017a). Pinning-controlled synchronization of delayed neural networks with distributed-delay coupling via impulsive control. *Neural Networks*, 85:1–9.

He, X., Wang, Z., Liu, Y., Qin, L., and Zhou, D. (2017b). Fault-tolerant control for an internet-based three-tank system: Accommodation to sensor bias faults. *IEEE Transactions on Industrial Electronics*, 64(3):2266–2275.

Henson, M. A. and Seborg, D. E. (1990). Input-output linearization of general nonlinear processes. *AIChE Journal*, 36(11):1753–1757.

Henson, M. A. and Seborg, D. E. (1991). An internal model control strategy for nonlinear systems. *AIChE Journal*, 37(7):1065–1081.

Huang, C. T. and Chou, C. J. (1994). Estimation of the underdamped second-order parameters from the system transient. *Industrial & Engineering Chemistry Research*, 33(1):174–176.

Huang, Y., Lou, H., Gong, J., and Edgar, T. (2000). Fuzzy model predictive control. *Fuzzy Systems, IEEE Transactions on*, 8(6):665–678.

Kalafatis, A., Arifin, N., Wang, L., and Cluett, W. R. (1995). A new approach to identification of pH processes based on the Wiener model. *Chemical Engineering Science*, 50:3696–3701.

Kautz, W. H. (1954). Transient synthesis in the time domain. *Transactions of the IRE Professional Group on Circuit Theory*, CT-1(3):29–39.

Khan, B., Rossiter, J. A., and Valencia-Palomo, G. (2011). Exploiting Kautz functions to improve feasibility in MPC. In *Preprints of the 18th IFAC World Congress Milano (Italy) August 28 – September 2, 2011*, pages 6777–6782.

Lakshminarayanan, S., L.Shah, S., and Nandhakumar, K. (1995). Identification of hammerstein using multivariate statistical tools. *Chemical Engineering Science*, 50 (22):3599–3613.

Ławryńczuk, M. (2010). Suboptimal nonlinear predictive control based on multivariable neural hammerstein models. *Applied Intelligace*, 32(2):173 – 192.

Ławryńczuk, M. (2013). Practical nonlinear predictive control algorithms for neural wiener models. *Journal of Process Control*, 23(5):696 – 714.

Ławryńczuk, M. (2015). Nonlinear predictive control for hammerstein-wiener systems. *ISA Transactions*, 55:49 – 62.

Ławryńczuk, M. (2016a). Modelling and predictive control of a neutralisation reactor using sparse support vector machine wiener models. *Neurocomputing*, 205:311 – 328.

Ławryńczuk, M. (2016b). Nonlinear predictive control of dynamic systems represented by wienerhammerstein models. *Nonlinear dynamics*, 86:1193 – 1214.

Linhares, L. L. S., Araújo, Jr., J. M., Araújo, F. M. U., and Yoneyama, T. (2015). A nonlinear system identification approach based on fuzzy wavelet neural network. *J. Intell. Fuzzy Syst.*, 28(1):225–235.

Ljung, L. (1999). *System Identification: Theory for the User*. Prentice-Hall, Upper Saddle River, NJ.

Lu, Q., Shi, P., Lam, H. K., and Zhao, Y. (2015). Interval type-2 fuzzy model predictive control of nonlinear networked control systems. *IEEE Transactions on Fuzzy Systems*, 23(6):2317–2328.

Mahmoodi, S., Poshtan, J., Jahed-Motlagh, M. R., and Montazeri, A. (2009). Nonlinear model predictive control of a pH neutralization process based on Wiener-Laguerre model. *Chemical Engineering Journal*, 146(3):328 – 337.

Mangan, N. M., Kutz, J. N., Brunton, S. L., and Proctor, J. L. (2017). Model selection for dynamical systems via sparse regression and information criteria. *arXiv preprint arXiv:1701.01773*.

Manohar, M. and Das, S. (2017). Current sensor fault-tolerant control for direct torque control of induction motor drive using flux linkage observer. *IEEE Transactions on Industrial Informatics*, PP(99):1–1.

Masnadi-Shirazi, M. A. and Aleshams, M. (2003). Laguerre discrete-time filter desgin. *Computers and Electrical Engineering*, 29:173–192.

Mayne, D. Q. (2014). Model predictive control: Recent developments and future promise. *Automatica*, 50(12):2967 – 2986.

Mittal, A. and Aadaleesan, P. (2012). A new hammerstein model for non-linear system identification. *algorithms*, 11:13.

Münker, T. and Nelles, O. (2016). Nonlinear system identification with regularized local fir model networks. *IFAC-PapersOnLine*, 49(5):61 – 66. 4th IFAC Conference on Intelligent Control and Automation SciencesICONS 2016.

Nahas, E., Henson, M., and Seborg, D. (1992). Nonlinear internal model control strategy for neural network models. *Computers & Chemical Engineering*, 16(12):1039 – 1057.

Nath, U. M., Dey, C., and Mudi, R. K. (2017). Fuzzy-based adaptive imc-pi controller for real-time application on a level control loop. In *Proceedings of the 5th International Conference on Frontiers in Intelligent Computing: Theory and Applications*, pages 387–395. Springer.

Ninness, B. (1996). Frequency domain estimation using orthonormal bases. *IFAC Proceedings Volumes*, 29(1):4309 – 4314. 13th World Congress of IFAC, 1996, San Francisco USA, 30 June - 5 July.

Niva, L. and Yli-Korpela, A. (2012). Control of a benchmark boiler process model with dmc and qdmc. *IFAC Proceedings Volumes*, 45(21):190–195.

Norquay, S. J., Palazoglu, A., and Romagnoli, J. A. (1999). Application of Wiener model predictive control (WMPC) to an industrial C_2-splitter. *Journal of Process Control*, 9(6):461–473.

Ogunnaike, B. A. and Ray, W. H. (1994). *Process dynamics, modeling, and control*. Oxford University Press, New York.

Oliveira, G. H., da Rosa, A., Campello, R. J., Machado, J. B., and Amaral, W. C. (2012). An introduction to models based on laguerre, kautz and other related orthonormal functions–part ii: non-linear models. *International Journal of Modelling, Identification and Control*, 16(1):1–14.

Othman, C., Cheikh, I. B., and Bouzaouache, H. (2016). A nonlinear internal model controller for affine nonlinear discrete-time systems. In *2016 17th International Conference on Sciences and Techniques of Automatic Control and Computer Engineering (STA)*, pages 48–53.

Pasieka, M., Grzesik, N., and Kuźma, K. (2017). Simulation modeling of fuzzy logic controller for aircraft engines. *International Journal of Computing*, 16(1):27–33.

Patwardhan, R. S., Lakshminarayanan, S., and Shah, S. L. (1998). Constrained nonlinear MPC using Hammerstein and Wiener models: PLS framework. *AIChE Journal*, 44(7):1611–1622.

Prakash, J. and Srinivasan, K. (2009). Design of nonlinear PID controller and nonlinear model predictive controller for a continuous stirred tank reactor . *ISA Transactions*, 48(3):273 – 282.

Propoi, A. I. (1963). Use of linear programming methods for synthesizing sampled-data automatic systems. *Automation and Remote Control*, 24 (7):837–844.

Qing-chao Wang, J.-z. Z. (2011). Wiener model identification and nonlinear model predictive control of a pH neutralization process based on Laguerre filters and least squares support vector machines. *Journal of Zhejiang University Science C*, 12(1):25–35.

Qiu, Z. (2017). *Composite Adaptive Internal Model Control: Theory and Applications to Engine Control*. PhD thesis, The University of Michigan.

Rahman, T. A. Z. (2016). Parametric modelling of twin rotor system using chaotic fractal search algorithm. In *2016 7th IEEE Control and System Graduate Research Colloquium (ICSGRC)*, pages 34–39.

Rawlings, J. and Mayne, D. (2009). *Model Predictive Control: Theory and Design*. Nob Hill Pub.

Reddy, R. and Saha, P. (2017a). Kautz filters based model predictive control for resonating systems. *International Journal of Dynamics and Control*, 5(3):477–495.

Reddy, R. and Saha, P. (2017b). Modelling and control of nonlinear resonating processes: part i—system identification using orthogonal basis function. *International Journal of Dynamics and Control*, 5(4):1222–1236.

Reddy, R. and Saha, P. (2017c). Modelling and control of nonlinear resonating processes: part ii—model based control using orthogonal basis function based wiener models. *International Journal of Dynamics and Control*, 5(4):1237–1251.

Richalet, J., Rault, A., Testud, J., and Papon, J. (1978). Model predictive heuristic control. *Automatica*, 14(5):413 – 428.

Rivals, I. and Personnaz, L. (2000). Nonlinear internal model control using neural networks: application to processes with delay and design issues. *IEEE Transactions on Neural Networks*, 11(1):80–90.

Rouhani, R. and Mehra, R. K. (1982). Model algorithmic control (mac); basic theoretical properties. *Automatica*, 18(4):401 – 414.

Saha, P. (1998). *Nonlinear model predictive control for chemical processes using Laguerre models*. PhD thesis, Indian Institute of Technology-Madras, Chennai, India.

Saha, P., Krishnan, S. H., Rao, V. S. R., and Patwardhan, S. C. (2004). Modeling and predictive control of MIMO nonlinear systems using Wiener-Laguerre models. *Chemical Engineering Communications*, 191(8):1083–1119.

Senthil, R., Janarthanan, K., and Prakash, J. (2006). Nonlinear state estimation using fuzzy kalman filter. *Industrial & Engineering Chemistry Research*, 45(25):8678–8688.

Seyab, R. A. and Cao, Y. (2008a). Differential recurrent neural network based predictive control. *Computers & Chemical Engineering*, 32(7):1533 – 1545.

Seyab, R. A. and Cao, Y. (2008b). Nonlinear system identification for predictive control using continuous time recurrent neural networks and automatic differentiation. *Journal of Process Control*, 18(6):568 – 581.

Seyab, R. K. A., Cao, Y., and Yang, S. H. (2006). Predictive control for the alstom gasifier problem. *IEE Proceedings - Control Theory and Applications*, 153(3):293–301.

Shafiee, G., Arefi, M. M., Jahed-Motlagh, M. R., and Jalali, A. A. (2008). Nonlinear predictive control of a polymerization reactor based on piecewise linear Wiener model. *Chemical Engineering Journal*, 143 (1-3):282–292.

Shen, W., Gao, X., Yang, F., Jiang, Y., Ye, H., and Huang, D. (2017). Identification of fir models using basis models of first-order plus time delays. In *2017 6th International Symposium on Advanced Control of Industrial Processes (AdCONIP)*, pages 239–244.

Srinivasagupta, D., Schttler, H., and Joseph, B. (2004). Time-stamped model predictive control: an algorithm for control of processes with random delays. *Computers & Chemical Engineering*, 28(8):1337 – 1346.

Stanisawski, R., Latawiec, K. J., Gaek, M., and ukaniszyn, M. (2014). Modeling and identification of a fractional-order discrete-time siso laguerre-wiener system. In *2014 19th International Conference on Methods and Models in Automation and Robotics (MMAR)*, pages 165–168.

Suykens, J. and Vandewalle, J. (1999). Least squares support vector machine classifiers. *Neural Processing Letters*, 9(3):293–300.

Tang, Y., Han, Z., Liu, F., and Guan, X. (2016). Identification and control of nonlinear system based on laguerre-elm wiener model. *Communications in Nonlinear Science and Numerical Simulation*, 38:192 – 205.

Tiels, K. and Schoukens, J. (2014). Wiener system identification with generalized orthonormal basis functions. *Automatica*, 50(12):3147 – 3154.

Totterman, S. and Toivonen, H. T. (2009). Support vector method for identification of Wiener models. *Journal of Process Control*, 19(7):1174 – 1181.

Vairetti, G., van Waterschoot, T., Moonen, M., Catrysse, M., and Jensen, S. H. (2014). An automatic model-building algorithm for sparse approximation of room impulse responses with orthonormal basis functions. In *Acoustic Signal Enhancement (IWAENC), 2014 14th International Workshop on*, pages 248–252. IEEE.

Vapnik, V. N. (1998). *Statistical learning theory*. Wiley, 1 edition.

Voorakaranam, S. and Joseph, B. (1999). Model predictive inferential control with application to a composites manufacturing process. *Industrial & Engineering Chemistry Research*, 38(2):433–450.

Wahlberg, B. (1991a). Identification of resonant systems using Kautz filters. In *Decision and Control, 1991., Proceedings of the 30th IEEE Conference on*, volume 2, pages 2005–2010.

Wahlberg, B. (1991b). System identification using Laguerre models. *Automatic Control, IEEE Transactions on*, 36(5):551–562.

Wahlberg, B. and Mäkilä, P. M. (1996). On approximation of stable linear dynamical systems using Laguerre and Kautz functions. *Automatica*, 32(5):693 – 708.

Wang, D., Ding, F., and Ximei, L. (2014). Least squares algorithm for an input nonlinear system with a dynamic subspace state space model. *Nonlinear Dynamics*, 75(1):49–61.

Wang, L. (2004). Discrete model predictive controller design using Laguerre functions. *Journal of Process Control*, 14(2):131 – 142.

Wang, L. (2009). *Model Predictive Control System Design and Implementation Using MATLAB*. Springer Publishing Company, Incorporated, 1st edition.

Wang, Q. C. and Zhang, J. Z. (2011). Wiener model identification and nonlinear model predictive control of a pH neutralization process based on Laguerre filters and least squares support vector machines. *Journal of Zhejiang University SCIENCE C*, 12(1):25–35.

Wang, S., Han, Z., Liu, F., and Tang, Y. (2015). Nonlinear system identification using least squares support vector machine tuned by an adaptive particle swarm optimization. *International Journal of Machine Learning and Cybernetics*, 6(6):981–992.

Wang, T., Gao, H., and Qiu, J. (2016). A combined adaptive neural network and nonlinear model predictive control for multirate networked industrial process control. *IEEE Transactions on Neural Networks and Learning Systems*, 27(2):416–425.

Wang, X., Ratnaweera, H., Holm, J. A., and Olsbu, V. (2017). Statistical monitoring and dynamic simulation of a wastewater treatment plant: A combined approach to achieve model predictive control. *Journal of Environmental Management*, 193:1 – 7.

Xi, Y.-G., LI, D.-W., and LIN, S. (2013). Model predictive control-status and challenges. *Acta Automatica Sinica*, 39(3):222 – 236.

Ying, C.-M. and Joseph, B. (1999a). Identification of stable linear systems using polynomial kernels. *Industrial & Engineering Chemistry Research*, 38(12):4712–4728.

Ying, C.-M. and Joseph, B. (1999b). Performance and stability analysis of lp-mpc and qp-mpc cascade control systems. *AIChE Journal*, 45(7):1521–1534.

Ying, C.-M. and Joseph, B. (1999c). System identification of chemical processes in frequency domain using polynomial model. *Submitted to Jl of Process Control*.

Yousefzadeh, A. and Jahanian, O. (2017). Using detailed chemical kinetics 3d-cfd model to investigate combustion phase of a cng-hcci engine according to control strategy requirements. *Energy Conversion and Management*, 133:524 – 534.

Zabidi, A., Tahir, N. M., Yassin, I. M., and Rizman, Z. I. (2017). The performance of binary artificial bee colony (babc) in structure selection of polynomial narx and narmax models. *International Journal on Advanced Science, Engineering and Information Technology*, 7(2):373–379.

Zabiri, H., Ariff, M., Tufa, L. D., and Ramasamy, M. (2014a). A comparison study between integrated obfarx-nn and obf-nn for modeling of nonlinear systems in extended regions of operation. In *Applied Mechanics and Materials*, volume 625, pages 382–385. Trans Tech Publ.

Zabiri, H., Fadzil, M., Tufa, L., Ramasamy, M., Zabiri, H., Ramasamy, M., Tufa, L. D., and Maulud, A. (2014b). Modeling of nonlinear systems using parallel obf-wavelet networks

model. *Recent advances in mathematical methods, mathematical models and simulation in science and egieering*, page 206.

Zabiri, H., Marappagounder, R., and Lemma, T. D. (2016). A study on the closed-loop performance in extrapolated regions of operations of nonlinear systems using parallel obf-nn models. *Journal of chemical egineering og japan*, 49(2):176–185.

Zabiri, H., Ramasamy, M., Tufa, L. D., and Maulud, A. (2013). Integrated obf-nn models with enhanced extrapolation capability for nonlinear systems. *Journal of Process Control*, 23(10):1562 – 1566.

Zenan Šehiċ, Z. v. G. (2012). Comparation study for PID and MPC controller based on orthonormal functions. volume 1, pages 1700–1704. EDIS - Publishing Institution of the University of Zilina.

Zhang, Q. (1997). Using wavelet network in nonparametric estimation. *Neural Networks, IEEE Transactions on*, 8(2):227–236.

Zhang, Q. and Benveniste, A. (1992). Wavelet networks. *Neural Networks, IEEE Transactions on*, 3(6):889–898.

Zheng, A., Kotheare, M. V., and Morari, M. (1994). Anti-windup design for internal model control. *International Journal of Control*, 60(5):1015–1024.

Appendix A

Detailed Derivation of Recursive Linear Kautz functions Model

By taking the inverse $\mathcal{Z}$-transform of the Kautz functions defined in Theorem 2.1 as

$$\Psi(k) = \mathcal{Z}^{-1}\Psi(z) \tag{A1}$$

and expressing the i^{th} pole-pairs of the Kautz model parameters as

$$\begin{aligned} h_1^{(i)} &= -\left(\beta_i + \beta_i^*\right) \\ h_2^{(i)} &= \beta_i\beta_i^* \end{aligned} \tag{A2}$$

the odd Kautz functions, given in Eq. 2.1 of Theorem 2.1, can further be derived as

$$\begin{aligned} \Psi_{2i-1}(z) &= C_o^{(i)}\left(1 - a_o^{(i)}z\right)\Gamma^{(i)}(z) \\ &= C_o^{(i)}\left(1 - a_o^{(i)}z\right) \times \frac{\left(1-\beta_i z\right)\left(1-\beta_i^* z\right)}{\left(z-\beta_i\right)\left(z-\beta_i^*\right)}\Gamma^{(i-1)}(z) \\ &= C_o^{(i)}\left(1 - a_o^{(i)}z\right) \times \frac{1-\left(\beta_i+\beta_i^*\right)z+\beta_i\beta_i^* z^2}{z^2-\left(\beta_i+\beta_i^*\right)z+\beta_i\beta_i^*} \times \frac{\Psi_{2(i-1)-1}(z)}{C_o^{(i-1)}\left(1 - a_o^{(i-1)}z\right)} \\ &= \frac{C_o^{(i)}\left(a_o^{(i)}z - 1\right)}{C_o^{(i-1)}\left(a_o^{(i-1)}z - 1\right)} \times \frac{h_2^{(i)}z^2 + h_1^{(i)}z + 1}{z^2 + h_1^{(i)}z + h_2^{(i)}} \times \Psi_{2(i-1)-1}(z) \\ &= \frac{C_o^{(i)}a_o^{(i)}h_2^{(i)}}{C_o^{(i-1)}a_o^{(i-1)}} \times \frac{\left(z - \frac{1}{a_o^{(i)}}\right)}{\left(z - \frac{1}{a_o^{(i-1)}}\right)} \times \frac{\left(z^2 + \frac{h_1^{(i)}}{h_2^{(i)}}z + \frac{1}{h_2^{(i)}}\right)}{z^2 + h_1^{(i)}z + h_2^{(i)}} \\ &\quad \times \Psi_{2(i-1)-1}(z) \\ &= \frac{C_o^{(i)}a_o^{(i)}h_2^{(i)}}{C_o^{(i-1)}a_o^{(i-1)}} \end{aligned}$$

$$\times \frac{z^3 + \left(\frac{h_1^{(i)}}{h_2^{(i)}} - \frac{1}{a_o^{(i)}}\right) z^2 + \left(\frac{1}{h_2^{(i)}} - \frac{h_1^{(i)}}{a_o^{(i)} h_2^{(i)}}\right) z - \frac{1}{a_o^{(i)} h_2^{(i)}}}{z^3 - \left(\frac{1}{a_o^{(i-1)}} - h_1^{(i)}\right) z^2 - \left(\frac{h_1^{(i)}}{a_o^{(i-1)}} - h_2^{(i)}\right) z - \frac{h_2^{(i)}}{a_o^{(i-1)}}}$$

$$\times \Psi_{2(i-1)-1}(z)$$

$$= p_{o,0}^{(i)} \times \frac{z^3 + p_{o,1}^{(i)} z^2 + p_{o,2}^{(i)} z + p_{o,3}^{(i)}}{z^3 - p_{o,4}^{(i)} z^2 - p_{o,5}^{(i)} z - p_{o,6}^{(i)}} \times \Psi_{2(i-1)-1}(z) \tag{A3}$$

and the even Kautz functions, given in Eq. 2.2 of Theorem 2.1, can further be derived as

$$\begin{aligned}
\Psi_{2i}(z) &= C_e^{(i)} \left(1 - a_e^{(i)} z\right) \Gamma^{(i)}(z) \\
&= C_e^{(i)} \left(1 - a_e^{(i)} z\right) \times \frac{(1 - \beta_i z)(1 - \beta_i^* z)}{(z - \beta_i)(z - \beta_i^*)} \Gamma^{(i-1)}(z) \\
&= C_e^{(i)} \left(1 - a_e^{(i)} z\right) \times \frac{1 - (\beta_i + \beta_i^*) z + \beta_i \beta_i^* z^2}{z^2 - (\beta_i + \beta_i^*) z + \beta_i \beta_i^*} \times \frac{\Psi_{2(i-1)}(z)}{C_e^{(i-1)} \left(1 - a_e^{(i-1)} z\right)} \\
&= \frac{C_e^{(i)} \left(a_e^{(i)} z - 1\right)}{C_e^{(i-1)} \left(a_e^{(i-1)} z - 1\right)} \times \frac{h_2^{(i)} z^2 + h_1^{(i)} z + 1}{z^2 + h_1^{(i)} z + h_2^{(i)}} \times \Psi_{2(i-1)}(z) \\
&= \frac{C_e^{(i)} a_e^{(i)} h_2^{(i)}}{C_e^{(i-1)} a_e^{(i-1)}} \times \frac{\left(z - \frac{1}{a_e^{(i)}}\right)}{\left(z - \frac{1}{a_e^{(i-1)}}\right)} \times \frac{\left(z^2 + \frac{h_1^{(i)}}{h_2^{(i)}} z + \frac{1}{h_2^{(i)}}\right)}{z^2 + h_1^{(i)} z + h_2^{(i)}} \\
&\quad \times \Psi_{2(i-1)}(z) \\
&= \frac{C_e^{(i)} a_e^{(i)} h_2^{(i)}}{C_e^{(i-1)} a_e^{(i-1)}} \\
&\quad \times \frac{z^3 + \left(\frac{h_1^{(i)}}{h_2^{(i)}} - \frac{1}{a_e^{(i)}}\right) z^2 + \left(\frac{1}{h_2^{(i)}} - \frac{h_1^{(i)}}{a_e^{(i)} h_2^{(i)}}\right) z - \frac{1}{a_e^{(i)} h_2^{(i)}}}{z^3 - \left(\frac{1}{a_e^{(i-1)}} - h_1^{(i)}\right) z^2 - \left(\frac{h_1^{(i)}}{a_e^{(i-1)}} - h_2^{(i)}\right) z - \frac{h_2^{(i)}}{a_e^{(i-1)}}} \\
&\quad \times \Psi_{2(i-1)}(z) \\
&= p_{e,0}^{(i)} \times \frac{z^3 + p_{e,1}^{(i)} z^2 + p_{e,2}^{(i)} z + p_{e,3}^{(i)}}{z^3 - p_{e,4}^{(i)} z^2 - p_{e,5}^{(i)} z - p_{e,6}^{(i)}} \times \Psi_{2(i-1)}(z)
\end{aligned} \tag{A4}$$

The suffices "o" and "e" indicate the corresponding parameters of the odd and even Kautz functions respectively. These suffices are collectively represented as suffice "g"

$$p_{g,0}^{(i)} = \frac{C_g^{(i)} a_g^{(i)} h_2^{(i)}}{C_g^{(i-1)} a_g^{(i-1)}} \tag{A5}$$

$$p_{g,1}^{(i)} = \frac{h_1^{(i)}}{h_2^{(i)}} - \frac{1}{a_g^{(i)}} \tag{A6}$$

$$p_{g,2}^{(i)} = \frac{1}{h_2^{(i)}} - \frac{h_1^{(i)}}{a_g^{(i)} h_2^{(i)}} \tag{A7}$$

$$p_{g,3}^{(i)} = -\frac{1}{a_g^{(i)} h_2^{(i)}} \tag{A8}$$

$$p_{g,4}^{(i)} = \frac{1}{a_g^{(i-1)}} - h_1^{(i)} \tag{A9}$$

$$p_{g,5}^{(i)} = \frac{h_1^{(i)}}{a_g^{(i-1)}} - h_2^{(i)} \tag{A10}$$

$$p_{g,6}^{(i)} = \frac{h_2^{(i)}}{a_g^{(i-1)}} \tag{A11}$$

The odd Kautz functions in Eq. A3 can be represented in discrete time domain as following

$$\begin{aligned} z^3 \Psi_{2i-1}(z) &= \left\{ p_{o,4}^{(i)} z^2 + p_{o,5}^{(i)} z + p_{o,6}^{(i)} \right\} \Psi_{2i-1}(z) \\ &\quad + p_{o,0}^{(i)} \left\{ z^3 + p_{o,1}^{(i)} z^2 + p_{o,2}^{(i)} z + p_{o,3}^{(i)} \right\} \Psi_{2(i-1)-1}(z) \end{aligned}$$

$$\begin{aligned} \Psi_{2i-1}(k+3) &= p_{o,4}^{(i)} \Psi_{2i-1}(k+2) + p_{o,5}^{(i)} \Psi_{2i-1}(k+1) \\ &\quad + p_{o,6}^{(i)} \Psi_{2i-1}(k) + p_{o,0}^{(i)} \left\{ \Psi_{2(i-1)-1}(k+3) \right. \\ &\quad + p_{o,1}^{(i)} \Psi_{2(i-1)-1}(k+2) + p_{o,2}^{(i)} \Psi_{2(i-1)-1}(k+1) \\ &\quad \left. + p_{o,3}^{(i)} \Psi_{2(i-1)-1}(k) \right\} \end{aligned} \tag{A12}$$

For $i = 1$ the structure of the Kautz functions is a bit different from the cases with $i \neq 1$,

$$\begin{aligned}
\Gamma^{(1)}(z) &= \frac{1}{(z-\beta_1)(z-\beta_1^*)} \\
\Psi_1(z) &= C_o^{(1)}\left(1-a_o^{(1)}z\right)\Gamma^{(1)}(z) = \frac{C_o^{(1)}\left(1-a_o^{(1)}z\right)}{(z-\beta_1)(z-\beta_1^*)} \\
&= \frac{C_o^{(1)}\left(1-a_o^{(1)}z\right)}{z^2-(\beta_1+\beta_1^*)z+\beta_1\beta_1^*} \\
&= \frac{C_o^{(1)}\left(1-a_o^{(1)}z\right)}{z^2+h_1^{(1)}z+h_2^{(1)}} \qquad \text{(A13)} \\
\Psi_1(k+2) &= -h_1^{(1)}\Psi_1(k+1) - h_2^{(1)}\Psi_1(k) \qquad \text{(A14)}
\end{aligned}$$

and long division of Eq.A13 leads to the following z-domain form

$$\begin{aligned}
\Psi_1(z) &= -C_o^{(1)}a_o^{(1)}z^{-1} + C_o^{(1)}\left\{1+a_o^{(1)}h_1^{(1)}\right\}z^{-2} \\
&\quad + C_o^{(1)}\left[a_o^{(1)}h_2^{(1)} - h_1^{(1)}\left\{1+a_o^{(1)}h_1^{(1)}\right\}\right]z^{-3} + \cdots \qquad \text{(A15)}
\end{aligned}$$

with

$$\begin{aligned}
\Psi_1(1) &= -C_o^{(1)}a_o^{(1)} \\
\Psi_1(2) &= C_o^{(1)}\left\{1+a_o^{(1)}h_1^{(1)}\right\} \\
\Psi_1(3) &= C_o^{(1)}\left\{a_o^{(1)}h_2^{(1)} - h_1^{(1)}\left(1+a_o^{(1)}h_1^{(1)}\right)\right\} \qquad \text{(A16)}
\end{aligned}$$

For any $i(i \neq 1)$, the general expression for the odd Kautz functions can be derived by using long division method on Eq. A3.

$$\begin{aligned}
\Psi_{2i-1}(z) &= p_{o,0}^{(i)} \times \left[1 + \left(p_{o,1}^{(i)} + p_{o,4}^{(i)}\right)z^{-1}\right. \\
&\quad \left. + \left\{\left(p_{o,2}^{(i)} + p_{o,5}^{(i)}\right) + p_{o,4}^{(i)}\left(p_{o,1}^{(i)} + p_{o,4}^{(i)}\right)\right\}z^{-2} + \cdots\right] \\
&\quad \times \Psi_{2(i-1)-1}(z) \\
&= p_{o,0}^{(i)} \times \left[1 + \left(p_{o,1}^{(i)} + p_{o,4}^{(i)}\right)z^{-1}\right.
\end{aligned}$$

$$
\begin{aligned}
&+\left\{\left(p_{o,2}^{(i)}+p_{o,5}^{(i)}\right)+p_{o,4}^{(i)}\left(p_{o,1}^{(i)}+p_{o,4}^{(i)}\right)\right\}z^{-2}+\cdots\Big] \\
&\times\left[\Psi_{2(i-1)-1}(0)\,z^{-1}+\Psi_{2(i-1)-1}(1)\,z^{-2}\right. \\
&\left.+\Psi_{2(i-1)-1}(2)\,z^{-3}+\cdots\right] \\
=\;& p_{o,0}^{(i)}\Psi_{2(i-1)-1}(0)\,z^{-1}+p_{o,0}^{(i)}\left\{\Psi_{2(i-1)-1}(1)+\Psi_{2(i-1)-1}(0)\left(p_{o,1}^{(i)}+p_{o,4}^{(i)}\right)\right\}z^{-2} \\
&+p_{o,0}^{(i)}\left(\Psi_{2(i-1)-1}(2)+\Psi_{2(i-1)-1}(1)\left(p_{o,1}^{(i)}+p_{o,4}^{(i)}\right)+\Psi_{2(i-1)-1}(0)\right. \\
&\left.\left\{\left(p_{o,2}^{(i)}+p_{o,5}^{(i)}\right)+p_{o,4}^{(i)}\left(p_{o,1}^{(i)}+p_{o,4}^{(i)}\right)\right\}\right)z^{-3}+\cdots
\end{aligned}
\tag{A17}
$$

Using Eq. A17 the samples at time instants 1,2 and 3 were found as following.

$$
\begin{aligned}
\Psi_{2i-1}(1) &= p_{o,0}^{(i)}\Psi_{2(i-1)-1}(0) \\
\Psi_{2i-1}(2) &= p_{o,0}^{(i)}\left\{\Psi_{2(i-1)-1}(1)+\Psi_{2(i-1)-1}(0)\left(p_{o,1}^{(i)}+p_{o,4}^{(i)}\right)\right\} \\
\Psi_{2i-1}(3) &= p_{o,0}^{(i)}\left(\Psi_{2(i-1)-1}(2)+\Psi_{2(i-1)-1}(1)\left(p_{o,1}^{(i)}+p_{o,4}^{(i)}\right)\right. \\
&\quad\left.+\Psi_{2(i-1)-1}(0)\left\{\left(p_{o,2}^{(i)}+p_{o,5}^{(i)}\right)+p_{o,4}^{(i)}\left(p_{o,1}^{(i)}+p_{o,4}^{(i)}\right)\right\}\right)
\end{aligned}
$$

Now, from Eq. A14

$$
\Psi_1(k+3) = -h_1^{(1)}\Psi_1(k+2)-h_2^{(1)}\Psi_1(k+1) \tag{A18}
$$

For $i=2$, using Eq.A12 and Eq.A18

$$
\begin{aligned}
\Psi_3(k+3) &= p_{o,4}^{(2)}\Psi_3(k+2)+p_{o,5}^{(2)}\Psi_3(k+1)+p_{o,6}^{(2)}\Psi_3(k) \\
&\quad+p_{o,0}^{(2)}\left\{\Psi_1(k+3)+p_{o,1}^{(2)}\Psi_1(k+2)+p_{o,2}^{(2)}\Psi_1(k+1)+p_{o,3}^{(2)}\Psi_1(k)\right\} \\
&= p_{o,4}^{(2)}\Psi_3(k+2)+p_{o,5}^{(2)}\Psi_3(k+1)+p_{o,6}^{(2)}\Psi_3(k) \\
&\quad+p_{o,0}^{(2)}\left\{\left[-h_1^{(1)}\Psi_1(k+2)-h_2^{(1)}\Psi_1(k+1)\right]\right. \\
&\quad\left.+p_{o,1}^{(2)}\Psi_1(k+2)+p_{o,2}^{(2)}\Psi_1(k+1)+p_{o,3}^{(2)}\Psi_1(k)\right\} \\
&= p_{o,4}^{(2)}\Psi_3(k+2)+p_{o,5}^{(2)}\Psi_3(k+1)+p_{o,6}^{(2)}\Psi_3(k) \\
&\quad+p_{o,0}^{(2)}\left\{\left(p_{o,1}^{(2)}-h_1^{(1)}\right)\Psi_1(k+2)+\left(p_{o,2}^{(2)}-h_2^{(1)}\right)\Psi_1(k+1)+p_{o,3}^{(2)}\Psi_1(k)\right\} \\
&= p_{o,0}^{(2)}\left(p_{o,1}^{(2)}-h_1^{(1)}\right)\Psi_1(k+2)+p_{o,4}^{(2)}\Psi_3(k+2)
\end{aligned}
$$

$$+p_{o,0}^{(2)}\left(p_{o,2}^{(2)}-h_2^{(1)}\right)\Psi_1(k+1)+p_{o,5}^{(2)}\Psi_3(k+1)$$
$$+p_{o,0}^{(2)}p_{o,3}^{(2)}\Psi_1(k)+p_{o,6}^{(2)}\Psi_3(k) \tag{A19}$$

For $i=3$ and using Eq.A12 and Eq. A19

$$\begin{aligned}\Psi_5(k+3) &= p_{o,4}^{(3)}\Psi_{o,5}(k+2)+p_{o,5}^{(3)}\Psi_5(k+1)+p_{o,6}^{(3)}\Psi_5(k)\\ &\quad +p_{o,0}^{(3)}\Big[\Psi_3(k+3)+p_{o,1}^{(3)}\Psi_3(k+2)\\ &\quad +p_{o,2}^{(3)}\Psi_3(k+1)+p_{o,3}^{(3)}\Psi_3(k)\Big]\end{aligned}$$

$$\begin{aligned}\Psi_5(k+3) &= p_{o,4}^{(3)}\Psi_5(k+2)+p_{o,5}^{(3)}\Psi_5(k+1)+p_{o,6}^{(3)}\Psi_5(k)+p_{o,0}^{(3)}\Big\{p_{o,4}^{(2)}\\ &\quad \Psi_3(k+2)+p_{o,0}^{(2)}\left(p_{o,1}^{(2)}-h_1^{(1)}\right)\Psi_1(k+2)\\ &\quad +p_{o,5}^{(2)}\Psi_3(k+1)+p_{o,0}^{(2)}\left(p_{o,2}^{(2)}-h_2^{(1)}\right)\Psi_1(k+1)\\ &\quad +p_{o,6}^{(2)}\Psi_3(k)+p_{o,0}^{(2)}p_{o,3}^{(2)}\Psi_1(k)+p_{o,2}^{(3)}\Psi_3(k+1)+p_{o,3}^{(3)}\Psi_3(k)\Big\}\\ &\quad +p_{o,0}^{(3)}p_{o,1}^{(3)}\Psi_3(k+2)\\ &= p_{o,4}^{(3)}\Psi_5(k+2)+p_{o,5}^{(3)}\Psi_5(k+1)+p_{o,6}^{(3)}\Psi_5(k)\\ &\quad +\Bigg[p_{o,0}^{(3)}\left(p_{o,4}^{(2)}+p_{o,1}^{(3)}\right)\Psi_3(k+2)+\left(\prod_{i=2}^{3}p_{o,0}^{(i)}\right)\left(p_{o,1}^{(2)}-h_1^{(1)}\right)\\ &\quad \Psi_1(k+2)+p_{o,0}^{(3)}\left(p_{o,5}^{(2)}+p_{o,2}^{(3)}\right)\Psi_3(k+1)+\left(\prod_{i=2}^{3}p_{o,0}^{(i)}\right)\\ &\quad \left(p_{o,2}^{(2)}-h_2^{(1)}\right)\Psi_1(k+1)+p_{o,0}^{(3)}\left(p_{o,6}^{(2)}+p_{o,3}^{(3)}\right)\Psi_3(k)+\left(\prod_{i=2}^{3}p_{o,0}^{(i)}\right)p_{o,3}^{(2)}\Psi_1(k)\Bigg]\end{aligned}$$

$$\begin{aligned}&= \left(\prod_{i=2}^{3}p_{o,0}^{(i)}\right)\left(p_{o,1}^{(2)}-h_1^{(1)}\right)\Psi_1(k+2)+p_{o,0}^{(3)}\left(p_{o,4}^{(2)}+p_{o,1}^{(3)}\right)\\ &\quad \Psi_3(k+2)+p_{o,4}^{(3)}\Psi_5(k+2)+\left(\prod_{i=2}^{3}p_{o,0}^{(i)}\right)\left(p_{o,2}^{(2)}-h_2^{(1)}\right)\\ &\quad \Psi_1(k+1)+p_{o,0}^{(3)}\left(p_{o,5}^{(2)}+p_{o,2}^{(3)}\right)\Psi_3(k+1)\\ &\quad +p_{o,5}^{(3)}\Psi_5(k+1)\end{aligned}$$

$$+\left(\prod_{i=2}^{3} p_{o,0}^{(i)}\right) p_{o,3}^{(2)} \Psi_1(k) + p_{o,0}^{(3)} \left(p_{o,6}^{(2)} + p_{o,3}^{(3)}\right) \Psi_3(k)$$
$$+p_{o,6}^{(3)} \Psi_5(k) \tag{A20}$$

similarly for $i = 4$, using Eq.A12, Eq.A19 and Eq.A20

$$\begin{aligned}
\Psi_7(k+3) &= p_{o,4}^{(4)} \Psi_7(k+2) + p_{o,5}^{(4)} \Psi_7(k+1) + p_{o,6}^{(4)} \Psi_7(k) \\
&\quad + p_{o,0}^{(4)} \Big[\Psi_5(k+3) + p_{o,1}^{(4)} \Psi_5(k+2) \\
&\quad + p_{o,2}^{(4)} \Psi_5(k+1) + p_{o,3}^{(4)} \Psi_5(k) \Big] \\
&= \left(\prod_{i=2}^{4} p_{o,0}^{(i)}\right) \left(p_{o,1}^{(2)} - h_1^{(1)}\right) \Psi_1(k+2) \\
&\quad + \left(\prod_{i=3}^{4} p_{o,0}^{(i)}\right) \left(p_{o,4}^{(2)} + p_{o,1}^{(3)}\right) \Psi_3(k+2) \\
&\quad + p_{o,0}^{(4)} \left(p_{o,4}^{(3)} + p_{o,1}^{(4)}\right) \Psi_5(k+2) + p_{o,4}^{(4)} \Psi_7(k+2) \\
&\quad + \left(\prod_{i=2}^{4} p_{o,0}^{(i)}\right) \left(p_{o,2}^{(2)} - h_2^{(1)}\right) \Psi_1(k+1) \\
&\quad + \left(\prod_{i=3}^{4} p_{o,0}^{(i)}\right) \left(p_{o,5}^{(2)} + p_{o,2}^{(3)}\right) \Psi_3(k+1) \\
&\quad + p_{o,0}^{(4)} \left(p_{o,5}^{(3)} + p_{o,2}^{(4)}\right) \Psi_5(k+1) + p_{o,5}^{(4)} \Psi_7(k+1) \\
&\quad + \left(\prod_{i=2}^{4} p_{o,0}^{(i)}\right) p_{o,3}^{(2)} \Psi_1(k) + \left(\prod_{i=3}^{4} p_{o,0}^{(i)}\right) \left(p_{o,6}^{(2)} + p_{o,3}^{(3)}\right) \\
&\quad \Psi_3(k) + p_{o,0}^{(4)} \left(p_{o,6}^{(3)} + p_{o,3}^{(4)}\right) \Psi_5(k) + p_{o,6}^{(4)} \Psi_7(k)
\end{aligned} \tag{A21}$$

The Eq. A18, Eq. A19, Eq. A20 and Eq. A21 together can be written in a compact matrix form as given by the Eq. 2.29 and by analyzing the above derived matrix equality given in Eq. 2.29, one can easily observe that the set of Kautz functions can be represented in recursive manner that satisfies the following difference equation

with initial conditions $\Psi(1), \Psi(2)$ and $\Psi(3)$.

$$\begin{bmatrix} \Psi_1(k+3) \\ \Psi_3(k+3) \\ \Psi_5(k+3) \\ \Psi_7(k+3) \\ \vdots \\ \Psi_{2n-1}(k+3) \end{bmatrix} = \Omega_{2,o} \begin{bmatrix} \Psi_1(k+2) \\ \Psi_3(k+2) \\ \Psi_5(k+2) \\ \Psi_7(k+2) \\ \vdots \\ \Psi_{2n-1}(k+2) \end{bmatrix} + \Omega_{1,o} \begin{bmatrix} \Psi_1(k+1) \\ \Psi_3(k+1) \\ \Psi_5(k+1) \\ \Psi_7(k+1) \\ \vdots \\ \Psi_{2n-1}(k+1) \end{bmatrix} + \Omega_{0,o} \begin{bmatrix} \Psi_1(k) \\ \Psi_3(k) \\ \Psi_5(k) \\ \Psi_7(k) \\ \vdots \\ \Psi_{2n-1}(k) \end{bmatrix}$$

where the n^{th} rows of the matrices $\Omega_{2,o}$, $\Omega_{1,o}$and $\Omega_{0,o}$ are

$$\Omega_{2,o}(n) = \begin{bmatrix} \left\{\prod_{i=2}^{n} p_{o,0}^{(i)}\right\}\left(p_{o,1}^{(2)} - h_1^{(1)}\right) \\ \left\{\prod_{i=3}^{n} p_{o,0}^{(i)}\right\}\left(p_{o,4}^{(2)} + p_{o,1}^{(3)}\right) \\ \left\{\prod_{i=4}^{n} p_{o,0}^{(i)}\right\}\left(p_{o,4}^{(3)} + p_{o,1}^{(4)}\right) \\ \vdots \\ \left\{\prod_{i=n-1}^{n} p_{o,0}^{(i)}\right\}\left(p_{o,4}^{(n-2)} + p_{o,1}^{(n-1)}\right) \\ p_{o,0}^{(n)}\left(p_{o,4}^{(n-1)} + p_{o,1}^{(n)}\right) \\ p_{o,4}^{(n)} \end{bmatrix}^T \tag{A22}$$

$$\Omega_{1,o}(n) = \begin{bmatrix} \left\{\prod_{i=2}^{n} p_{o,0}^{(i)}\right\}\left(p_{o,2}^{(2)} - h_2^{(1)}\right) \\ \left\{\prod_{i=3}^{n} p_{o,0}^{(i)}\right\}\left(p_{o,5}^{(2)} + p_{o,2}^{(3)}\right) \\ \left\{\prod_{i=4}^{n} p_{o,0}^{(i)}\right\}\left(p_{o,5}^{(3)} + p_{o,2}^{(4)}\right) \\ \vdots \\ \left\{\prod_{i=n-1}^{n} p_{o,0}^{(i)}\right\}\left(p_{o,5}^{(n-2)} + p_{o,2}^{(n-1)}\right) \\ p_{o,0}^{(n)}\left(p_{o,5}^{(n-1)} + p_{o,2}^{(n)}\right) \\ p_{o,5}^{(4)} \end{bmatrix}^T \tag{A23}$$

$$\Omega_{0,o}(n) = \begin{bmatrix} \left\{\prod_{i=2}^{n} p_{o,0}^{(i)}\right\} p_{o,3}^{(2)} \\ \left\{\prod_{i=3}^{n} p_{o,0}^{(i)}\right\}\left(p_{o,6}^{(2)} + p_{o,3}^{(3)}\right) \\ \left\{\prod_{i=4}^{n} p_{o,0}^{(i)}\right\}\left(p_{o,6}^{(3)} + p_{o,3}^{(4)}\right) \\ \vdots \\ \left\{\prod_{i=n-1}^{n} p_{o,0}^{(i)}\right\}\left(p_{o,6}^{(n-2)} + p_{o,3}^{(n-1)}\right) \\ p_{o,0}^{(n)}\left(p_{o,6}^{(n-1)} + p_{o,3}^{(n)}\right) \\ p_{o,6}^{(4)} \end{bmatrix}^T \tag{A24}$$

Similarly, starting from Eq. A4 one can easily obtain similar structure for even Kautz functions in a recursive form as,

$$\begin{bmatrix} \Psi_2(k+3) \\ \Psi_4(k+3) \\ \Psi_6(k+3) \\ \Psi_8(k+3) \\ \vdots \\ \Psi_{2n}(k+3) \end{bmatrix} = \Omega_{2,e} \begin{bmatrix} \Psi_2(k+2) \\ \Psi_4(k+2) \\ \Psi_6(k+2) \\ \Psi_8(k+2) \\ \vdots \\ \Psi_{2n}(k+2) \end{bmatrix} + \Omega_{1,e} \begin{bmatrix} \Psi_2(k+1) \\ \Psi_4(k+1) \\ \Psi_6(k+1) \\ \Psi_8(k+1) \\ \vdots \\ \Psi_{2n}(k+1) \end{bmatrix}$$

$$+\Omega_{0,e}\begin{bmatrix}\Psi_2(k)\\ \Psi_4(k)\\ \Psi_6(k)\\ \Psi_8(k)\\ \vdots\\ \Psi_{2n}(k)\end{bmatrix} \tag{A25}$$

where the n^{th} rows of the matrices $\Omega_{2,e}$, $\Omega_{1,e}$and $\Omega_{0,e}$ are

$$\Omega_{2,e}(n) = \begin{bmatrix}\left\{\prod_{i=2}^{n} p_{e,0}^{(i)}\right\}\left(p_{e,1}^{(2)} - h_1^{(1)}\right)\\ \left\{\prod_{i=3}^{n} p_{e,0}^{(i)}\right\}\left(p_{e,4}^{(2)} + p_{e,1}^{(3)}\right)\\ \left\{\prod_{i=4}^{n} p_{e,0}^{(i)}\right\}\left(p_{e,4}^{(3)} + p_{e,1}^{(4)}\right)\\ \vdots\\ \left\{\prod_{i=n-1}^{n} p_{e,0}^{(i)}\right\}\left(p_{e,4}^{(n-2)} + p_{e,1}^{(n-1)}\right)\\ p_{e,0}^{(n)}\left(p_{e,4}^{(n-1)} + p_{e,1}^{(n)}\right)\\ p_{e,4}^{(n)}\end{bmatrix}^T \tag{A26}$$

$$\Omega_{1,e}(n) = \begin{bmatrix}\left\{\prod_{i=2}^{n} p_{e,0}^{(i)}\right\}\left(p_{e,2}^{(2)} - h_2^{(1)}\right)\\ \left\{\prod_{i=3}^{n} p_{e,0}^{(i)}\right\}\left(p_{e,5}^{(2)} + p_{e,2}^{(3)}\right)\\ \left\{\prod_{i=4}^{n} p_{e,0}^{(i)}\right\}\left(p_{e,5}^{(3)} + p_{e,2}^{(4)}\right)\\ \vdots\\ \left\{\prod_{i=n-1}^{n} p_{e,0}^{(i)}\right\}\left(p_{e,5}^{(n-2)} + p_{e,2}^{(n-1)}\right)\\ p_{e,0}^{(n)}\left(p_{e,5}^{(n-1)} + p_{e,2}^{(n)}\right)\\ p_{e,5}^{(4)}\end{bmatrix}^T \tag{A27}$$

$$\Omega_{0,e}(n) = \begin{bmatrix} \left\{\prod_{i=2}^{n} p_{e,0}^{(i)}\right\} p_{e,3}^{(2)} \\ \left\{\prod_{i=3}^{n} p_{e,0}^{(i)}\right\} \left(p_{e,6}^{(2)} + p_{e,3}^{(3)}\right) \\ \left\{\prod_{i=4}^{n} p_{e,0}^{(i)}\right\} \left(p_{e,6}^{(3)} + p_{e,3}^{(4)}\right) \\ \vdots \\ \left\{\prod_{i=n-1}^{n} p_{e,0}^{(i)}\right\} \left(p_{e,6}^{(n-2)} + p_{e,3}^{(n-1)}\right) \\ p_{e,0}^{(n)} \left(p_{e,6}^{(n-1)} + p_{e,3}^{(n)}\right) \\ p_{e,6}^{(4)} \end{bmatrix}^T \tag{A28}$$

Now, the Eq. A22 and Eq. A25 can be represented in a single equation as

$$\mathbf{\Psi}(k+3) = \mathbf{\Omega}_2\mathbf{\Psi}(k+2) + \mathbf{\Omega}_1\mathbf{\Psi}(k+1) + \mathbf{\Omega}_0\mathbf{\Psi}(k) \tag{A29}$$

where

$$\mathbf{\Psi}(k) = \begin{bmatrix} \Psi_1(k) \\ \Psi_2(k) \\ \Psi_3(k) \\ \vdots \\ \Psi_{2N}(k) \end{bmatrix} \tag{A30}$$

$$\mathbf{\Omega}_p(2i-1, 2j-1) = \begin{cases} \Omega_{p,o}(i,j), & i = j, i \in [1\ N], j \in [1\ N] \\ \Omega_{p,o}(i,j), & i \neq j, i \in [2\ N], j \in [1\ i] \\ 0, & Otherwise \end{cases}$$

$$\mathbf{\Omega}_p(2i, 2j) = \begin{cases} \Omega_{p,e}(i,j), & i = j, i \in [1\ N], j \in [1\ N] \\ \Omega_{p,e}(i,j), & i \neq j, i \in [2\ N], j \in [1\ i] \\ 0, & Otherwise \end{cases}$$

where $p = 0, 1, 2$

Appendix B

Stability of Linear MPC

Control Lyapunov Function at sampling instant k

$$V(k) = \sum_{j=1}^{N_p} X(k+j/k)^T Q X(k+j/k) + \sum_{j=0}^{N_p-1} \Delta u^*(k+j)^T R \Delta u^*(k+j) \quad \text{(B1)}$$

where

$$X(k+j/k) = \Lambda^j X(k) + \sum_{i=0}^{j-1} \Lambda^{j-i-1} \Upsilon \mathbf{\Psi}(i)^T \eta_k^* \quad \text{(B2)}$$

$$\Delta u(k+j) = \mathbf{\Psi}(j)^T \eta_k^* \quad \text{(B3)}$$

where η_k^* is the optimal coefficient vector solution for the defined cost function at sampling instant k.

Control Lyapunov Function At sampling instant $k+1$,

$$V(k+1) = \sum_{j=1}^{N_p} X(k+j+1/k+1)^T Q X(k+j+1/k+1) + \sum_{j=0}^{N_p-1} \Delta u^*(k+j+1)^T R \Delta u^*(k+j+1) \quad \text{(B4)}$$

where

$$X(k+j+1/k) = \Lambda^j X(k+1) + \sum_{i=0}^{j-1} \Lambda^{j-i-1} \Upsilon \mathbf{\Psi}(i)^T \eta_{k+1}^* \quad \text{(B5)}$$

$$\Delta u(k+j+1) = \mathbf{\Psi}(j)^T \eta_{k+1}^* \quad \text{(B6)}$$

where η^*_{k+1} is the optimal coefficient vector solution for the defined cost function at sampling instant $k+1$.

At sampling instant $k+1$ a feasible solution(not optimal) can be obtained by using the one step ahead prediction resulting from the solution(η^*_k) at sampling instant k as

$$X(k+1) = \Lambda X(k) + \Upsilon \Delta u^*(k) \tag{B7}$$

i.e, the sub-optimal solution at $k+1$ can be obtained by shifting the optimal solution at k one step forward. Therefore, the sub optimal cost is evaluated by applying input sequence $[\mathbf{\Psi}(1)^T\eta^*_k, \mathbf{\Psi}(2)^T\eta^*_k \cdots, \mathbf{\Psi}(k+N_p-1)^T\eta^*_k, C_{mpc}(X(k+N_p))]$.

$$\begin{aligned} V_{sub-opt}(k+1) &= \sum_{j=1}^{N_p}[X(k+j+1/k+1)^T Q X(k+j+1/k+1)] \\ &\quad + \sum_{j=0}^{N_p-1}[\Delta u_{sub-opt}(j)^T R \Delta u_{sub-opt}(j)] \end{aligned}$$

where

$$\begin{aligned} X(k+j+1/k+1) &= \Lambda^j X(k+1) + \sum_{i=0}^{j-1} \Lambda^{j-i-1} \Upsilon \Delta u_{sub-opt}(i) \\ \Delta u_{sub-opt}(j) &= [\mathbf{\Psi}(1)^T\eta^*_k, \mathbf{\Psi}(2)^T\eta^*_k, \cdots, \\ &\quad \mathbf{\Psi}(k+N_p-1)^T\eta^*_k, \\ &\quad C_{mpc}(X(k+N_p))] \end{aligned} \tag{B8}$$

From Eq. B2, the state space predictions using the optimal solution at sampling instant k can be further expressed as,

$$X(k+1/k) = \Lambda^1 X(k) + \Upsilon \mathbf{\Psi}(0)^T \eta^*_k \tag{B9a}$$

$$\begin{aligned} X(k+2/k) &= \Lambda^2 X(k) + \sum_{i=0}^{1} \Lambda^{1-i} \Upsilon \mathbf{\Psi}(i)^T \eta^*_k \\ &= \Lambda^2 X(k) + \Lambda^1 \Upsilon \mathbf{\Psi}(0)^T \eta^*_k + \Upsilon \mathbf{\Psi}(1)^T \eta^*_k \end{aligned} \tag{B9b}$$

$$\begin{aligned} X(k+3/k) &= \Lambda^3 X(k) + \sum_{i=0}^{2} \Lambda^{2-i} \Upsilon \mathbf{\Psi}(i)^T \eta^*_k \\ &= \Lambda^3 X(k) + \Lambda^2 \Upsilon \mathbf{\Psi}(0)^T \eta^*_k + \Lambda \Upsilon \mathbf{\Psi}(1)^T \eta^*_k \end{aligned}$$

$$+\Upsilon\mathbf{\Psi}(2)^T\eta_k^* \tag{B9c}$$

$$\vdots$$

$$\begin{aligned} X(k+N_p/k) &= \Lambda^{N_p}X(k) + \sum_{i=0}^{N_p-1}\Lambda^{j-i-1}\Upsilon\mathbf{\Psi}(i)^T\eta_k^* \\ &= \Lambda^{N_p}X(k) + \sum_{i=0}^{N_p-1}\Lambda^{N_p-i-1}\Upsilon\mathbf{\Psi}(i)^T\eta_k^* \\ &= \Lambda^{N_p}X(k) + \Lambda^{N_p-1}\Upsilon\mathbf{\Psi}(0)^T\eta_k^* \\ &\quad +\Lambda^{N_p-2}\Upsilon\mathbf{\Psi}(1)^T\eta_k^* + \Lambda^{N_p-3}\Upsilon\mathbf{\Psi}(2)^T\eta_k^* + \dots \\ &\quad +\Upsilon\mathbf{\Psi}(N_p-1)^T\eta_k^* \end{aligned} \tag{B9d}$$

Similarly, using Eq. B8, the state space predictions using the sub-optimal solution at sampling instant $k+1$ can be further expressed as,

$$\begin{aligned} X(k+2/k+1) &= \Lambda X(k+1) + \Upsilon\Delta u_{sub-opt}(0) \\ &= \Lambda\{\Lambda^1 X(k) + \Upsilon\mathbf{\Psi}(0)^T\eta_k^*\} + \Upsilon\mathbf{\Psi}(1)^T\eta_k^* \\ &= \Lambda^2 X(k) + \Lambda^1\Upsilon\mathbf{\Psi}(0)^T\eta_k^* + \Upsilon\mathbf{\Psi}(1)^T\eta_k^* \end{aligned} \tag{B10a}$$

$$\begin{aligned} X(k+3/k+1) &= \Lambda^2 X(k+1) + \sum_{i=0}^{1}\Lambda^{1-i}\Upsilon\Delta u_{sub-opt}(i) \\ &= \Lambda^2\{\Lambda^1 X(k) + \Upsilon\mathbf{\Psi}(0)^T\eta_k^*\} \\ &\quad +\Lambda\Upsilon\Delta u_{sub-opt}(0) + \Upsilon\Delta u_{sub-opt}(1) \\ &= \Lambda^3 X(k) + \Lambda^2\Upsilon\mathbf{\Psi}(0)^T\eta_k^* + \Lambda\Upsilon\mathbf{\Psi}(1)^T\eta_k^* \\ &\quad +\Upsilon\mathbf{\Psi}(2)^T\eta_k^* \end{aligned} \tag{B10b}$$

$$\begin{aligned} X(k+4/k+1) &= \Lambda^3 X(k+1) + \sum_{i=0}^{2}\Lambda^{2-i}\Upsilon\Delta u_{sub-opt}(i) \\ &= \Lambda^3\{\Lambda^1 X(k) + \Upsilon\mathbf{\Psi}(0)^T\eta_k^*\} \\ &\quad +\Lambda^2\Upsilon\Delta u_{sub-opt}(0) \\ &\quad +\Lambda\Upsilon\Delta u_{sub-opt}(1) + \Upsilon\Delta u_{sub-opt}(2) \\ &= \Lambda^4 X(k) + \Lambda^3\Upsilon\mathbf{\Psi}(0)^T\eta_k^* + \Lambda^2\Upsilon\mathbf{\Psi}(1)^T\eta_k^* \\ &\quad +\Lambda\Upsilon\mathbf{\Psi}(2)^T\eta_k^* + \Upsilon\mathbf{\Psi}(3)^T\eta_k^* \dots \end{aligned}$$

$$
\begin{aligned}
X(k+N_p/k+1) &= \Lambda^{N_p-1}X(k+1) + \sum_{i=0}^{N_p-2}\Lambda^{N_p-i-2}\Upsilon\Delta u_{sub-opt}(i) \\
&= \Lambda^{N_p-1}\{\Lambda^1 X(k) + \Upsilon\mathbf{\Psi}(0)^T\eta_k^*\} \\
&\quad +\Lambda^{N_p-2}\Upsilon\Delta u_{sub-opt}(0) \\
&\quad +\Lambda^{N_p-3}\Upsilon\Delta u_{sub-opt}(1) \\
&\quad +\ldots+\Upsilon\Delta u_{sub-opt}(N_p-2) \\
&= \Lambda^{N_p}X(k) + \Lambda^{N_p-1}\Upsilon\mathbf{\Psi}(0)^T\eta_k^* \\
&\quad +\Lambda^{N_p-2}\Upsilon\mathbf{\Psi}(1)^T\eta_k^* + \Lambda^{N_p-3}\Upsilon\mathbf{\Psi}(2)^T\eta_k^* + \ldots \\
&\quad +\Upsilon\mathbf{\Psi}(N_p-1)^T\eta_k^* \qquad \text{(B10c)}
\end{aligned}
$$

From Eq. B9 and Eq. B10, One can easily observe that,

$$
\begin{aligned}
X(k+2/k) &= X(k+2/k+1) \qquad \text{(B11a)} \\
X(k+3/k) &= X(k+3/k+1) \qquad \text{(B11b)} \\
X(k+4/k) &= X(k+4/k+1) \qquad \text{(B11c)} \\
&\vdots \\
X(k+N_p/k) &= X(k+N_p/k+1) \qquad \text{(B11d)}
\end{aligned}
$$

Now the $V_{sub-opt}(k+1)$ can be further rearranged as

$$
\begin{aligned}
V_{sub-opt}(k+1) &= \sum_{j=1}^{N_p}[X(k+j+1/k+1)^T Q X(k+j+1/k+1)] \\
&\quad + \sum_{j=0}^{N_p-1}[\Delta u_{sub-opt}(j)^T R\Delta u_{sub-opt}(j)] \\
&= X(k+2/k+1)^T Q X(k+2/k+1) \\
&\quad +X(k+3/k+1)^T Q X(k+3/k+1)+\cdots \\
&\quad +X(k+N_p+1/k+1)^T Q X(k+N_p+1/k+1) \\
&\quad +\Delta u^*(k+1)^T R\Delta u^*(k+1) \\
&\quad +\Delta u^*(k+2)^T R\Delta u^*(k+2) \\
&\quad +\cdots+C_{mpc}(X(k+N_p))^T R C_{mpc}(X(k+N_p))
\end{aligned}
$$

$$
\begin{aligned}
&= V(k) - X(k+1/k)^T Q X(k+1/k) \\
&\quad -\Delta u^*(k)^T R \Delta u^*(k) \\
&\quad +X(k+N_p/k+1)^T Q X(k+N_p/k+1) \\
&\quad +C_{mpc}(X(k+N_p))^T R C_{mpc}(X(k+N_p))
\end{aligned} \tag{B12}
$$

Using the assumption in Theorem 3.2,

$$
\begin{aligned}
V_{sub-opt}(k+1) &= V(k) - X(k+1/k)^T Q X(k+1/k) \\
&\quad -\Delta u^*(k)^T R \Delta u^*(k)
\end{aligned} \tag{B13}
$$

Let us denote the optimal value of the cost function at sampling instant $k+1$ as $V(k+1)$ and any sub-optimal cost function value $V_{sub-opt}(k+1)$ should follow that $V(k+1) \leq V_{sub-opt}(k+1)$, which means

$$
\begin{aligned}
V(k+1) &\leq V_{sub-opt}(k+1) \\
&\leq V(k) - X(k+1/k)^T Q X(k+1/k) \\
&\quad -\Delta u^*(k)^T R \Delta u^*(k) \\
V(k+1) - V(k) &\leq -X(k+1/k)^T Q X(k+1/k) \\
&\quad -\Delta u^*(k)^T R \Delta u^*(k)
\end{aligned} \tag{B14}
$$

Which implies that the Control Lyapunov Function (CLF) is a decreasing function and hence the asymptotic stability is proved.

Appendix C

Detailed derivation of state-space linear Kautz Model

Using Theorem 2.1 the state space Kautz model given in Eqs. (2.42) and (2.43) can be derived in the following state space form (q is shift operator).

$$\varphi_1(k) = \Psi_1(q)\, u(k)$$

$$
\begin{aligned}
&= C_1^{(1)} \left(1 - a_1^{(1)} q\right) \Gamma^{(1)}(q)\, u(k) \\
&= C_1^{(1)} \left(1 - a_1^{(1)} q\right) \frac{1}{(q-\beta_1)(q-\beta_1^*)} u(k) \\
&= C_1^{(1)} \left(q^{-1} - a_1^{(1)}\right) \frac{q}{q^2 + h_1^{(1)} q + h_2^{(1)}} u(k)
\end{aligned} \tag{C1}
$$

where

$$h_1^{(1)} = -(\beta_1 + \beta_1^*) \tag{C2}$$

$$h_2^{(1)} = \beta_1 \beta_1^* \tag{C3}$$

Define the following states

$$x_1(k) = \frac{q}{q^2 + h_1^{(1)} q + h_2^{(1)}} u(k) \tag{C4}$$

$$x_2(k) = x_1(k-1) \tag{C5}$$

Using Eqs. (C4) and (C5) in Eq.(C1) one obtains

$$\varphi_1(k) = C_1^{(1)} \left[x_2(k) - a_1^{(1)} x_1(k)\right] \tag{C6}$$

Similarly

$$
\begin{aligned}
\varphi_2(k) &= \Psi_2(q)\, u(k) \\
&= C_2^{(1)} \left(1 - a_2^{(1)} q\right) \Gamma^{(1)}(q)\, u(k) \\
&= \cdots \\
&= C_2^{(1)} \left[x_2(k) - a_2^{(1)} x_1(k)\right]
\end{aligned} \tag{C7}
$$

Further

$$
\begin{aligned}
\varphi_3(k) &= \Psi_3(q)\, u(k) \\
&= C_1^{(2)} \left(1 - a_1^{(2)} q\right) \Gamma^{(2)}(q)\, u(k) \\
&= C_1^{(2)} \left(1 - a_1^{(2)} q\right) \frac{(1-\beta_1 q)(1-\beta_1^* q)\, u(k)}{(q-\beta_2)(q-\beta_2^*)(q-\beta_1)(q-\beta_1^*)}
\end{aligned}
$$

$$
\begin{aligned}
&= C_1^{(2)}\left(q^{-1}-a_1^{(2)}\right)\times \\
&\left(\frac{h_2^{(1)}q^2+h_1^{(1)}q+1}{q^2+h_1^{(2)}q+h_2^{(2)}}\right)\left(\frac{q}{q^2+h_1^{(1)}q+h_2^{(1)}}\right)u\left(k\right) \\
&= C_1^{(2)}\left(q^{-1}-a_1^{(2)}\right)\frac{h_2^{(1)}q^2+h_1^{(1)}q+1}{q^2+h_1^{(2)}q+h_2^{(2)}}x_1\left(k\right) \qquad \text{(C8)}
\end{aligned}
$$

where

$$h_1^{(2)} = -\left(\beta_2+\beta_2^*\right) \qquad \text{(C9)}$$

$$h_2^{(2)} = \beta_2\beta_2^* \qquad \text{(C10)}$$

Define the following states

$$x_3\left(k\right) = \frac{h_2^{(1)}q^2+h_1^{(1)}q+1}{q^2+h_1^{(2)}q+h_2^{(2)}}\times x_1\left(k\right) \qquad \text{(C11)}$$

$$x_4\left(k\right) = x_3\left(k-1\right) \qquad \text{(C12)}$$

Using Eqs.(C11) and (C12) in Eq.(C8), one obtains the regressors (similar to Eqs. C6 and C7) as

$$\varphi_3\left(k\right) = C_1^{(2)}\left[x_4\left(k\right)-a_1^{(2)}x_3\left(k\right)\right] \qquad \text{(C13)}$$

$$\varphi_4\left(k\right) = C_2^{(2)}\left[x_4\left(k\right)-a_2^{(2)}x_3\left(k\right)\right] \qquad \text{(C14)}$$

The derivation of regressors can further be continued and a generalized expression can be given as in Eqs. (2.45)−(2.50).

Further, upon applying inverse transformation on the Eq. (C4) and thereupon using Eq. (C5), following discrete time domain state space expression can be obtained

$$
\begin{aligned}
x_1\left(k+1\right) &= -h_1^{(1)}x_1\left(k\right)-h_2^{(1)}x_1\left(k-1\right)+u(k) \\
&= -h_1^{(1)}x_1\left(k\right)-h_2^{(1)}x_2\left(k\right)+u(k) \qquad \text{(C15)} \\
x_2\left(k+1\right) &= x_1\left(k\right) \qquad \text{(C16)}
\end{aligned}
$$

Similarly, upon applying inverse transformation the above Eq. (C11) and thereupon using

Eqs. (C12) and (C15)

$$\begin{aligned} x_3(k+1) &= -h_1^{(2)} x_3(k) - h_2^{(2)} x_3(k-1) + h_2^{(1)} x_1(k+1) \\ &\quad + h_1^{(1)} x_1(k) + x_1(k-1) \\ &= \cdots \\ &= h_1^{(1)} \left(1 - h_2^{(1)}\right) x_1(k) + \left\{1 - \left(h_2^{(1)}\right)^2\right\} x_2(k) \\ &\quad - h_1^{(2)} x_3(k) - h_2^{(2)} x_4(k) + h_2^{(1)} u(k) \end{aligned} \tag{C17}$$

$$x_4(k+1) = x_3(k) \tag{C18}$$

Similar to Eqs.(C11) and (C12),

$$x_5(k) = \frac{h_2^{(2)} q^2 + h_1^{(2)} q + 1}{q^2 + h_1^{(3)} q + h_2^{(3)}} \times x_3(k) \tag{C19}$$

$$x_6(k) = x_5(k-1) \tag{C20}$$

and applying inverse transformation on Eq. (C19) and thereupon using Eqs. (C20) and (C17)

$$\begin{aligned} x_5(k+1) &= h_1^{(1)} h_2^{(2)} \left(1 - h_2^{(1)}\right) x_1(k) + \\ &\quad h_2^{(2)} \left\{1 - \left(h_2^{(1)}\right)^2\right\} x_2(k) + h_1^{(2)} \left(1 - h_2^{(2)}\right) x_3(k) \\ &\quad + \left\{1 - \left(h_2^{(2)}\right)^2\right\} x_4(k) - h_1^{(3)} x_5(k) - h_2^{(3)} x_6(k) \\ &\quad + h_2^{(2)} h_2^{(1)} u(k) \end{aligned} \tag{C21}$$

$$x_6(k+1) = x_5(k) \tag{C22}$$

Likewise,

$$x_7(k+1) = \begin{bmatrix} h_1^{(1)} h_2^{(2)} h_2^{(3)} \left(1 - h_2^{(1)}\right) x_1(k) + \\ h_2^{(2)} h_2^{(3)} \left\{1 - \left(h_2^{(1)}\right)^2\right\} x_2(k) + \\ h_1^{(2)} h_2^{(3)} \left(1 - h_2^{(2)}\right) x_3(k) + \\ h_2^{(3)} \left\{1 - \left(h_2^{(2)}\right)^2\right\} x_4(k) + \\ h_1^{(3)} \left(1 - h_2^{(3)}\right) x_5(k) + \\ \left\{1 - \left(h_2^{(3)}\right)^2\right\} x_6(k) - \\ h_1^{(4)} x_7(k) - h_2^{(4)} x_8(k) + \\ h_2^{(3)} h_2^{(2)} h_2^{(1)} u(k) \end{bmatrix} \tag{C23}$$

$$x_8(k+1) = x_7(k) \tag{C24}$$

and

$$x_9(k+1) = \begin{bmatrix} h_1^{(1)} h_2^{(2)} h_2^{(3)} h_2^{(4)} \left(1 - h_2^{(1)}\right) x_1(k) + \\ h_2^{(2)} h_2^{(3)} h_2^{(4)} \left\{1 - \left(h_2^{(1)}\right)^2\right\} x_2(k) + \\ h_1^{(2)} h_2^{(3)} h_2^{(4)} \left(1 - h_2^{(2)}\right) x_3(k) + \\ h_2^{(3)} h_2^{(4)} \left\{1 - \left(h_2^{(2)}\right)^2\right\} x_4(k) + \\ h_1^{(3)} h_2^{(4)} \left(1 - h_2^{(3)}\right) x_5(k) + \\ h_2^{(4)} \left\{1 - \left(h_2^{(3)}\right)^2\right\} x_6(k) + \\ h_1^{(4)} \left\{1 - h_2^{(4)}\right\} x_7(k) + \\ \left\{1 - \left(h_2^{(4)}\right)^2\right\} x_8(k) \\ -h_1^{(5)} x_9(k) - h_2^{(5)} x_{10}(k) \\ +h_2^{(4)} h_2^{(3)} h_2^{(2)} h_2^{(1)} u(k) \end{bmatrix} \tag{C25}$$

$$x_{10}(k+1) = x_9(k) \tag{C26}$$

The above expressions in Eqs.(C15), (C16), (C17), (C18), (C21), (C22), (C23), (C24),

(C25) and (C26) can further be represented in a compact matrix form as,

$$\begin{bmatrix} x_1(k+1) \\ x_2(k+1) \\ x_3(k+1) \\ x_4(k+1) \\ x_5(k+1) \\ x_6(k+1) \\ x_7(k+1) \\ x_8(k+1) \\ x_9(k+1) \\ x_{10}(k+1) \end{bmatrix} = F \times \begin{bmatrix} x_1(k) \\ x_2(k) \\ x_3(k) \\ x_4(k) \\ x_5(k) \\ x_6(k) \\ x_7(k) \\ x_8(k) \\ x_9(k) \\ x_{10}(k) \end{bmatrix} + \begin{bmatrix} 1 \\ 0 \\ h_2^{(1)} \\ 0 \\ h_2^{(1)}h_2^{(2)} \\ 0 \\ h_2^{(1)}h_2^{(2)}h_2^{(3)} \\ 0 \\ h_2^{(1)}h_2^{(2)}h_2^{(3)}h_2^{(4)} \\ 0 \end{bmatrix} \times u(k)$$

and

$$F = \begin{bmatrix} F_1 & F_2 & F_3 & F_4 \end{bmatrix}$$

where

$$F_1 = \begin{bmatrix} -h_1^{(1)} & -h_2^{(1)} \\ 1 & 0 \\ h_1^{(1)}\left(1-h_2^{(1)}\right) & 1-\left(h_2^{(1)}\right)^2 \\ 0 & 0 \\ h_1^{(1)}h_2^{(2)}\left(1-h_2^{(1)}\right) & h_2^{(2)}\left\{1-\left(h_2^{(1)}\right)^2\right\} \\ 0 & 0 \\ h_1^{(1)}\prod_{i=2}^{3}h_2^{(i)}\left(1-h_2^{(1)}\right) & \prod_{i=2}^{3}h_2^{(i)}\left\{1-\left(h_2^{(1)}\right)^2\right\} \\ 0 & 0 \\ h_1^{(1)}\prod_{i=2}^{4}h_2^{(i)}\left(1-h_2^{(1)}\right) & \prod_{i=2}^{4}h_2^{(i)}\left\{1-\left(h_2^{(1)}\right)^2\right\} \\ 0 & 0 \end{bmatrix}$$

and

$$F_2 = \begin{bmatrix} 0 & 0 \\ 0 & 0 \\ -h_1^{(2)} & -h_2^{(2)} \\ 1 & 0 \\ h_1^{(2)}\left(1-h_2^{(2)}\right) & 1-\left(h_2^{(2)}\right)^2 \\ 0 & 0 \\ h_1^{(2)}h_2^{(3)}\left(1-h_2^{(2)}\right) & h_2^{(3)}\left\{1-\left(h_2^{(2)}\right)^2\right\} \\ 0 & 0 \\ h_1^{(2)}\prod_{i=3}^{4}h_2^{(i)}\left(1-h_2^{(2)}\right) & \prod_{i=3}^{4}h_2^{(i)}\left\{1-\left(h_2^{(2)}\right)^2\right\} \\ 0 & 0 \end{bmatrix}$$

and

$$F_3 = \begin{bmatrix} 0 & 0 \\ 0 & 0 \\ 0 & 0 \\ 0 & 0 \\ -h_1^{(3)} & -h_1^{(3)} \\ 1 & 0 \\ h_1^{(3)}\left(1-h_2^{(3)}\right) & 1-\left(h_2^{(3)}\right)^2 \\ 0 & 0 \\ h_1^{(3)}h_2^{(4)}\left(1-h_2^{(3)}\right) & h_2^{(4)}\left\{1-\left(h_2^{(3)}\right)^2\right\} \\ 0 & 0 \end{bmatrix}$$

and

$$F_4 = \begin{bmatrix} 0 & 0 & 0 & 0 \\ 0 & 0 & 0 & 0 \\ 0 & 0 & 0 & 0 \\ 0 & 0 & 0 & 0 \\ 0 & 0 & 0 & 0 \\ 0 & 0 & 0 & 0 \\ -h_1^{(4)} & -h_2^{(4)} & 0 & 0 \\ 1 & 0 & 0 & 0 \\ h_1^{(4)}\left\{1-h_2^{(4)}\right\} & 1-\left(h_2^{(4)}\right)^2 & -h_1^{(5)} & -h_2^{(5)} \\ 0 & 0 & 1 & 0 \end{bmatrix}$$

The complete state space model can be derived as given in Eq. (2.54) whose $(2n-1)^{th}$ row will be

$$x_{2n-1}(k+1) = \begin{bmatrix} h_1^{(1)}\prod_{i=2}^{n-1} h_2^{(i)}\left(1-h_2^{(1)}\right) \\ \prod_{i=2}^{n-1} h_2^{(i)}\left\{1-\left(h_2^{(1)}\right)^2\right\} \\ h_1^{(2)}\prod_{i=3}^{n-1} h_2^{(i)}\left(1-h_2^{(2)}\right) \\ \prod_{i=3}^{n-1} h_2^{(i)}\left\{1-\left(h_2^{(2)}\right)^2\right\} \\ h_1^{(3)}\prod_{i=4}^{n-1} h_2^{(i)}\left(1-h_2^{(3)}\right) \\ \prod_{i=4}^{n-1} h_2^{(i)}\left\{1-\left(h_2^{(3)}\right)^2\right\} \\ \vdots \\ h_1^{(n-1)}\left(1-h_2^{(n-1)}\right) \\ 1-\left(h_2^{(n-1)}\right)^2 \\ -h_1^{(n)} \\ -h_2^{(n)} \end{bmatrix}^T \begin{bmatrix} x_1(k) \\ x_2(k) \\ x_3(k) \\ x_4(k) \\ x_5(k) \\ x_6(k) \\ \vdots \\ x_{2(n-1)-1}(k) \\ x_{2(n-1)}(k) \\ x_{2n-1}(k) \\ x_{2n}(k) \end{bmatrix} + \left\{\prod_{i=1}^{n-1} h_2^{(i)}\right\} u(k) \tag{C27}$$

and

$$x_{2n}(k+1) = x_{2n-1}(k) \tag{C28}$$

which would eventually yield the Eqs.(2.58)−(2.60)